UC Berkeley
UC Berkeley Electronic Theses and Dissertations

Title

Physiology and Biotechnological Applications of Microbial (Per)chlorate Reduction

Permalink

https://escholarship.org/uc/item/2rz4s2v3

Author

Wang, Ouwei

Publication Date

2018

Peer reviewed|Thesis/dissertation

**Physiology and Biotechnological Applications of
Microbial (Per)chlorate Reduction**

By

Ouwei Wang

A dissertation submitted in partial satisfaction of

the requirements for the degree of

Doctor of Philosophy

In

Microbiology

in the

Gradate Division

of the

University of California at Berkeley

Committee in charge:

Professor John D. Coates, Chair
Professor Arash Komeili
Professor Peter H. Quail

Summer 2018

Abstract

Physiology and Biotechnological Applications of
Microbial (Per)chlorate Reduction

by
Ouwei Wang

Doctor of Philosophy in Microbiology
University of California at Berkeley
Professor John D. Coates, Chair

Respiration is a set of metabolic reactions and processes that release chemical energy to fuel cellular activity. While humans can only breathe oxygen, microorganisms are able to respire other terminal electron acceptors such as chlorate and perchlorate [collectively (per)chlorate]. My graduate thesis aims to elucidate the molecular mechanisms and physiology of (per)chlorate respiration in the model (per)chlorate reducing bacteria, *Azospira suillum* PS; and to transform our fundamental knowledge of perchlorate reduction into applied technologies to solve practical industrial problems.

The first chapter of this dissertation is a published review article. This chapter represents an overview of my thesis and summarizes the potential biotechnological applications of (per)chlorate reduction, including enzymatic perchlorate detection; enhanced xenobiotic bioremediation; oil reservoir bio-souring control; chemostat hygiene control; aeration enhancement in industrial bioreactors; and biogenic oxygen production for planetary exploration.

The second chapter of this dissertation is a published research article. This chapter aims to identify the redundancy between perchlorate and nitrate reduction pathways. Our results demonstrate two genes (*pcrQ* and *pcrO*) that encode electron transfer cytochromes are essential for perchlorate respiration; but completely redundant and fully replaceable with their respective homologous genes *napC* and *napO* in the denitrification pathway. While (per)chlorate reducers are known to preferentially reduce nitrate in the presence of both nitrate and perchlorate, by rewiring the terminal electron transport pathways in PS we were able to engineer strains that preferentially reduce perchlorate or concurrently reduce both nitrate and perchlorate.

The third chapter of this dissertation is a transcriptomic analysis of PS under different growth conditions. These data establish the expression profiles of proteins involved in

the nitrate, chlorate, perchlorate, and aerobic respiration pathways. This information also serves as a hypothesis-generating foundation for future investigations in microbial (per)chlorate reduction.

The fourth chapter of this dissertation describes a biocide/biocide-resistant system for bacteriophage and microbial contamination prevention and treatment during biomanufacturing. This technology is based on the biocide chlorite(ClO_2^-), a toxic intermediate generated during perchlorate respiration, and the corresponding detoxifying enzyme, chlorite dismutase (Cld).

The fifth chapter of this dissertation discusses the implications of this research for future investigations regarding the biology and the biotechnology of microbial (per)chlorate reduction.

The sixth chapter is the conclusion of this dissertation.

Table of Contents

Acknowledgments

Chapter 1
Biotechnological Applications of Microbial (Per)chlorate Reduction

Abstract

While the microbial degradation of a chloroxyanion-based herbicide was first observed nearly ninety years ago, only recently have researchers elucidated the underlying mechanisms of perchlorate and chlorate respiration [collectively, (per)chlorate respiration]. Although the obvious application of these metabolisms lies in the bioremediation and attenuation of (per)chlorate in contaminated environments, a diversity of alternative and innovative biotechnological applications has been proposed based on the unique metabolic abilities of dissimilatory (per)chlorate-reducing bacteria (DPRB). This is fueled in part by the unique ability of these organisms to generate molecular oxygen as a transient intermediate of the central pathway of (per)chlorate respiration. This ability, along with other novel aspects of the metabolism, have resulted in a wide and disparate range of potential biotechnological applications being proposed; including enzymatic perchlorate detection; gas gangrene therapy; enhanced xenobiotic bioremediation; oil reservoir bio-souring control; chemostat hygiene control; aeration enhancement in industrial bioreactors; and biogenic oxygen production for planetary exploration. While previous reviews focus on the fundamental science of microbial (per)chlorate reduction (for example see Youngblut et al, 2016), here we provide an overview of the emerging biotechnological applications of (per)chlorate respiration and the underlying organisms and enzymes to environmental and biotechnological industries.

1.1 Introduction

The oxyanions of chlorine, perchlorate (ClO_4^-) and chlorate (ClO_3^-), are highly soluble, strong oxidants that are deposited in the environment through both anthropogenic and natural processes [1-8]. Perchlorate is a common commodity chemical with a diverse range of industrial uses ranging from pyrotechnics to lubricating oils [4], but it is predominantly used as an energetics booster or oxidant in solid rocket fuels by the munitions industry [4, 9-11]. Although a powerful oxidant, under most environmental conditions perchlorate is highly stable on account of the high energy of activation associated with its reduction [9, 10]. Perchlorate is toxic to humans as it inhibits the uptake of iodine by the thyroid gland, disrupting the production of thyroid hormones, potentially leading to hypothyroidism [12-14]. For humans, oral ingestion is the primary source of perchlorate exposure as contamination is widespread in soil, fertilizers, and groundwater, allowing it to readily move into our food chain [15].

In contrast to perchlorate, chlorate is far more chemically reactive than perchlorate [16]. It is currently used to produce chlorine dioxide in bleaching and disinfection processes [17] and as a precursor for the manufacture of perchlorate. Historically it was widely used as the active component of herbicide during the early twentieth century [18, 19]. Chlorate is also toxic to humans causing oxidative damage to red blood cells resulting in methemoglobin formation[20, 21]. In both plant and microbial cells, chlorate can be a substrate for respiratory or assimilatory nitrate reductases, which reduce it to chlorite (ClO_2^-) [22], a compound with demonstrated broad-spectrum biocidal activity against gram negative and positive bacteria [23-29], bacteriophages [28], fungi [24], and algae [26]. Because of this, chlorite is often used to treat freshwater copepod parasites [30] and as an active ingredient in topical wound treatments.

In the 1920's, bacteria were discovered that used chlorate, (and presumably perchlorate although this is not a prerequisite [19]) as a terminal electron acceptors for anaerobic energy production [31]. Recent studies have identified the molecular mechanisms underlying this unique biochemistry (Figure 1)[18] . Dissimilatory (per)chlorate reducing bacteria (DPRB) use a highly conserved perchlorate reductase PcrABC to reduce perchlorate to chlorate and subsequently chlorite. The chlorite is rapidly removed by another highly conserved enzyme, chlorite dismutase (Cld), to produce molecular oxygen (O_2) and innocuous chloride (Cl^-) [18, 32]. The oxygen produced is then respired by the same organism, generally through the use of a high-affinity cytochrome *cbb3*-oxidase [18, 19, 32]. Specialized dissimilatory chlorate-reducing bacteria (DCRB) respire only chlorate and not perchlorate using an analogous pathway involving chlorite and Cld, but the chlorate is initially reduced via a specialized chlorate reductase (ClrABC), a structurally and evolutionarily distinct enzyme from the PcrABC

2

that can reduce chlorate but not perchlorate [33-37]. Owing to the unique ability to degrade (per)chlorate and generate molecular oxygen under anaerobic conditions, DPRB, perchlorate reductase, chlorate reductase, and chlorite dismutase provide innovative solutions to outstanding problems in current industrial processes. In this review, we provide an overview of the potential applications of microbial (per)chlorate reduction, and the underlying genes, and enzymes.

1.2 (Per)chlorate Bioremediation

The primary application of microbial (per)chlorate reduction is the bio-attenuation of perchlorate-contaminated water sources [38]. Bioremediation of perchlorate can be much more effective than other remediation strategies, as perchlorate is completely and irreversibly reduced to innocuous chloride [38]. For example, although ion exchange based technology is a widely used and effective method for perchlorate removal, it does not uniquely bind to perchlorate, rather the ion exchange resins also bind other common co-contaminating anions such as nitrate which are often present in concentrations several orders of magnitude higher than perchlorate. As such, much of the ion exchange capacity is lost in binding these analogous compounds [38]. Furthermore, ion exchange technologies concentrate perchlorate and other ions into a recalcitrant brine, which often poses disposal issues in its own right [18, 38-40]. In contrast, perchlorate metabolism by DPRB completely converts perchlorate into innocuous chloride [38]. This can be used as an independent treatment strategy or can be applied in combination with ion exchange methods using halophilic DPRB [41-44] or salt-tolerant communities [40, 45-47] to treat perchlorate-laden waste brines that are extracted from ion exchange resins that would otherwise pose significant health and disposal issues.

Perchlorate bioremediation can be achieved in-situ or ex-situ using various types of bioreactors. While laboratory-scale autotrophic reactors using hydrogen [48-51], reduced iron [52], or sulfur compounds [53] as the electron donor have been developed, most industrial-scale fixed or fluidized-bed reactors are operated as heterotrophic reactors using either simple alcohols or acetate as the electron donor [18, 54]. Among the different types, fluidized-bed heterotrophic (with ethanol as the electron donor) bioreactors have emerged as the most successful for perchlorate treatment with capacities up to 34×10^6 L·day^{-1}, reducing perchlorate concentrations to below 6 ppb (6 µg.L^{-1}), the maximum concentration limit that is allowed in the state of California [18, 55].

Conventional bioreactors always depend on the continuous addition of a chemical electron donor and are subject to bio-fouling issues due to microbial growth [54, 56-58]. Furthermore, disposal of the excess biomass generated represents a significant

3

operational cost of the treatment process, while any residual labile electron donor in the reactor effluent can stimulate microbial growth in water distribution systems and contribute to the formation of toxic trihalomethanes during disinfection by chlorination [59]. These issues led to the proposal of a diversity of alternative advanced reactor designs. An innovative and unorthodox bioreactor concept was developed in 2007 based on the electrochemical stimulation of microbial perchlorate reduction [58, 60, 61] (Figure 2). In these packed-bed bioelectrical reactors, DPRB use electrons that are provided through a negatively charged cathode set at a redox potential of 500mV as an electron donor. Preliminary studies suggested that electrons were either directly consumed off the electrode surface or indirectly through the use of anthraquinone-2,6-disulfonate as a recyclable electron shuttle [58, 62]. However, subsequently, it was demonstrated that these reactors did not function mechanistically as initially perceived [58, 62]. Remarkably, it was shown that living DPRB cells were not required for perchlorate reduction in the bioelectrical reactors. Rather, catalytic amounts of oxygen contaminating the bioelectrical packed-bed reactors reacted with electrochemically reduced anthraquinone-2,6-disulfonate to form superoxide and hydrogen peroxide, leading to DPRB cell lysis and active enzyme release [58, 62]. The observed perchlorate reduction and removal was primarily mediated through interconnected enzymatic electrocatalysis mechanisms, in which the cathode-reduced anthraquinone-2,6-disulfonate functioned as a direct electron donor for the perchlorate reductase enzyme PcrAB that was released from the dying lysing microbial cells [58, 62]. While the underlying mechanism of perchlorate attenuation was not dependent on living cells, the technology still shows great promise and could be improved by the use of nanocarbon conductive interlinks between the electrode surface and the cell or by the identification of DPRB that can use electrons directly off the electrode surface similar to the mechanism used by a diversity of iron reducing species [63, 64]. Alternatively, the redox potential on the cathode could be increased to allow for electrochemical H_2 generation, which could support an autotrophic DPRB population. Although further work is needed to develop the technology to commercial application, the advantages are substantial in being able to control the rate of metabolism and perchlorate treatment independently from biomass growth (Figure 2).

1.3 Enzymatic Bioassay for the Detection of Perchlorate

Ion chromatography and mass spectrometry are commonly used for the detection and quantification of perchlorate in environmental samples [65-67]. Although sensitive, these methods are slow, costly, and require specialized personnel and laboratories. Therefore, an enzymatic bioassay that offers a cost-effective alternative with the potential for high throughput application was developed using a mixture of purified perchlorate reductase (PcrAB), nicotine adenine dinucleotide (NADH), and the electron shuttle phenazine methosulfate (PMS) [68, 69]. In this bioassay, PMS mediates the
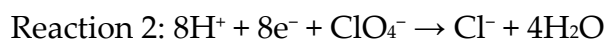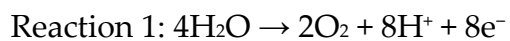
4

transfer of electrons from NADH to PcrAB, which subsequently reduces perchlorate to chlorite (Figure 3). The enzymatically produced chlorite is subsequently dismutated by Cld to produce O_2, which chemically reacts with the PMS resulting in further NADH oxidation. This additional PMS cycle provides an effective twofold signal amplification (Figure 3). The perchlorate concentration is indirectly measured by the oxidation of NADH, which is monitored as absorbance changes at 340 nm [68, 69]. A perchlorate detection range of 2–17,000 ppb ($\mu g.L^{-1}$) was achieved when the bioassay was coupled with a solid-phase extraction step to purify and concentrate the perchlorate [68, 69]. This step, based on styrene divinyl benzene syringe columns pretreated with decyltrimethylammonium bromide (DTAB), allowed for the selective extraction and concentration of perchlorate from solutions with numerous co-occurring ions including nitrate, phosphate, sulfate, iron, and chloride [68, 69]. Although this bioassay is sensitive to air due to the slow oxygen-induced inactivation of perchlorate reductase, this issue was avoided by covering all of the reactions with mineral oil [68]. Alternatively, an oxygen insensitive enzyme, such as suitable nitrate reductase that is capable of reducing perchlorate, could conceptually be used to replace the PcrAB, although this might significantly impact the assay lower limit of detection. Youngblut et al. [32] recently demonstrated that the PcrAB is a specialized member of the DMSO reductase superfamily, with a relatively high perchlorate affinity (K_M = 6 μM), unlike the closely related nitrate reductase, which has a much lower affinity for perchlorate (K_M = 1.1 mM).

1.4 Bioeletrochemical O_2 Production from Perchlorate

Perchlorate has been detected and inferred on Mars at concentrations between 0.5% and 1% [70, 71]. Similarly, perchlorate has also been detected in lunar and meteorite samples [72], suggesting its prevalence across the solar system and possibly beyond. Due to unrestricted UV radiation and the lack of biotic perchlorate diagenesis processes, the quantity of perchlorate in the surface regolith of Mars is three to four orders of magnitude higher when compared with soils on Earth, and offers an attractive resource for human exploration and survival. Traditionally, perchlorate is used as an energetic booster or oxidant in solid rocket fuel. However, perchlorate on Mars could also serve as a source of O_2 for human consumption [73]. For example, humans respire 550–650 liters of oxygen per day. Based on the estimated mass fraction of perchlorate in Martian regolith, a daily supply of oxygen for one astronaut could be obtained by the complete dissociation of perchlorate contained in 60 kg of regolith. Perchlorate can be extracted from Martian regolith easily with water, which can be recycled for reuse with minimal effort. Because of the large molecular volume and single anionic charge, perchlorate has a low affinity for cations, and, as a result, perchlorate salts are generally highly soluble and completely dissociate into perchlorate and the relevant counter ion in aqueous solutions. Furthermore, perchlorate does not sorb to any significant extent to soils or

sediments and, in the absence of any biological interactions, its mobility and fate are largely influenced by the hydrology of the environment [74]. As such, the extraction of perchlorate laden rock simply requires water.

The method of O_2 production from the extracted perchlorate takes advantage of electrochemistry combined with enzymatic reduction (Figure 4) previously developed for microbial perchlorate attenuation in a bioelectrical reactor (BER) [58]. Electrochemical consumption of perchlorate in the cathodic chamber mediated by an active perchlorate reductase enzyme can be coupled to electrolysis of water releasing pure O_2 with no contaminating gases in the anodic chamber. Furthermore, because water is formed in the cathodic chamber at a rate that is identical to that consumed in the anodic chamber (reactions 1–3) (Figure 4), the system is not limited by water availability.

$$\text{Reaction 1: } 4H_2O \rightarrow 2O_2 + 8H^+ + 8e^-$$
$$\text{Reaction 2: } 8H^+ + 8e^- + ClO_4^- \rightarrow Cl^- + 4H_2O$$
$$\text{Combined reaction: } ClO_4^- \rightarrow Cl^- + 2O_2$$

The technology is composed of a simple poised potential electrochemical cell containing a cathode and an anode. The redox potential on the cathode can be set at 500–750 mV relative to a reference electrode. The anode voltage is left free floating at ≥1.5 volt, while power can be provided through a photovoltaic cell. The cathode chamber is filled with an aqueous extract of regolith containing perchlorate and amended with pure enzyme or lysed cells with demonstrated perchlorate reduction capacity. The cathode chamber can be further amended with a soluble electron shuttle, such as 2,6-anthraquinone disulphonate (100 µM), to mediate electron transfer from the electrode surface to the active enzyme. Preliminary studies demonstrated the bioelectrochemical reduction of ~1 mM perchlorate over 8 h [58], which equates to the production of ~2 mM O_2 (or ~45 mL from a 1 L bioreactor), suggesting that some process optimization is required to achieve a goal of 550–650 liters of oxygen per day. However, the rate of oxygen production is directly correlated to the rate of perchlorate reduction, which is a function of enzyme concentration in the cathodic chamber, thus it is easy to envision straightforward approaches for rate improvement. The anodic chamber is filled with water and the electrical requirements can either be supplied from photovoltaic cells or from alternative electrical sources. When the water content of the anode chamber is depleted, it can be refilled with water produced in the cathode chamber. While this process may not be suitable to scale up to satisfy the sole needs of a human colony, it could offer an emergency O_2 alternative, taking advantage of the natural resources of the planet.

1.5 Oil Reservoir Bio-Souring Control

Off-shore petroleum extraction often involves injection of sulfate-rich (~28 mM) seawater into the oil reservoir, which increases the reservoir pressure and facilitates crude oil recovery [75, 76]. However, this practice frequently leads to the bio-generation of hydrogen sulfide (H_2S) by sulfate reducing microorganisms (SRM) [75, 77]. This phenomenon, termed bio-souring, poses significant health and operational risks due to the toxic, explosive, and corrosive nature of hydrogen sulfide gas, and has an estimated associated annual cost of \$90 billion globally [18, 78]. Presently, the most common practice for bio-souring control is the addition of nitrate into the injected seawater to stimulate nitrate respiration [75, 77-79]. Microbial nitrate reduction is thermodynamically more favorable than microbial sulfate reduction (NO_3^-/N_2 $E°' = +750$ mV, SO_4^-/HS_2 $E°' = -217$ mV), and, as such, should bio-competitively exclude sulfate reduction [75, 79, 80]. However, while bio-competitive exclusion may effectively reduce souring in some natural environments, the favorable thermodynamics of nitrate reduction does not exclude the potential for the co-occurrence of sulfate reduction if the electron donor is saturating [81], as is the case in an oilfield. In addition, sulfate reduction can persist in deeper reservoirs as nitrate penetration is limited due to rapid depletion through microbial respiration, as seawater is often a rich source of nitrate reducing organisms [16, 75, 79, 82]. Furthermore, many SRM, including *Desulfovibrio* spp., *Desulfobulbus* spp., and *Desulfomonas* spp., can alternatively use nitrate as a terminal electron acceptor, foreshadowing rapid SRM activity and H_2S rebound during any interruption of nitrate treatment [83].

Recent studies have exploited perchlorate and DPRB as an alternative method for oil reservoir bio-souring control. Perchlorate treatment has several advantages over nitrate (Figure 5). First, microbial perchlorate respiration is thermodynamically more favorable ($E°' = +797$ mV) than either nitrate or sulfate reduction [18, 19, 76], therefore ensuring the bio-competitive exclusion of SRM by DPRB. Second, sulfide causes electron transport chain short-circuiting in DPRB, in which the perchlorate reductase directly oxidizes sulfide to produce elemental sulfur [84]. Due to the highly conserved nature of the perchlorate reductase, all DPRB tested to date rapidly and preferentially oxidize sulfide, even in the presence of labile physiological electron donors (e.g., acetate, lactate etc.) [76, 84]. The DPRB retain the ability to grow on other electron donors once the sulfide is completely biologically removed [76, 84]. Finally, perchlorate acts as a competitive inhibitor of the ATP sulfurylase, which is a highly conserved key enzyme in the sulfate reduction pathway [78]. A proof-of-concept study of a flow-through column system mimicking an oil reservoir environment with the potential to sour has confirmed dramatic SRM activity inhibition by the addition of perchlorate at concentrations as low as 3.5 mM [16].

1.6 Xenobiotic Bioremediation by DPRB and DCRB

Anthropogenic activities, such as industrial discharges and accidental spills, often result in the release of highly toxic xenobiotics, such as benzene, toluene, ethylbenzene, or xylene (BTEX) into groundwater, soil, or sediments [85-87]. Aerobic microorganisms, especially *Pseudomonas* species, utilize oxygen as a co-substrate for oxygenase enzymes to effectively cleave chemically stable aromatic rings [88, 89]. However, this combined with the utilization of O_2 as an electron acceptor for respiration leads to a rapid depletion of oxygen. As such, the contaminated environment becomes anoxic and dominated by anaerobic microbial metabolism [90]. Under anoxic conditions, microbial metabolisms dependent on energy consuming reductive de-aromatization steps to cleave the ring [91, 92], and the rate of degradation is significantly slower than when O_2 is available [93].

Owing to their unique ability to generate molecular oxygen under anaerobic conditions, it had long been postulated that DPRB and DCRB are capable of stimulating oxygenase-dependent anaerobic metabolisms [18, 94-96]. This was first shown in anoxic co-cultures of DPRB with obligate aerobic hydrocarbon utilizing *Pseudomonas* spp. [95, 96]. In these studies, degradation of benzene and naphthalene was demonstrated under anoxic conditions when the cultures were amended with chlorite. The chlorite was directly dismutated into O_2 and Cl^- by the active DPRB (Figure 6) and the biogenic O_2 was subsequently available for the aerobic *Pseudomonas* to use as a co-substrate and an electron acceptor for the hydrocarbon metabolism in an oxygenase-dependent manner. An expansion of these studies showed that degradation of both monoaromatic and polycylic aromatic hydrocarbons could be stimulated in contaminated anoxic sediment upon bioaugmentation with DPRB and addition of chlorite [96]. Subsequent studies have similarly demonstrated that methane degradation can be correspondingly stimulated in a co-culture of an aerobic methanotroph with a DPRB [97].

These findings led to the postulation that DPRB, with the appropriate gene content, may exist that can completely catabolize xenobiotics independently under anoxic conditions in an oxygenase-dependent manner using perchlorate as their sole electron acceptor (Figure 7). Indeed, recent studies have confirmed that the DPRB *Arcobacter* sp. CAB and the DCRB *Dechloromarinus chlorophilus* NSS use aerobic pathways under anaerobic conditions to couple (per)chlorate reduction to the degradation of such aromatic compounds as catechol, phenylacetate, and benzoate [41, 42]. Under these conditions, some of the biogenic O_2 is reused by the cell for the appropriate catabolic pathway (Figure 7). Remarkably, in some of these organisms, internal oxygen consumption is not a prerequisite for aromatic compound degradation coupled to (per)chlorate reduction, as demonstrated by the ability of *Sedimenticola selenatireducens* CUZ to utilize both anaerobic and aerobic catabolic pathways to degrade phenylacetate and benzoate during (per)chlorate respiration [41, 42]. The production of oxygen by

DPRB and DCRB makes these organisms excellent candidates for the bioremediation of a broad diversity of recalcitrant xenobiotic compounds under anoxic or oxygen-limiting conditions, both in situ and in bioreactors.

1.7 Genetic Optimization of DPRB and DCRB
The recent development of genetic systems for both DPRB and DCRB allows for the construction of (per)chlorate-reducing organisms with improved phenotypic characteristics [33-36, 98, 99]. Marker-less gene deletion strains can now be generated by antibiotic selection via suicide plasmid genomic integration, and subsequent plasmid excision via sucrose (*sacB*) or streptomycin (*rpsL*) counter-selection [33-36, 98, 99]. In addition, gene complementation and enzyme over-expression can be achieved with the pSC101 and pBBR1MCS series of broad range plasmids [33-36, 98, 99]. Furthermore, bar-coded transposon mutant libraries of the DPRB *Azospira suillum* PS and the DCRB *Pseudomonas stutzeri* PDA are available for rapid gene-fitness profiling under diverse conditions [36, 99]. These bar-coded transposon mutant libraries allow for rapid beneficial or detrimental gene identification under different growth conditions (e.g., high salinity, high temperature, high pressure, etc.). Equipped with these molecular tools, engineers have been able to manipulate DPRB and DCRB genomes according to their fitness profiles to achieve desired phenotypes with potential biotechnological application [36, 99]. As an example, reactive chlorine species such as chlorite and hypochlorite are produced as toxic intermediates during (per)chlorate respiration. Melnyk and co-workers were able to construct a strain of *A. suillum* that was resistant to reactive chlorine species by knocking out the anti-sigma factor *nrsF*, which is a repressor of the sigma factor *sigF* that activates the expression of hypochlorite scavenging methionine-rich peptide (mrpX) and methionine sulfoxide reductase (yedY1) [99]. The *nrsF* deletion strain showed an increased tolerance and enhanced growth rate with high concentration of chlorate, presumably due to heightened resistance to reactive chlorine species produced as part of the respiratory pathway [99].

1.8 Chlorite Mediated Bioreactor Hygiene Control
The biotechnology industry uses living organisms for the development or biotransformation of its products from raw materials. In 2015, this industry generated $107.7 billion of revenue in the United States (US) alone and has an estimated global market value of $890 billion (www.statista.com/topics/1634/biotechnology-industry). Bioprocessing and biotransformation with bioreactors frequently suffer from contamination with environmental microbes or bacterial phages [100-103]. Robust long-term operations often rely on costly antibiotic addition, which is economically infeasible for bio-commodity production. A proposed alternative is the use of chlorite and Cld as a biocide/biocide-resistance system for bioprocessing hygiene control. Chlorite is a low-cost biocide with activity against a broad range of microorganisms and viruses [23-29],

and chlorite dismutase provides specific resistance to chlorite. For example, under aerobic conditions, the DPRB *Azospira suillum* PS grew normally in the presence of 40 µM chlorite, while a *cld* gene deletion mutant failed to grow (Coates lab, unpublished observations). Additionally, heterologous expression of Cld in non-(per)chlorate reducing *Shewanella oneidensis* MR-1 protected the strain against chlorite toxicity (Coates lab, unpublished observations). In theory, it should be possible to construct a chlorite hyper-resistant industrial strain by the heterologous expression of Cld. However, one key difficulty is balancing the optimization of Cld activity with chlorite resistance. High Cld activity would lead to rapid chlorite removal, decreasing the selection against contaminant strains. Future studies could utilize directed evolution approaches to optimize and construct a Cld mutant that has low enzymatic activity, but can still confer resistance to the production strain.

1.9 Chlorite Mediated Aeration Enhancement

The physical properties of molecular oxygen, such as its low aqueous solubility (40 mg/L at 1 atm, 25 °C) and low mass transfer rate through the air-water interface, impose technical challenges in both laboratory enzymology experiments and industry scale bioprocessing [104-109]. Owing to the large oxygen demand in high cell density bioreactors, operators sometimes use expensive pure oxygen instead of air for aeration, along with an increased pressure and agitation rate to enhance the oxygen mass transfer [105]. Dassama and co-workers demonstrated that the addition of purified Cld and chlorite in aqueous solution resulted in a "burst" of oxygen generation of >5 mM in less than 1 ms [110]. This efficient enzymatic oxygen-generation system has been applied to increase the yield of unstable (half-life < 1–10 seconds) oxygenated intermediates [110], and to elucidate the biochemical mechanisms of oxygenases and oxidases [107, 110, 111]. The addition of purified Cld is implausible in industry-scale bioprocessing plants due to the large volume of industrial bioreactors and the high cost that is associated with Cld purification. However, the aeration problem could be solved by expressing Cld in the process organisms, which, in combination with chlorite addition, results in oxygen generation. Chlorite is extremely cheap (approximately $1 per kg), and only requires mild agitation as a result of its high solubility in water. Preliminary evidence of the potential for this approach was apparent in the demonstration of enhanced oxygenase-dependent benzene and naphthalene degradation under anaerobic conditions by the addition of chlorite and DPRB [95, 96]. Further studies are needed for the materialization and validation of this approach.

1.10 Gas Gangrene Treatment

A major medical problem in deep tissue wound therapy relates to the prevention and treatment of gas gangrene. At a basic level, gas gangrene can result from development of anaerobic conditions in deep wounds and infection by obligatory anaerobic *Clostridia*

species producing necrotizing tissue toxins. Gas gangrene is generally fatal if left untreated. Furthermore, many *Clostridia* species have developed resistances to a broad range of antibiotics, necessitating the application of alternative treatment technologies. These are often complex, expensive, and of limited success. Apart from amputation of the infected region, current treatments of gas gangrene involve cumbersome hypobaric chambers to increase oxygen levels in infected tissue or "maggot therapy", in which live maggots are sutured into the wound to graze on the necrotic tissue and *Clostridium* cells.

A novel alternative treatment was proposed that takes advantage of the activity of Cld purified from DPRB, which produces oxygen in copious quantities from aqueous solutions of chlorite, stored as a dry stable sodium salt under oxic or anoxic conditions. Studies have shown that the purified enzyme is stable and functions optimally at circumneutral pH and 35 °C [112]. From a very simplistic perspective, one can envision the mechanistic basis of such a treatment, whereby the oxygen produced and evolved as gaseous O_2 [95, 96] could inhibit the development and progression of the Clostridial gangrenous infection in deep wounds over the long term. Furthermore, chlorite itself has known biocidal activity against a broad range of microorganisms and viruses [23-29],, and as such would have an immediate antibiotic effect prior to the long term development of oxic conditions.

1.11 Conclusions

Exciting research in the field of microbial (per)chlorate reduction in the past 20 years has revealed the unique physiological and biochemical characteristics of microbial (per)chlorate reduction and its associated enzymatic and genetic mechanisms. This understanding provides many opportunities to leverage the novel capabilities of these organisms and apply this knowledge to solve outstanding problems in the environmental and biotechnological industries. Aside from perchlorate bioremediation, many of the other topics outlined here require commercial validation, while others are still at the preliminary proof-of-concept stage. Such early stage technologies offer excellent prospects for researchers and industrialists alike, who wish to contribute to the realization and translation of these concepts.

Figures
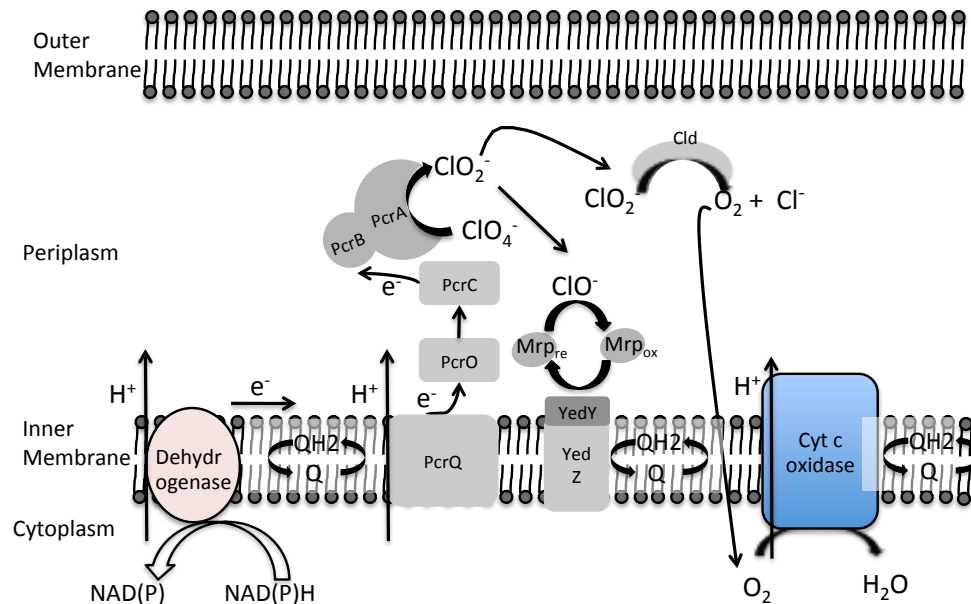
Figure 1-1. A schematic of the current model for the biochemical pathway of perchlorate reduction. As part of this pathway, hypochlorite (ClO⁻) is inadvertently produced at the chlorite dismutase. Perchlorate reducing bacteria have evolved a detoxification process based on a methionine rich peptide that chemically reacts with ClO⁻ to produce methionine sulfoxide, which is subsequently re-reduced by the methionine sulfoxide reductase (YedY) using reducing equivalents from the quinone oxidoreductase (YedZ). QH—quinone pool; Pcr—Perchlorate reductase; Cld—Chlorite dismutase; CytOx—Cytochrome oxidase; and, MRP—methionine rich peptide. For the biochemical pathway of chlorate reduction, PcrABC is replaced by chlorate reductase ClrABC, however, the process by which ClrABC receives electrons from the quinone pool is currently not well understood.
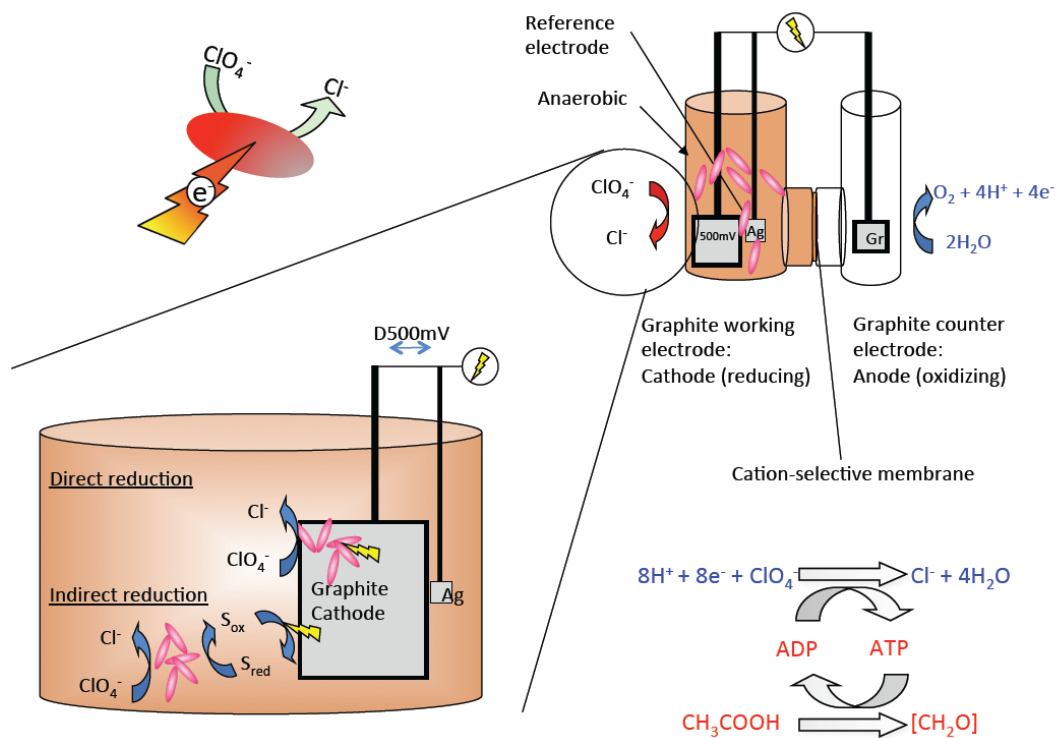
Figure 1-2. A schematic diagram of a packed-bed bioelectrical reactor for perchlorate bioremediation. DPRB use electrons provided through a negatively charged cathode as the direct of indirect (with electron shuttle) electron donor to reduce perchlorate to innocuous chloride. S ox – oxidized electron shuttle; S red – reduced electron shuttle

A bioassay for perchlorate

Monitor NADH concentration at 340 nm
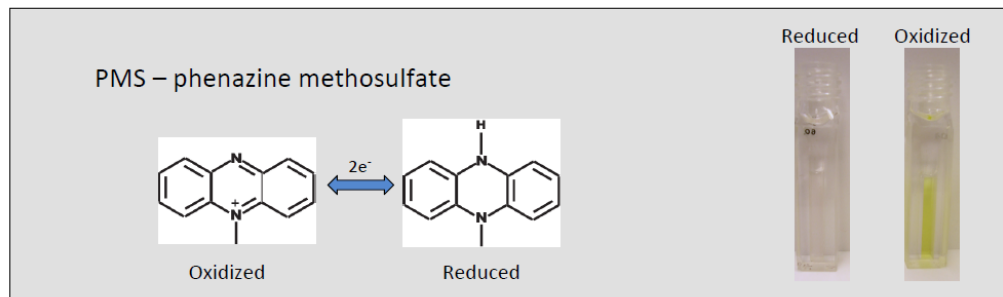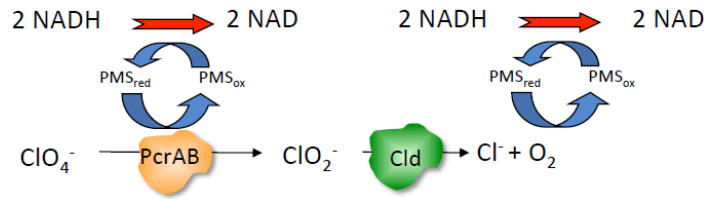
Figure 1-3. Schematic for the high throughput bioassay (with a perchlorate detection range of 2 – 17000 ppb) using perchlorate reductase (PcrAB), chlorite dismutase (Cld) nicotine adenine dinucleotide (NADH), and the electron shuttle phenazine methosulfate (PMS).
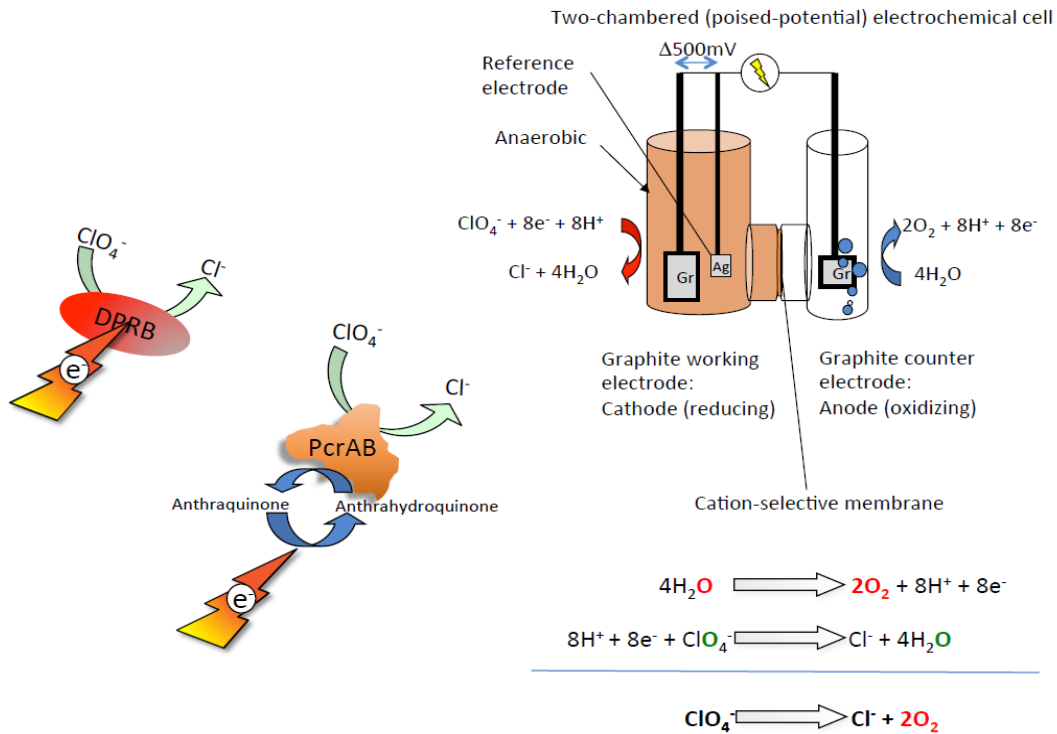
Figure 1-4. A schematic diagram of a bioelectrical reactor developed for bioelectrochemical oxygen production from perchlorate. Electrochemical consumption of perchlorate in the cathodic chamber mediated by active perchlorate reductase enzymes or lysed DPRB cells are coupled to electrolysis of water releasing pure O2 in the anodic chamber.

Two phases of inhibition

- ClO_4^- is selectively inhibitory to SRM
- Increased (more electropositive) redox potential

  — Direct

- Competitive thermodynamic inhibition
- Sulfate is removed, not recycled

  — Indirect

Organic Carbon

SRM

CO_2

SO_4^{2-}

HS^-

DPRB

S^o

ClO_4^-

Cl^-
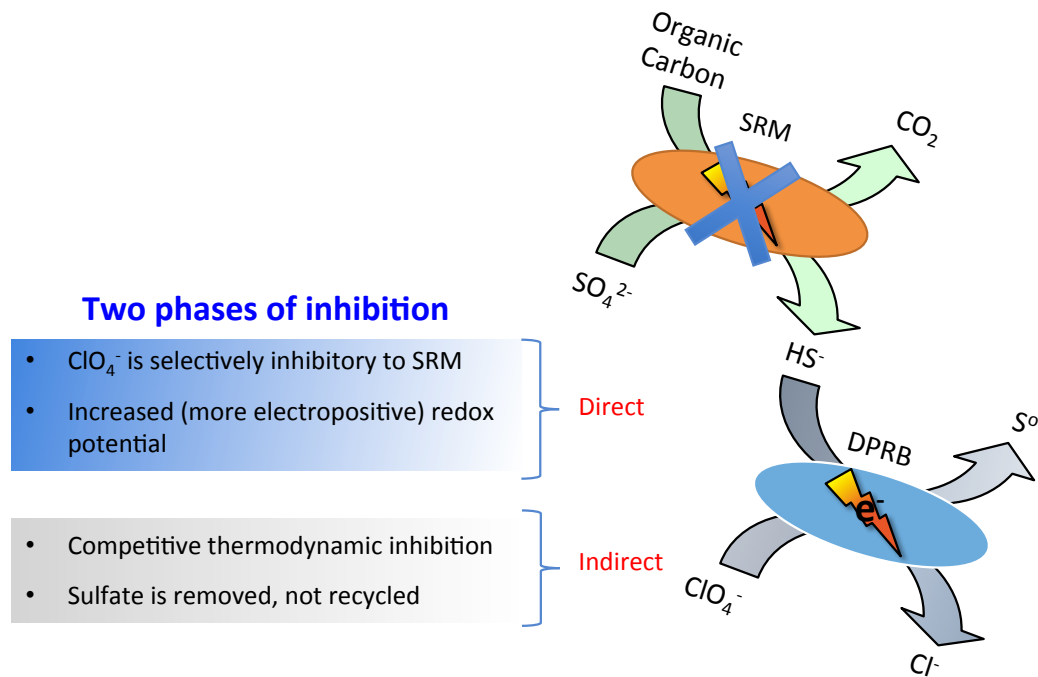
Figure 1-5. A model illustrating different modes of inhibition of sulfate reducing microorganisms (SRM) by perchlorate and dissimilatory perchlorate-reducing bacteria (DPRB).
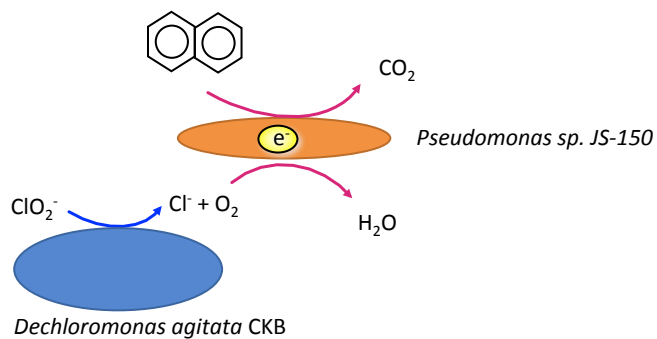
Figure 1-6. A model of oxygenase-dependent degradation for a xenobiotic degrading co-culture in the absence of O_2. Pre-requisite oxygen is supplied to the obligatory aerobic xenobiotic degrading organism by the dissimilatory perchlorate reducing bacterium (DPRB) as a result of the dismutation of added chlorite.
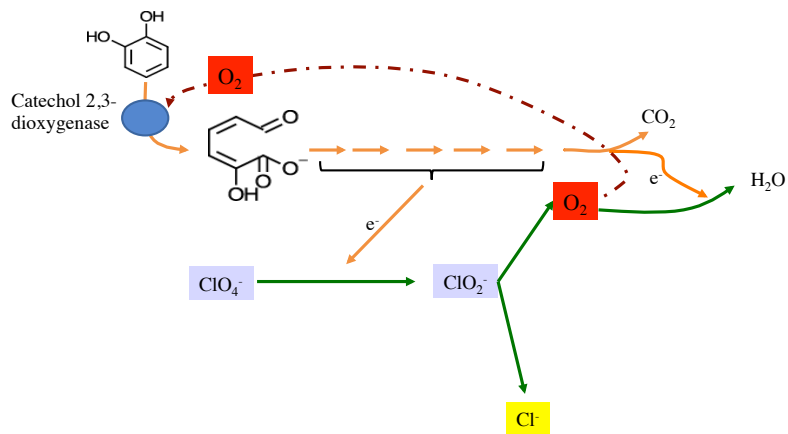
Figure 1-7. A simplified model illustrating the oxygenase-dependent, anaerobic catechol degradation pathway in the DPRB *Arcobacter* sp. CAB. Green, orange, and red arrows indicates perchlorate reduction pathway, catechol degradation pathway, flow of oxygen or electrons, respectively.

Chapter 2
Functional Redundancy in Perchlorate and Nitrate Electron Transport Chains and Rewiring Respiratory Pathways to Alter Terminal Electron Acceptor Preference

Abstract

Most dissimilatory perchlorate reducing bacteria (DPRB) are also capable of respiratory nitrate reduction, and preferentially utilize nitrate over perchlorate as a terminal electron acceptor. The similar domain architectures and phylogenetic relatedness of the nitrate and perchlorate respiratory complexes suggests a common evolutionary history and a potential for functionally redundant electron carriers. In this study, we identify key genetic redundancies in the electron transfer pathways from the quinone pool(s) to the terminal nitrate and perchlorate reductases in *Azospira suillum* PS (hereafter referred to as PS). We show that the quinol dehydrogenases, (PcrQ and NapC) and the soluble cytochrome electron carriers (PcrO and NapO) are functionally redundant under anaerobic growth conditions. We demonstrate that, when grown diauxically with both nitrate and perchlorate, the endogenous expression of NapC and NapO during the nitrate reduction phase was sufficient to completely erase any growth defect in the perchlorate reduction phase caused by deletion of *pcrQ* and/or *pcrO*. We leveraged our understanding of these genetic redundancies to make PS mutants with altered electron acceptor preferences. Deletion of the periplasmic nitrate reductase catalytic subunit, *napA*, led to preferential utilization of perchlorate even in the presence of equimolar nitrate, and deletion of the electron carrier proteins *napQ* and *napO*, resulted in concurrent reduction of nitrate and perchlorate. Our results demonstrate that nitrate and perchlorate respiratory pathways in PS share key functionally redundant electron transfer proteins and that mutagenesis of these proteins can be utilized as a strategy to alter the preferential usage of nitrate over perchlorate.

Introduction

Perchlorate (ClO_4^-) is deposited in the environment by both industrial activities and natural processes [1-6]. Due to the lack of regulations for perchlorate disposal before 1997 and the high water solubility, perchlorate contamination is widespread and has been detected in a diversity of drinking water supplies [1, 2]. Perchlorate-contaminated water poses a potential health risk as it accumulates in food sources, inhibiting the uptake of iodine by the thyroid gland [13]. This can disrupt thyroid hormone production leading to hypothyroidism, physical, and neuropsychological development anomalies [12, 13, 113, 114].

Most approaches to long-term robust perchlorate remediation rely on microbial bioattenuation either *in situ* or *ex situ* through the use of bioreactors. Despite its human toxicity, perchlorate can be used as a terminal electron acceptor by dissimilatory perchlorate-reducing microorganisms (DPRM) during anaerobic respiration [112, 115-117]. DPRM are phylogenetically diverse and can be isolated from many environments [112, 118]. All isolated Gram-negative DPRM are facultative anaerobes, and the majority are capable of alternatively using nitrate as an electron acceptor [42, 115, 118-120]. When both perchlorate and nitrate are present, pure or mixed culture DPRM either preferentially or concurrently reduce nitrate, even though perchlorate respiration is energetically more favorable ($E^{\circ\prime}$ = +797 mV for the reduction of ClO_4^- to Cl^-, $E^{\circ\prime}$ = +750 mV for the reduction of NO_3^- to N_2) [44, 115, 121]. This occurs regardless of whether the culture was previously grown on oxygen, nitrate, or perchlorate [115, 121]. The only known exception is *Sedimenticola selenatireducens* CUZ, in which, perchlorate is preferentially utilized if the inoculum is pre-grown on perchlorate [118]. Preferential utilization of nitrate by DPRM is non-intuitive and presents an obstacle to the facile bioremediation of perchlorate, as electron donor additions preferentially drive denitrification rather than perchlorate reduction in a bioreactor [122, 123]. In most contaminated environments, nitrate concentrations can dominate perchlorate concentrations by several orders of magnitude. As such, attenuating perchlorate to regulatory standards often necessitates that the majority (>90%) of the applied electron donor is used to consume the nitrate. Consequently, new strategies to influence this electron acceptor utilization preference could improve treatment efficiency especially in environments where nitrate concentrations dominate [116].

Previous comparative analysis of the genomes of DPRM identified a horizontally transferred perchlorate reduction genomic island (PRI) associated with perchlorate metabolism [124]. Genomic and genetic analysis of PS perchlorate reduction machinery identified a PRI containing 17 genes and defined which genes are essential for respiratory perchlorate reduction [98]. The genes *pcrABC* code for subunits of the perchlorate reductase complex [32, 98]. From biochemical and genomic evidence, it is

clear that reduced tetraheme *c*-type cytochrome PcrC donates electrons, via the iron-sulfur cluster protein PcrB, to the perchlorate reductase catalytic subunit PcrA, which reduces perchlorate to chlorite (ClO_2^-) as the initial step in the pathway [32, 84, 98, 116]. However, the precise electron transfer pathway from the quinone pool to PcrC has remained obscure. In the PRI, two proteins annotated as having redox active cofactors are likely candidates for electron carriers during perchlorate reduction. PcrO (*dsui_0143, pcrO),* a diheme *c*-type cytochrome, and PcrQ (*dsui_0143, pcrQ),* a tetraheme c-type cytochrome that likely functions as a quinol dehydrogenase [98]. Consistent with a role in electron transfer during perchlorate respiration, Δ*pcrQ* and Δ*pcrO* strains displayed slower growth kinetics with perchlorate as an electron acceptor, however, remarkably, neither gene was essential for perchlorate reduction [98]. This observation led to the central hypothesis and motivation for this study that functionally redundant electron transport proteins, likely from the nitrate respiratory pathway, are capable of complementing for the function of *pcrQ* and *pcrO* (Figrue. 2-1).

Materials and Methods

Bacterial strain cultivation and characterization

Wild type *Azospira suillum* PS [125] (Isolated by the Coates lab, ATCC^R BAA-33, hereafter referred to as wtPS) and mutant strains were revived from freezer stocks by streaking out for single colonies on ALP medium agar plates [98]. One liter of ALP medium is composed of 0.49 g monobasic sodium phosphate dihydrate, 0.97 g dibasic anhydrous sodium phosphate, 0.1 g potassium chloride, 0.25 g ammonium chloride, 0.82 g sodium acetate, 2.0 g yeast extract, 7.6 g of a 60% (wt/wt) sodium lactate solution, 1.10 g sodium pyruvate, and 10 ml of both vitamin mix and mineral mix as previously described [126]. To make solid ALP medium for plates, 15 g/liter agar was added. For aerobic cultivation, single colonies from plates were picked into LMM medium and cultivated at 37°C with vigorous shaking (250 rpm). LMM minimal medium is composed of the same ingredients as ALP, but omitting acetate, pyruvate, and yeast extract). For anaerobic cultivation, liquid overnight aerobic cultures were used to inoculate anoxic LMM medium amended with 5mM each of sodium nitrate and sodium perchlorate. Media were made anoxic by flushing with oxygen-free N_2, and sealed with butyl rubber stoppers prior to autoclaving. Anaerobic cultures were cultivated in anaerobic tubes (Bellco) with a nitrogen headspace at 37°C without shaking.

All phenotypic analyses to compare strains were carried out in microplate cultures. For microplate growth experiments, 2.5µl of overnight stationary phase PS culture was used to inoculate 250µl of LMM medium supplemented with nitrate (5mM), perchlorate (2.5mM), or both nitrate and perchlorate (5mM each). After inoculation, 80 µl of mineral oil was added to each sample to prevent evaporation. The concentration of perchlorate under the perchlorate-only condition was lowered to avoid unpredictably long lag periods seen with high perchlorate concentrations (unpublished data), possibly due to enzymatic substrate inhibition observed previously for the PcrAB [32]. Strain characterization experiments were conducted in flat-bottom 96-well plates (Corning Costar, Tewksbury, MA) in an anaerobic chamber filled with 98% N_2 and 2% H_2 (Coy Labs, Grass Lake, MI). Note PS cannot use hydrogen as an electron donor for energy metabolism [125] and does not contain any known hydrogenase. The optical density at 600 nm was measured with a spectrophotometer (Tecan Sunrise, Männedorf, Switzerland) at 37°C without shaking. All growth data were plotted and calculated with the Prism 7 software.

To test the preferential utilization of nitrate and perchlorate, 0.5mL of overnight aerobic grown cells were transferred to anaerobic tubes containing 10mL LMM medium with 5 mM each of sodium perchlorate and sodium nitrate. Cell growth was measured spectrophotometrically at 600 nm. All experimental analyses were performed in three biological replicates.

23

Strain construction

In-frame gene deletions and complementation experiments in PS were conducted as previously described [98]. Briefly, the suicide vector pNPTS138 (Dickon Alley via Kathleen Ryan, UC, Berkeley) with a gene deletion cassette was transformed into PS by electroporation using a method previously described for *Zymomonas mobilis* [127]. Transformed PS cells were plated on ALP agar plates with 50 μg kanamycin/mL medium (ALP-KAN) to select for integration of the suicide vector into the chromosome. Resulting PS colonies were picked into ALP liquid medium, cultivated overnight, and plated on ALP-KAN and ALP-sucrose (6%) agar plates to select for colonies that were sensitive to kanamycin and resistant to sucrose. Colony PCR was used to screen for crossover mutants containing the gene deletion. The pBBR1MCS2 plasmid was used as the complementation vector to express *pcrQ, pcrO, napC, napO in trans* [128]. The PCR-amplified *pcrQ, pcrO, napC, napO* genes with their native ribosomal binding sites (defined as 20 nucleotides upstream of the start codon) were cloned downstream of the *nap* or *pcr* native promoters to generate complementation vectors. A 20 to 500 nucleotides region upstream of the first gene of the operon was treated as the native promoter [98]. Complementation vectors were transformed into PS by electroporation as previously described [98]. Strains, plasmids, and primers used for this study are listed in Tables 2-1, 2-2 and 2-3 respectively.

Analytical procedures

Perchlorate and nitrate concentrations were measured via ion chromatography using a ICS 1500 (Dionex) equipped with an Ion Pac AS25 column (4 × 250 mm, Thermo Scientific) with a mobile phase of 36 mM NaOH at a flow rate of 1.0 mL/min. Analyses were detected by conductivity suppressed with an ASRS 300 (4 mm, Dionex) in recycle mode. The suppressor controller was set at 90 mA for analysis. The injection volume was 10 μL. Cultures were sampled anaerobically using sterile 1ml syringes, filtered with 0.2 μm syringe filters and diluted in deionized water.

Results and Discussion

Addition of both nitrate and perchlorate rescues single deletion mutants in either quinol dehydrogenases (*ΔpcrQ*, *ΔnapC*) or electron transfer cytochromes (*ΔpcrO*, *ΔnapO*)

The *pcrQ* and *pcrO* genes are highly conserved among phylogenetically diverse DPRB, suggesting that, as in PS, they are important for perchlorate metabolism. However, the observation that *pcrQ* and *pcrO* are not absolutely essential for perchlorate reduction in PS suggests than their role can be partially complemented by other functionally redundant proteins in the PS genome [124, 129]. PS can also effectively utilize nitrate as an alternative terminal electron acceptor wherein the nitrate is reduced to nitrogen gas. BLAST-P searches with protein sequences against the PS genome (taxid:640081) identified two proteins (NapC and NapO) from the periplasmic nitrate reductase *nap* operon that are homologous to PcrQ and PcrO. PcrQ is 79% identical to the PS NapC homolog (locus tag: Dsui_1176) [130]. Both PcrQ and NapC are tetraheme *c*-type cytochromes belonging to the NapC/NirT family [130], and NapC is known to function as a quinol dehydrogenase that mediates electron transfer between quinone pool and soluble periplasmic nitrate reductase [130-132]. PcrO is 55% identical to NapO (Dsui_1177), and like PcrO, NapO is also a diheme *c*-type cytochrome. Both NapO and PcrO are homologous to the structurally characterized gamma subunit in the ethylbenzene dehydrogenase complex from *Aromatoleum aromaticum* [133]. Of note, to our knowledge, no previous studies have identified NapO as a part of a denitrification metabolism [132, 134-138].

It was previously observed that under nitrate reducing conditions, *pcrQ* and *pcrO* single deletion mutants (*ΔpcrQ*, *ΔpcrO*) had no growth defect and were in fact similar to wtPS [98]. When grown with perchlorate, *ΔpcrQ* and *ΔpcrO* mutants displayed slightly slower growth kinetics but reach the same final optical density as wtPS [98]. When grown diauxically with both nitrate and perchlorate, *ΔpcrQ* and *ΔpcrO* displayed no growth defect compared with wtPS [98]. These results suggested that other genes in the PS genome are functionally redundant with *pcrQ* and *pcrO*. We hypothesized that rescue of *ΔpcrQ* and *ΔpcrO* growth defects in diauxic growth conditions is due to functional redundancy with *napC* and *napO* from the nitrate reduction pathway, which is induced by the presence of nitrate. Similarly, *napC* and *napO* would also not be essential for nitrate reduction because by corollary their electron transfer role should be rescued by *pcrQ* and *pcrO*. To demonstrate functional redundancies between the quinol dehydrogenases and the electron transfer cytochromes, *napC* and *napO* deletion mutants were constructed (*ΔnapC, ΔnapO*) and the growth phenotypes under nitrate, perchlorate, and diauxic growth conditions were tested. *ΔnapC* and *ΔnapO* mutants failed to grow when nitrate was the sole electron acceptor (Figure 2-2a). Under

perchlorate growth conditions, both the *ΔnapC* and *ΔnapO* showed no growth defect compared to wtPS (Figure 2-2b). Interestingly, *ΔpcrQ* and *ΔpcrO* showed a more severe growth defect compared to the previous study [98], likely due to the LMM minimal medium used in this study lacks yeast extract, which could contain trace amount of nitrate to partially induce the expression of nitrate reduction pathway. However, under diauxic growth conditions, all mutants reached the same final optical density as wtPS (Figure 2-2c). *ΔnapC* and *ΔnapO* grew with an increased lag phase, and slightly slower growth rate comparing to wtPS over both phases of the diauxic growth assay (Figure 2-2d, Table 2-4). *ΔpcrQ* and *ΔpcrO* displayed no growth defect compared to wtPS, consistent with previous study [98]. Taken together, these results support the hypothesis that the homologous quinol dehydrogenases (PcrQ and NapC) and soluble periplasmic electron transfer proteins (PcrO and NapO) are functionally redundant, and independently capable of rescuing growth defects due to the absence of their homologues counterparts. A summary of the growth rates of these strains can be found in Table 2-4.

ΔnapC and ΔnapO growth over both phases of diauxic growth curves is not due to nitrate reduction by PcrABC

Biochemical results show that the perchlorate reductase enzyme complex, PcrABC, can reduce several substrates other than perchlorate, including nitrate [32, 69, 139]. Thus, one explanation for the rescue of the *ΔnapC* and *ΔnapO* growth defects under the diauxic growth condition is that expression of the *pcr* genes leads to production of a fully functional perchlorate and nitrate reductase that facilitates respiratory nitrate and perchlorate reduction. To address this possibility, we deleted *pcrA* in *ΔnapC* and *ΔnapO* single mutants to construct *ΔnapCΔpcrA and ΔnapOΔpcrA* double mutants. With nitrate as the sole electron acceptor, *ΔnapCΔpcrA* and *ΔnapOΔpcrA* strains displayed the identical growth defect as *ΔnapC* and *ΔnapO* (Figure 2-2a, d). As expected, *ΔnapCΔpcrA, ΔnapOΔpcrA, and ΔpcrA* were not viable when perchlorate was the sole electron acceptor. When grown diauxically with both nitrate and perchlorate, all strains with *pcrA* deletion are incapable of growing over the second perchlorate growth phase (Figure 2-2e). *ΔnapCΔpcrA* grew over the nitrate phase of the diauxic growth curve with a similar rate to wtPS and *ΔpcrA*, while *ΔnapOΔpcrA* grew with a prolonged lag phase and a slightly slower growth rate (Table 2-4). Both double mutants *ΔnapCΔpcrA* and *ΔnapOΔpcrA* reached the same final optical density as *ΔpcrA* in the diauxic growth condition (Figure 2-2e). These results confirm that *ΔnapC* and *ΔnapO* electron transfer functions to the nitrate reductase complex are rescued by perchlorate induced electron carriers and that their phenotypes are not due to nitrate reduction by PcrABC.

There are two *nap* operons in PS, *napDAGHB* and *napCOF*, which are located in different regions in the genome. Based on previous work with *Escherichia coli* K-12, NapG and NapH form an alternate non-essential quinol dehydrogenase that transfer electrons to NapAB, via NapC [132]. While deletion of *napGH* in *E.coli* resulted in a mild growth defect [132], deletion of *napGH* in PS did not result in any significant growth defect under all conditions tested (Figure 2-3). This indicates that under the tested conditions NapGH is not donating electrons to either PcrQ or NapC. Further investigations are needed to define the exact function of NapGH in PS.

Functional redundancy of *napC /pcrQ* and, *napO /pcrO*

While NapC is homologous with PcrQ and NapO is homologous with PcrO, and our results clearly show cross-complementation of mutant growth defects by some component of the nitrate or perchlorate regulon, we sought to conclusively demonstrate the functional redundancy of the homologs PcrQ/NapC and PcrO/NapO. We constructed *ΔpcrQΔnapC* and *ΔpcrOΔnapO* and confirmed that, while capable of aerobic growth, these strains were incapable of anaerobic growth in any of nitrate, perchlorate or diauxic growth conditions (Figure 2-4a, b, Table 2-5).

To further confirm the functional redundancy between *napC* and *pcrQ*, and between *napO* and *pcrO*, we attempted to complement the double deletion mutants *ΔpcrQΔnapC* and *ΔpcrOΔnapO* by introducing *pcrQ*, *napC* and *pcrO*, *napO in trans*, under either the *pcr* or *nap* promoter. *ΔpcrQΔnapC* and *ΔpcrOΔnapO* harboring different complementation plasmids were subjected to growth experiments under nitrate and perchlorate diauxic growth conditions (Figure 2-4c, d). Consistent with a functional redundancy, *ΔpcrQΔnapC* on nitrate or perchlorate was complemented by either *pcrQ* or *napC*, and *ΔpcrOΔnapO* was complemented by either *pcrO* or *napO* (Figure 2-4c, d). The complementation was achieved under either the *pcr* or *nap* promoter. All complemented strains reached the same optical density as wtPS but displayed defective growth kinetics, which was likely due to the disruption of NapC, NapO, PcrQ, or PcrO protein expression level by increased gene copy number *in trans* and/or regulatory issues associated with the use of native *nap* or *pcr* promoters. Taken together, these results show that the components of the electron transport conduits from the quinone pool to NapAB or PcrABC, are functionally redundant. No other electron transfer protein expressed in PS under our growth conditions could function as quinol dehydrogenase or intermediate electron carrier to the nitrate or perchlorate reductase complexes.

Four redundant electron transfer routes are functional from the quinone pool to either terminal reductases - PcrABC or NapAB

Based on our results, there are four viable electron transfer routes from the quinone pool to PcrABC and NapAB as exemplified in Figure 2-5. To show that all four routes are functional and can sustain growth, we constructed four double deletion mutants, *napC/napO*, *napC/pcrO*, *pcrQ/napO*, and *pcrQ/pcrO* (*ΔnapCΔnapO*, *ΔnapCΔpcrO*, *ΔpcrQΔnapO*, and *ΔpcrQΔpcrO*). These combinatorial double mutants in either the perchlorate or nitrate reduction pathways abolished all electron bifurcations and result in a single electron transfer route from the quinone pool to either PcrABC or NapAB (Figure 2-5). The growth phenotypes of these mutants were determined under nitrate and perchlorate diauxic conditions. The purpose of the diauxic condition was to ensure that the induction of both denitrification and perchlorate reduction pathways. Under the conditions tested, all four mutant strains were viable and able to grow to the same optical density as wtPS (Figure 2-6a). These results suggested that all four electron transfer routes are capable to transfer electrons to PcrABC.

To conclusively demonstrate *ΔnapCΔnapO*, *ΔnapCΔpcrO*, *ΔpcrQΔnapO*, and *ΔpcrQΔpcrO* can also transfer electrons to NapAB, four PS triple deletion mutants that contain *pcrA* deletion in the background of *napCnapO*, *napCΔpcrO*, *pcrQΔnapO*, and *pcrQpcrO* (*ΔpcrAΔnapCΔnapO*, *ΔpcrΔnapCΔpcrO*, *ΔpcrAΔpcrQΔnapO*, and *ΔpcrAΔpcrQΔpcrO*) were constructed and assayed for growth under nitrate and perchlorate diauxic conditions, with *ΔpcrA* and wtPS as controls. The resulting growth phenotypes are shown in Fig. 4b. All mutant strains reached a final optical density that was similar to *ΔpcrA*. A summary of the growth rates of these strains can be found in Table 2-6. Of note, in mutants that harbor only one electron transfer route to PcrABC or NapAB, disruption of *nap* gene(s) always resulted in defective growth kinetics, indicating while NapC and NapO can fully replace the role of PcrQ and PcrO, PcrQ and PcrO can only partially rescue a growth defect as a result of lacking NapC and NapO.

The concluding redundancies that exist in these pathways are summarized in Figure 2-1. While PcrC from the perchlorate respiratory chain seems to lack a functional homolog in the nitrate respiratory chain, the same is also true for PcrB. Neither PcrC (tetraheme *c*-type cytochrome) nor PcrB (iron-sulfur cluster protein) are similar to NapB (diheme *c*-type cytochrome). However, PcrABC and NapAB could be considered as functional homologs as they both carries out the final step in terminal electron acceptor reduction.

Although extensive, such electron transfer branching and redundancy has been observed in other microorganisms. In *Shewanella oneidensis,* the Mtr metal respiratory

system is highly modular and redundant, and multiple electron transfer routes exist to reduce several terminal electron acceptors, such as DMSO, iron oxide, and ferric citrate [140]. A later study showed that *S. oneidensis* produces several interconnected functional electron transfer chains simultaneously [141]. It has been proposed that the modular electron transfer machinery enables the organism to quickly adapt to a variety of environmental electron acceptors, as well as offers a fitness benefit in redox-stratified environments [141]. Also, the redundancies in these electron transfer chains have implications for the past and future co-evolution of these respiratory metabolisms.

Rewiring PS to Alter the Nitrate/Perchlorate Preferential Usage

The efficiency of perchlorate bioattenuation is often significantly impacted by the preferential use of nitrate by perchlorate reducing microorganisms [115]. The rational construction of a perchlorate reducing strain that can preferentially reduce perchlorate or co-reduce both nitrate and perchlorate could significantly reduce operational costs and lead to more efficient remediation practices [115]. We sought to leverage our understanding of electron flow in PS to alter the preferential usage of anaerobic electron acceptors. In a *napA* deletion strain (*ΔnapA*), both nitrate and perchlorate reductions depend on the *in vivo* activity of perchlorate reductase PcrABC. Previous biochemical studies have demonstrated that a that PcrABC has a lower Km for perchlorate than for nitrate [32]. Consistent with this reasoning, during anaerobic growth with equimolar nitrate and perchlorate, *ΔnapA* PS strains preferentially reduced perchlorate over nitrate (Figure 2-7a, b). Interestingly, a 60-hour lag phase was observed in *ΔnapA*, which is similar to the 20-40 hours lag phase observed in wtPS when perchlorate was the sole acceptor (Figure 2-2b, Figure 2-4). Despite the fact that under nitrate and perchlorate diauxic growth conditions wtPS always preferentially uses nitrate, the presence of nitrate actually enhances the onset of perchlorate reduction (see wtPS growth in Figure 2-2b, c, Figure 2-4a, Figure 2-7a) [98, 121]. Presumably, this nitrate-dependent enhancement of perchlorate reduction is relying on the nitrate reduction pathway, which is interrupted in *ΔnapA* (unlike *ΔnapC* and *ΔnapO*, expression of *pcr* proteins will not initiate nitrate reduction in *ΔnapA* until depletion of perchlorate). In addition, the futile expression of a non-functional nitrate reduction complex in the absence of NapA, and the increased perchlorate concentration could also contribute to the prolonged lag phase. The rise of a suppressor mutant is implausible as the three biological replicates entered the log phase at a similar time, plus *ΔnapA* would be expected to grow under nitrate and perchlorate diauxic conditions even in the absence of any additional mutation.

Another approach to altering electron acceptor preference is to maintain NapA expression, but disrupt expression of electron carriers to NapAB, namely NapC and

NapO. In the double deletion mutant *ΔnapCΔnapO*, nitrate reduction depends solely on the expression PcrQ and PcrO, which functionally replace NapC and NapO in the electron transport pathway. Thus, under diauxic growth conditions, reconstitution of functional nitrate reductase respiratory complexes comprised of NapAB-PcrQO and nitrate reduction will only occur upon expression and reconstitution of functional perchlorate reductase complexes comprised of PcrABCOQ. Consistent with this model, *ΔnapCΔnapO* reduced both nitrate and perchlorate concomitantly (Figure. 2-7c). It is important to note, that in this case, we do not know the extent to which nitrate may be co-reduced by PcrABCOQ in *ΔnapCΔnapO* strains, but in *ΔnapA* nitrate was only reduced by PcrABC after complete removal of perchlorate, suggesting that reduction of nitrate reduction by NapA is likely a major pathway (Figure 2-7b, c).

Important outstanding questions related to regulation of nitrate and perchlorate reduction

While we have successfully identified redundant electron carriers in the nitrate and perchlorate respiratory chains in this work, independent regulation of nitrate and perchlorate respiratory pathways plays an important role in controlling environmental electron acceptor preferential usage. As such, dissecting regulatory mechanisms remains an important goal for future studies. In nitrate reducing Alpha- and Gamma-proteobacteria, nitrate metabolism is globally regulated by the Crp/Fnr family of transcriptional regulators that sense redox changes [142-145], as well as the NarXL and NarQP two component systems that sense environmental activators, such as nitrate and nitrite [142, 146]. However, there is little known about the nitrate regulatory circuit in Betaproteobacteria (e.g. PS). The nitrate/nitrite sensors NarXL and NarQP are absent in PS. Multiple Crp/Fnr transcriptional regulators are present in PS, but there is difficulty in predicting which transcriptional regulator is involved in nitrate metabolism regulation.

The perchlorate metabolism regulatory circuit is also not well characterized in PS. The PAS domain containing the protein PcrP, histidine kinase sensor PcrS, and response regulator PcrR comprise the putative transcriptional regulatory system that senses internal and/or external signals [98]. Based on homology to other systems, PcrS is likely regulated by PcrP to influence the phosphorylation state of PcrR which in turn interacts with RpoN to induce transcription of the *pcr* operon [98], However, the regulatory signal(s) that influence *pcr* operon induction via PcrPSR transcriptional regulatory system are still unknown.

Conclusion

Nitrate often co-occurs in perchlorate-contaminated environments. As such, nitrate inhibition of perchlorate metabolism presents an obstacle in the bioattenuation of perchlorate in these environments, as electron donor amendment will stimulate unproductive nitrate reduction rather than perchlorate reduction. This study improves our understanding of nitrate and perchlorate respiratory pathways in dissimilatory perchlorate reducing bacteria (DPRB) and identifies key functionally redundant electron carrier proteins in these pathways. These redundancies are important to consider for the past and future co-evolution of perchlorate and nitrate respiratory pathways as well as other oxyanion respiratory pathways by related enzymes. We leverage the redundancy in PS to construct mutant strains with altered electron acceptor preference. While thorough knowledge of the regulatory signals that influence the expression of nitrate and perchlorate respiratory pathways remains important, this study demonstrates that nitrate/perchlorate electron acceptor preference can be altered by "rewiring" the electron transport chains without mutation of regulatory pathways.
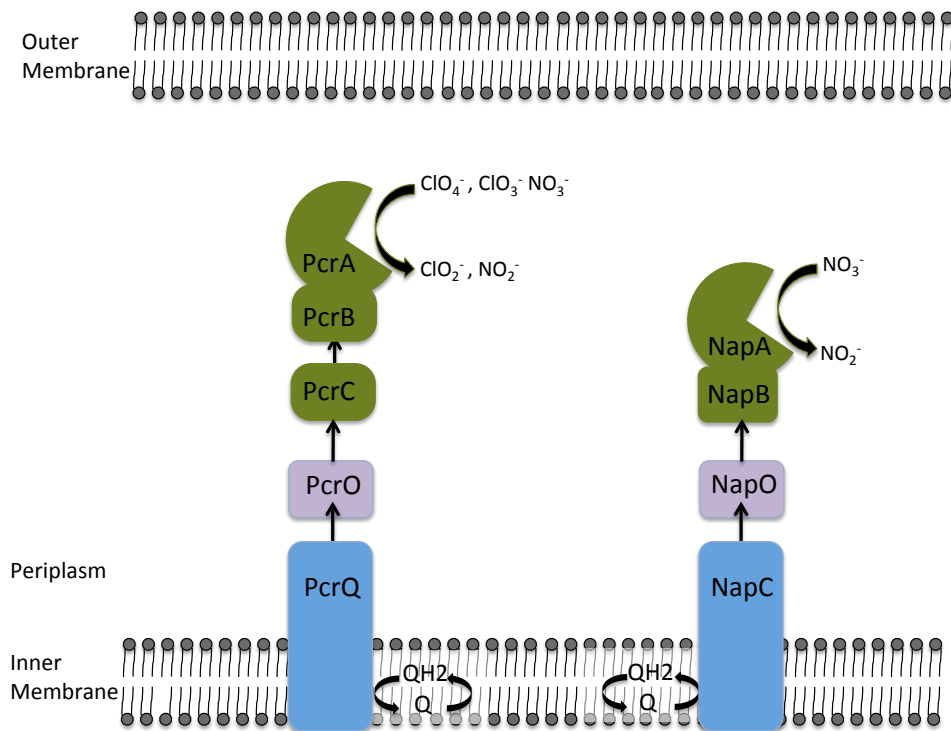
Figure 2-1. A model displaying proposed electron transfer networks between the quinone pool and PcrABC/NapAB respiratory complexes in *Azospira suillum* PS. Arrows indicate the canonical electron transfer pathways. The nitrate and perchlorate reductase complexes are painted green. Redundant electron transfer proteins are painted with the same color.
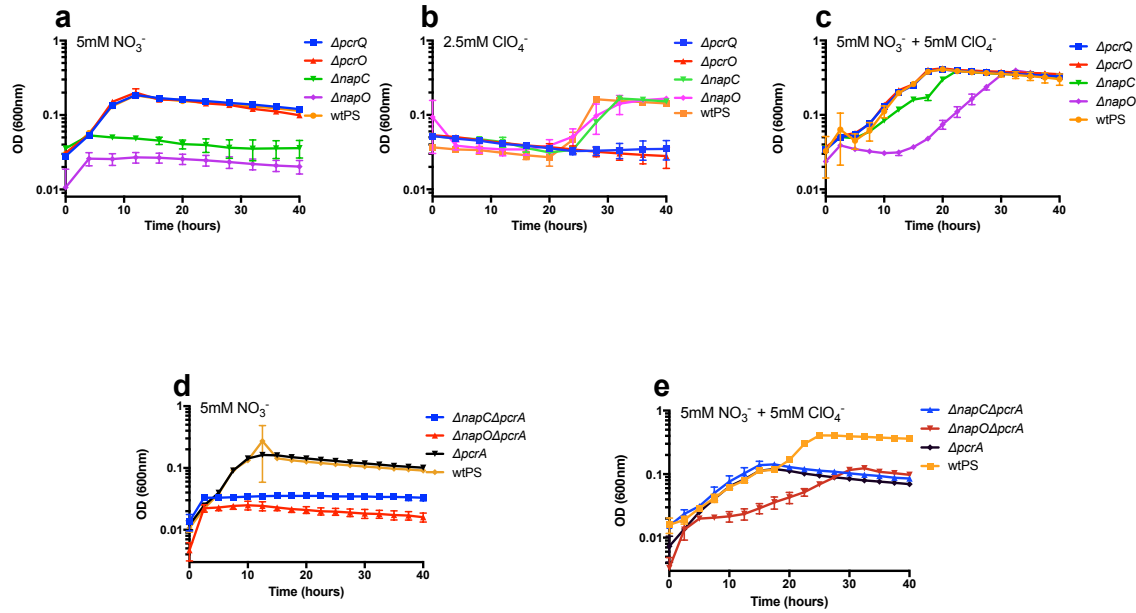
Figure 2-2. Growth of wtPS, *ΔpcrQ*, *ΔnapC*, *ΔpcrO* and *ΔnapO* in LMM medium containing nitrate (a), perchlorate (b), both nitrate and perchlorate (c). Growth of wtPS, *ΔpcrA*, *ΔnapCΔpcrA*, and *ΔpcrOΔpcrA* in LMM medium containing nitrate(d) and both nitrate and perchlorate (e). Error bars represent standard deviations of biological triplicate samples.
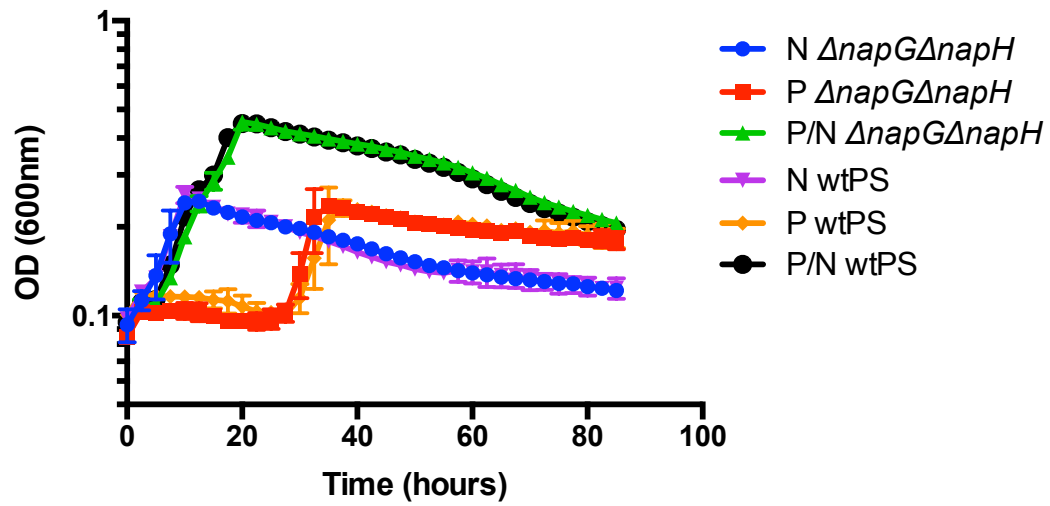
Fig 2-3. Growth of *ΔnapGΔnapH* on LMM medium containing nitrate (N), perchlorate (P), both nitrate and perchlorate (PN).
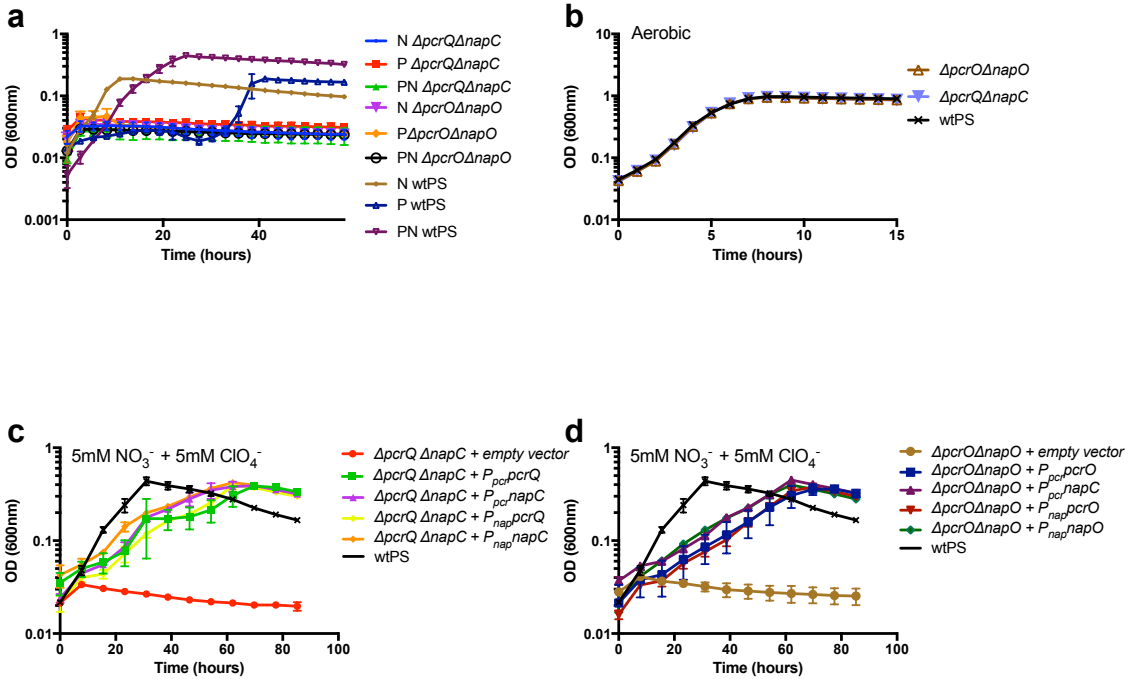
Figure 2-4. Growth of *ΔpcrQΔnapC* and *ΔpcrOΔnapO*. (a) Growth phenotype of wtPS, *ΔpcrQΔnapC* and *ΔpcrOΔnapO* on LMM medium containing nitrate (N), perchlorate (P), both nitrate and perchlorate (PN), and (b) aerobic were tested. (c,d) Growth of *ΔpcrQΔnapC* with complementation vectors expressing *pcrQ or napC*, and *ΔpcrOΔnapO* with complementation vectors expressing *pcrO or napO*, respectively on LMM medium with nitrate and perchlorate. Complementation tests were conducted with either *pcr* or *nap* promoter (P_{pcr} and P_{nap}). Error bars represent standard deviations of biological triplicate samples.

Four alternatives for electron transfer to PcrA
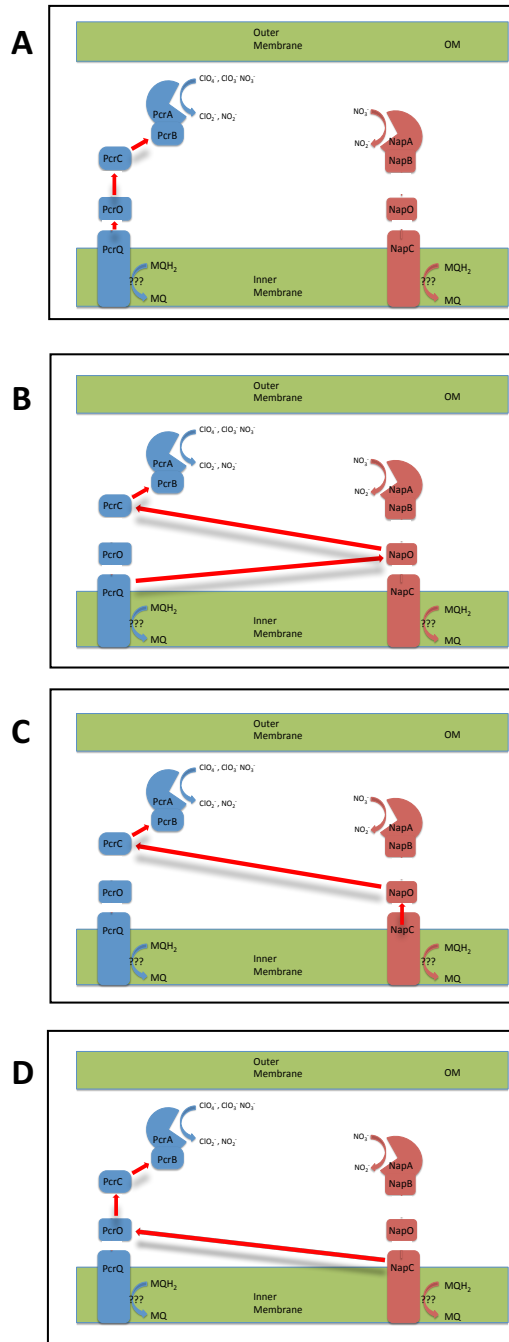
Figure 2-5. A model illustrating four possible electron transfer routes to from quinone pool to PcrABC respiratory complexes in *Azospira suillum* PS. Arrows indicate electron transfer pathways.

a

5mM NO$_3^-$ + 5mM ClO$_4^-$

OD (600nm)

Time (hours)

- $\Delta napC\Delta napO$
- $\Delta napC\Delta pcrO$
- $\Delta pcrQ\Delta napO$
- $\Delta pcrQ\Delta pcrO$
- wtPS

b

5mM NO$_3^-$ + 5mM ClO$_4^-$

OD (600nm)

Time (hours)

- $\Delta napC\Delta napO\Delta pcrA$
- $\Delta napC\Delta pcrO\Delta pcrA$
- $\Delta pcrQ\Delta napO\Delta pcrA$
- $\Delta pcrQ\Delta pcrO\Delta pcrA$
- $\Delta pcrA$
- wtPS
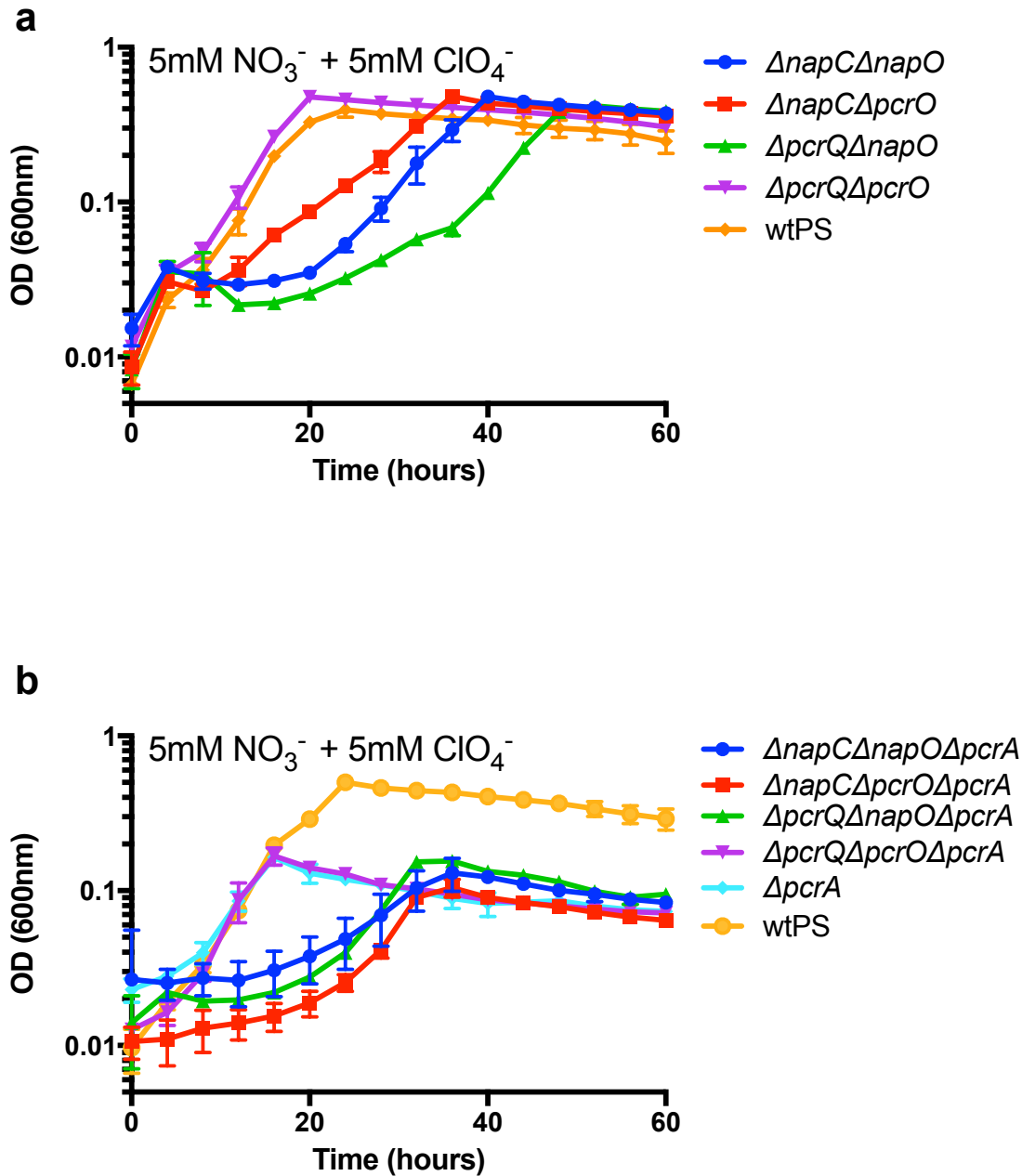
Figure 2-6. Growth of wtPS, $\Delta napC\Delta napO$, $\Delta napC\Delta pcrO$, $\Delta pcrQ\Delta napO$, and $\Delta pcrQ\Delta pcrO$ (a), and $\Delta pcrA$, $\Delta pcrA\Delta napC\Delta napO$, $\Delta pcrA\Delta napC\Delta pcrO$, $\Delta pcrA\Delta pcrQ\Delta napO$, and $\Delta pcrA\Delta pcrQ\Delta pcrO$ (b) on LMM medium with 5mM nitrate and 5mM perchlorate. Error bars represent standard deviations of biological triplicate samples.

37

a 5mM NO$_3^-$ + 5mM ClO$_4^-$, wtPS

b 5mM NO$_3^-$ + 5mM ClO$_4^-$, $\Delta napA$

c 5mM NO$_3^-$ + 5mM ClO$_4^-$, $\Delta napC\Delta napO$

Figure 2-7. Growth and concentration of nitrate or perchlorate in cultures of wtPS (a), *ΔnapA* (b), and *ΔnapCΔnapO*(c), in LMM medium with 5mM nitrate and 5mM perchlorate. Error bars represent standard deviations of biological triplicate samples.

Table 2-1. Primers used in this study; the names of all primers and sequences used in this study are listed here; a brief description of the primer is also supplied.

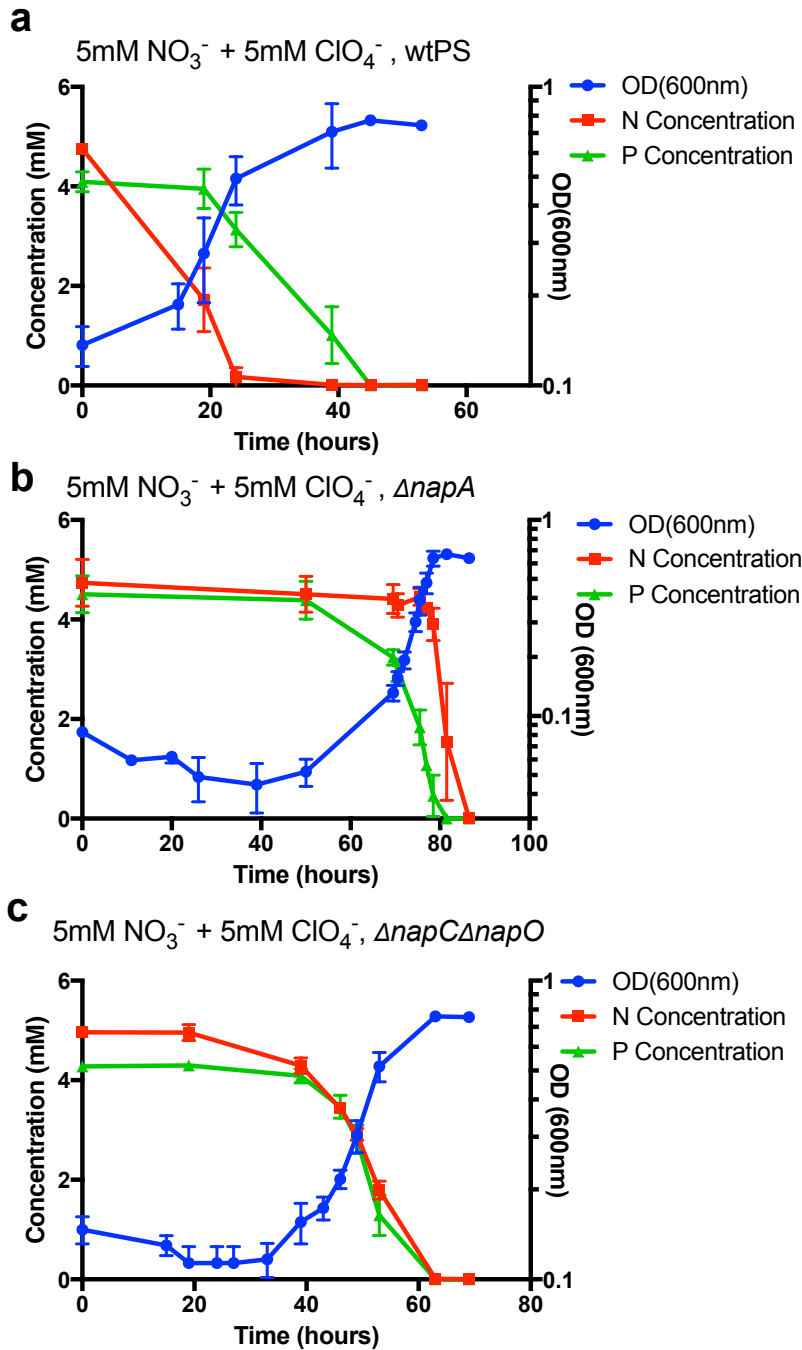| Primer ID	Primer Sequence or Reference	Brief Description of Primer
napA a	GNNGAATTCCTGTAGGCATGCCAGGAGAC	deletion of napA
napA b	GNNACTAGTCTTGATAAAGTCGCGACGGGT	deletion of napA
napA c	GNNACTAGTCTGGTCTTCGTGCCCTTCTTC	deletion of napA
napA d	GNNGGATCCGGGAATGAACATGCTGTGGC	deletion of napA
napC a	GNNGAATTCCTGGGCTACACCCTGCTG	deletion of napC
napC b	GNNACTAGTCTTCTTGAGGGTGGCCCAAAG	deletion of napC
napC c	GNNACTAGTCACAAACCCCAGAACATGCC	deletion of napC
napC d	GNNGGATCCGTGAATGGCGAAGCCGAAG	deletion of napC
napo a	GNNGAATTCTTCCAGTGTTTAGGCAGCGT	deletion of napO
napo b	GNNACTAGTGATGGCGGTTTGCTTGAAC	deletion of napO
napo c	GNNACTAGTCACCACGTTTCCTTCGGCTA	deletion of napO
napo d	GNNGGATCCCCGGCTGCTGTATGAGGAAA	deletion of napO
napGH a	GNNGAATTCCAGCAGGTCAAGCCCCAG	deletion of napG and napH
napGH b	GNNACTAGTAGGGGAGTTGGAAAGATCGC	deletion of napG and napH
napGH c	GNNACTAGTCAGACAGACCATCGCAAGACC	deletion of napG and napH
napGH d	GNNGGATCCTGCTGGATGCCGAGAACTTT	deletion of napG and napH
PS0143a	Melnyk et al 2013	deletion of pcrO
PS0143b	Melnyk et al 2013	deletion of pcrO
PS0143c	Melnyk et al 2013	deletion of pcrO
PS0143d	Melnyk et al 2013	deletion of pcrO
PS0144a	Melnyk et al 2013	deletion of pcrQ
PS0144b	Melnyk et al 2013	deletion of pcrQ
PS0144c	Melnyk et al 2013	deletion of pcrQ
PS0144d	Melnyk et al 2013	deletion of pcrQ
pcrQ comF	GNNGGATCCTTAAGTATGCCAATTTAATGAAAAA CATTCTCAAATCG	Complementation with pcrQ
pcrQ comR	GNNACTAGTCGATAATTGGTGTCAGGGATATGCG	Complementation with pcrQ
pcrO comF	GNNGGATCCAATCGTCTGGAGTATTTAAATGAAA AAAAGTGC	Complementation with pcrO
pcrO comR	GNNACTAGTAAAACGCCCTCTGCATTTCG	Complementation with pcrO
napC comF	GNNGGATCCCAGGGAGAGAAAGCGCATCATG	Complementation with napC
napC comR	GNNACTAGTGGATTCGACGCAGATTACTCGTC	Complementation with napC
napO comF	GNNGGATCCAGAATGGAGAGTTACACCATGTTCA AG	Complementation with napO
napO comR	GNNACTAGTCCAACTCGCGAAGATTTGCG	Complementation with napO
nap-promoterF	GNNGAATTCCTGTAGGCATGCCAGGAGAC	construction of nap promoter fragment

Table 2-2. Strains used in this study; all strains are listed here; a brief description of strain genotype is also supplied.

Strain	Species	Plasmid	Genotype	Reference
OW13	*Azospira suillum* PS	none	*ΔnapO*	This work
OW17	*Azospira suillum* PS	none	*ΔpcrOΔnapO*	This work
OW19	*Azospira suillum* PS	none	*ΔpcrAΔnapC*	This work
OW20	*Azospira suillum* PS	none	*ΔpcrAΔnapO*	This work
OW22	*Azospira suillum* PS	none	*ΔnapGH*	This work
OW38	*Azospira suillum* PS	none	*ΔnapCΔnapO*	This work
OW39	*Azospira suillum* PS	none	*ΔnapCΔpcrO*	This work
OW40	*Azospira suillum* PS	none	*ΔpcrQΔnapO*	This work
OW52	*Azospira suillum* PS	pBBR1MCS2	*ΔpcrQΔnapC*	This work
OW53	*Azospira suillum* PS	pOW26	*ΔpcrQΔnapC*	This work
OW54	*Azospira suillum* PS	pOW28	*ΔpcrQΔnapC*	This work
OW55	*Azospira suillum* PS	pOW31	*ΔpcrQΔnapC*	This work
OW56	*Azospira suillum* PS	pOW33	*ΔpcrQΔnapC*	This work
OW57	*Azospira suillum* PS	pBBR1MCS2	*ΔpcrOΔnapO*	This work
OW58	*Azospira suillum* PS	pOW27	*ΔpcrOΔnapO*	This work
OW59	*Azospira suillum* PS	pOW29	*ΔpcrOΔnapO*	This work
OW60	*Azospira suillum* PS	pOW32	*ΔpcrOΔnapO*	This work
OW61	*Azospira suillum* PS	pOW34	*ΔpcrOΔnapO*	This work
OW7	*Azospira suillum* PS	none	*ΔnapA*	This work
OW77	*Azospira suillum* PS	none	*ΔnapCΔnapOΔpcrA*	This work
OW78	*Azospira suillum* PS	none	*ΔnapCΔpcrOΔpcrA*	This work
OW79	*Azospira suillum* PS	none	*ΔpcrQΔnapOΔpcrA*	This work
OW80	*Azospira suillum* PS	none	*ΔpcrQΔpcrOΔpcrA*	This work
PS	*Azospira suillum* PS	none	wild-type	Coates Lab,
RAM035	*Azospira suillum* PS	none	ΔpcrA	Melnyk et al 2013
RAM038	*Azospira suillum* PS	none	*ΔpcrQ*	Melnyk et al 2013
RAM051	*Azospira suillum* PS	none	*ΔPcrO*	Melnyk et al 2013
RAM082	*Azospira suillum* PS	none	*ΔnapCΔPcrQ*	This work
RAM125	*Azospira suillum* PS	none	*ΔNapC*	This work
RAM126	*Azospira suillum* PS	none	*ΔpcrQΔNapC*	This work

Table 2-3. Plasmids used in this study; plasmids are listed here by name, and the markers carried are described, along with a brief description and source

Plasmid	Markers	Description	Reference
pOW12	KanR , SucS	pNPTS138 with napGH deletion insert	This study
pOW26	KanR	pRAM62 with pcrQ	This study
pOW27	KanR	pRAM62 with pcrO	This study
pOW28	KanR	pRAM62 with napC	This study
pOW29	KanR	pRAM62 with napO	This study
pOW30	KanR	pBBR1MCS2 with napC promoter	This study
pOW31	KanR	pOW30 with pcrQ	This study
pOW32	KanR	pOW30 with pcrO	This study
pOW33	KanR	pOW30 with napC	This study
pOW34	KanR	pOW30 with napO	This study
pOW35	KanR , SucS	pNPTS138 with napCO deletion insert	This study
pOW9	KanR , SucS	pNPTS138 with napO deletion insert	This study
pRAM44	KanR , SucS	pNPTS138 with PcrA deletion insert	Melnyk et al 2013
pRAM51	KanR , SucS	pNPTS138 with PcrO deletion insert	Melnyk et al 2013
pRAM55	KanR , SucS	pNPTS138 with PcrQ deletion insert	Melnyk et al 2013
pRAM62	KanR	pBBR1MCS2 with pcrA promoter	Melnyk et al 2013
pRAM74	KanR , SucS	pNPTS138 with PcrQO deletion insert	This study
pRAM94	KanR , SucS	pNPTS138 with napC deletion insert	This study

Table 2-4. Specific growth rates (hr $^{-1}$) of different mutants in Figure 2-2

Genotype	growth rate (nirate)	growth rate (perchlorate)	growth rate (diauxic nitrate)	growth rate (diaxuic perchlorate)
wild-type	0.247±0.006	0.197±0.009	0.273±0.044	0.167±0.016
ΔpcrQ	0.215±0.004	0	0.224±0.008	0.167±0.008
ΔpcrO	0.239±0.008	0	0.201±0.003	0.206±0.009
ΔnapC	0	0.251±0.008	0.137±0.003	0.201±0.017
ΔnapO	0	0.170±0.033	0.199±0.033	0.141±0.030
ΔpcrA	0.290±0.009	0	0.213±0.063	0
ΔnapCΔpcrA	0	0	0.214±0.082	0
ΔnapOΔpcrA	0	0	0.070±0.018	0

Table 2-5. Specific growth rates (hr $^{-1}$) of different mutants in Figure. 2-4a, 4b

Genotype	growth rate (nirate)	growth rate (perchlorate)	growth rate (diauxic nitrate)	growth rate (diaxuic perchlorate)	growth rate (aerobic)
Wild-type	0.300±0.01	0.355±0.091	0.167±0.006	0.110±0.004	0.560±0.007
ΔpcrQΔnapC	0	0	0	0	0.579±0.007
ΔpcrOΔnapO	0	0	0	0	0.575±0.007

Table 2-6. Specific growth rates (hr $^{-1}$) of different mutants in Figure 2-6

Genotype	Growth Rate (diauxic nitrate)	Growth Rate (diauxic perchlorate)
wild-type	0.220±0.050	0.167±0.016
ΔnapCΔnapO	0.143±0.017	0.144±0.004
ΔnapCΔpcrO	0.134±0.042	0.0970±0.003
ΔpcrQΔpcrO	0.251±0.042	0.0620±0.002
ΔpcrQΔnapO	0.073±0.013	0.157±0.002
ΔpcrA	0.207±0.025	0
ΔnapCΔnapOΔpcrA	0.069±0.02	0
ΔnapCΔpcrOΔpcrA	0.085±0.01	0
ΔpcrQΔnapOΔpcrA	0.107±0.005	0
ΔpcrQΔpcrOΔpcrA	0.215±0.012	0

Chapter 3
Transcriptomic analysis of *Azospira suillum* PS under different physiological conditions

Abstract

Azospira suillum PS (formally *Dechlorosoma suillum* strain PS) is a motile Gram-negative, facultative anaerobic Beta-proteobacterium within the *Rhodocyclaceae* family. PS is metabolically versatile and able to reduce nitrate, perchlorate, chlorate [collectively (per)chlorate)], and molecular oxygen. While the genetic and biochemical mechanisms of nitrate and (per)chlorate reduction pathways in PS have been recently elucidated, the expression profiles of these genes are still unknown. Here, we report the transcriptome of PS grown with lactate as the sole electron donor and carbon source, but different terminal electron acceptors (perchlorate, chlorate, nitrate, and oxygen). Our results suggest that (1) the (per)chlorate reduction genes are constitutively expressed at a baseline level but also specifically induced under (per)chlorate reduction conditions; (2) denitrification, rather than ammonification, by the periplasmic nitrate reductase NapAB, is the dominant nitrate reduction pathway under the tested conditions; (3) molecular oxygen reduction under aerobic and (per)chlorate reducing conditions is mediated by a cytochrome *cbb₃* oxidase that is constitutively expressed. The results of this study serve as a hypotheses-generating foundation for future investigations, in addition to providing new insight into this metabolically versatile model organism

Introduction

Azospira suillum PS (formally *Dechlorosoma suillum* strain PS) is a motile, Gram-negative, facultative anaerobic Beta-proteobacterium within the *Rhodocyclaceae* family [147]. PS was isolated from a swine waste lagoon because of its unique ability to grow by dissimilartory (per)chlorate reduction [125]. As mentioned in earlier chapters, (per)chlorate reducers, including PS use a highly conserved perchlorate reductase PcrABCOQ to reduce perchlorate to chlorate and subsequently chlorite. The produced chlorite is rapidly removed by another highly conserved enzyme, chlorite dismutase (Cld), to produce molecular oxygen (O_2) and innocuous chloride (Cl^-) [18, 32]. The produced oxygen is then internally respired within the same organism [18, 19, 32]. Owing to the unique ability to produce and consume molecular oxygen under anaerobic conditions, (per)chlorate respiration is in between the realms of aerobic and anaerobic metabolisms. The ability to utilize (per)chlorate in PS and other (per)chlorate reducers is conferred by a horizontally transferred (per)chlorate reduction genomic island (PRI), which harbors the core and auxiliary perchlorate reduction genes [148].

The first mature genetic system in (per)chlorate reducing bacteria was developed for PS, since then it became the model organism for studying the molecular and biochemical mechanisms of microbial (per)chlorate respiration [98]. Strain PS is metabolically versatile and able to reduce nitrate, perchlorate, and oxygen (Figure 3-1) [125]. While the genetic and biochemical mechanisms of nitrate and perchlorate reduction pathways have been recently elucidated [18, 32, 149, 150], their related gene expression profiles are still unknown.

Microbial perchlorate reduction is dependent on several factors, including the absence of alternative electron acceptors [19]. While the presence of molecular oxygen inhibits perchlorate reduction, oxygen is produced during perchlorate respiration (Figure 1-1)[32]. Thus perchlorate metabolism is uniquely in between the realms of aerobic and anaerobic metabolisms. While the presence of nitrate also inhibits perchlorate reduction [121], nitrate actually stimulates the onset of perchlorate reduction [121, 150]. To understand the underlying inhibition and stimulation mechanisms, it is essential to learn whether the expression profiles of perchlorate reduction align more with anaerobic (nitrate reduction) or aerobic metabolism.

To address above mentioned questions and to build a model of carbon and electron flow in PS, we conducted RNA-seq experiments with cells grown with lactate as the sole electron donor and carbon source, but different terminal electron acceptors (perchlorate, chlorate, nitrate, and oxygen). We predict that perchlorate reduction genes are specifically induced under chlorate and perchlorate reducing conditions, whereas the oxygen reducing cytochrome *c* oxidase is expressed under aerobic, chlorate, and

perchlorate reducing conditions. We further hypothesizing that PS would perform complete oxidation of lactate through the tricarboxylic acid cycle (TCA cycle) with NADH serving as the predominant electron carrier, in addition to incomplete oxidation of lactate with formate serving as the electron carrier, similar to a previous report on the chlorate reducing organism *Shewanella algae* ACDC [34]. The results of this study not only provide new insight into this metabolically versatile model organism, but also serve as a hypotheses-generating foundation for future investigations in microbial (per)chlorate reduction.

Material and Methods

Bacterial culturing

Wild type *Azospira suillum* PS [125] (Isolated by the Coates lab, ATCC[R] BAA-33, hereafter referred to as wtPS) and mutant strains were revived from freezer stocks by streaking out for single colonies on ALP medium agar plates [98]. One liter of ALP medium is composed of 0.49 g monobasic sodium phosphate dihydrate, 0.97 g dibasic anhydrous sodium phosphate, 0.1 g potassium chloride, 0.25 g ammonium chloride, 0.82 g sodium acetate, 2.0 g yeast extract, 7.6 g of a 60% (wt/wt) sodium lactate solution, 1.10 g sodium pyruvate, and 10 ml of both vitamin mix and mineral mix as previously described [126]. To make solid ALP medium for plates, 15 g/liter agar was added. LMM minimal medium is composed of the same ingredients as ALP, but omitting acetate, pyruvate, and yeast extract).

For aerobic cultivation, liquid overnight aerobic PS cultures in LMM medium were transferred into fresh LMM medium (1:100 dilution) and cultivated at 37°C with vigorous shaking (250 rpm), and harvested at mid-log growth phase (~4 hours, OD ~ 0.4). For anaerobic cultivation, overnight aerobic PS cultures in LMM medium were used as the inoculum (1:20 dilution) for anaerobic cultures in LMM amended with 10mM each of sodium nitrate, sodium chlorate, or sodium perchlorate. A lower dilution was used to minimize the unpredictable lagging growth phase associated with the transition from aerobic to nitrate and perchlorate metabolisms. Media were made anoxic by flushing with oxygen-free N_2, and sealed with butyl rubber stoppers prior to autoclaving. Anaerobic cultures were cultivated in anaerobic tubes (Bellco) with a nitrogen headspace at 37°C without shaking. The anaerobic samples were harvested at mid-log growth phase (OD ~ 0.4, ~12-24 hours for nitrate and chlorate, ~24-72 hours for perchlorate). Approximately 1×10^7 cells from each sample were centrifuged, washed, resuspended in Trizol (Life Technologies), and stored in -80 °C freezer for subsequent RNA extraction.

RNA extraction, sample preparation, data analysis and visualization

Wild type PS cells grown with oxygen, nitrate, chlorate or perchlorate as the terminal electron acceptors were centrifuged and resuspended in Trizol (Life Technologies) at mid-log phase. RNA was extracted and treated with DNase (DNase I, Life Technologies) according to the manufacturer's instructions. The rRNA removal (RiboZero kit, Epicentre), complementary DNA synthesis, library preparation (PrepX RNA-Seq Sample and Library Preparation Kits, WaferGen), and 100bp single-end hi-seq sequencing, were performed at the Vincent J. Coates Genomics Sequencing Laboratory. The sequencing reads were preprocessed to cut off 5 bases on the 5' end with seqtk (https://github.com/lh3/seqtk), quality trimmed with sickle

(https://github.com/ucdavis-bioinformatics/sickle), and quality checked with the FastQC tool. Read mapping and differential expression analysis were conducted with the bacterial RNA-Seq data analysis tool Rockhopper [151]. All data were visualized using the Prism 7 software.

Results

(Per)chlorate reduction genes are constitutively expressed at a baseline level and specifically induced under perchlorate and chlorate reducing conditions

All seventeen catalytic and auxiliary perchlorate reduction proteins are encoded on a horizontally transferred PRI, in addition to a non-PRI encoded sigma factor *rpoN* (locus tag: dsui_0704) that is predicted to activate the transcription of the perchlorate reduction operon. These genes can be further divided into four groups; (1) 7 genes encode the catalytic (per)chlorate reductase (*pcrABCDQO*, dsui_143, locus tag: dsui_144, dsui_146-149) and chlorite dismutase (*cld*, locus tag: dsui_0145); (2) 3 genes (*pcrPSR* locus tag: dsui_150-152) that comprise a histidine kinase sensory system, which is predicted to interact with the sigma factor RpoN; (3) 5 genes (*yedYZ, sigF, nrsF, mtrX* locus tag: dsui_154-158) that is involved in inadvertently produced hypochlorite detoxification and stress responses [152]; and (4) 2 genes (dsui_0153, *moa* (locus tag: dsui_142) of unknown function.

Our data indicated the genes encoding the catalytic enzymes were constitutively expressed at a low level, even under nitrate and aerobic conditions (Figure 3-2a). The sigma factor *rpoN* transcription remained remarkably stable across all conditions (Figure 3-2a, b), thus was used as a "standard" gene that represented active expression. The total normalized reads of *pcrA* and *cld* under aerobic and nitrate reducing conditions were of the same magnitude of *rpoN*, indicating a baseline level expression even in the absence of perchlorate and chlorate. While this observation could be caused by artificial sequencing error or extraction biases, a previous study demonstrated the deletion of *cld* led to chlorite hypersensitivity even under aerobic conditions [152], consistent with our results. We reasoned that the histidine kinase sensory system would be constitutively expressed, as they were needed across diverse growth conditions to detect the induction signals. Indeed, *pcrPSR* that encoded the histidine kinase sensory system were actively transcribed under aerobic and nitrate condition (Figure 3-2a, b).

The transcription of (per)chlorate reduction catalytic and stress response genes was specifically induced under perchlorate and chlorate growth conditions (Figure 3-2b). Under perchlorate and chlorate reducing conditions, the transcription of *pcrABCDQO, cld, yedYZ, sigF, nrsF,* and *mtrX* was on average was 33.01 ± 8.59 and 43.19 ± 18.61 fold higher than their aerobic baseline level (Figure 3-2b). The *pcrPSR* transcription was only moderately higher (1.76 ± 0.90 and 5.51 ± 4.06 fold) under the same condition (Figure 3-2b), likely to avoid unwanted crosstalk [153]. The transcription of the two genes of unknown function (dsui_0153, *moaA*) was also induced under perchlorate and chlorate reducing conditions.

Denitrification by the periplasmic nitrate reductase NapAB is the dominant nitrate reducing pathway under tested conditions

Strain PS constrains two complete nitrate reduction pathways (Figure 3-3): the denitrification pathway, and the dissimilatory nitrate reduction pathway (ammonification). In PS both pathways rely on the periplasmic nitrate reductase NapAB (locus tag: dsui_0507, dsui_0508) to reduce nitrate (NO_3^-) to nitrite (NO_2^-). In the denitrification pathway, NO_2^- is reduced by the nitrite reductase NirS (two paralogs in PS, locus tag: *nirS1* dsui_2076, *nirS2* dsui_3318) to nitric oxide (NO). The NO is then reduced to nitrous oxide (N_2O) by the respiratory nitric oxide reductase NorBC (locus tag: dsui_3109, dsui_3110). The N_2O is then finally reduced to nitrogen gas (N_2) by the nitrous-oxide reductase NosZ (two paralogs in PS locus tag: *nosZ1* Dsui_0882, *nosZ2* Dsui_3309). In contrast, in the ammonification pathway NO_2^- is directly reduced to ammonia (NH_3) by the NADH-depend nitrite reductase NirBD (locus tag: dsui_1825-1826)[154].

The transcription of most denitrification genes (*napAB, nirS1, nirS2, norBC*) was specifically induced under nitrate reduction conditions (compared to aerobic conditions), except *nosZ1* and *nosZ2* (Figure 3-4a). While the transcription of *nosZ1* was not detected, the total normalized reads of *nosZ2* suggested it was constitutively expressed, thus implied that *nosZ2* was the dominate nitrous oxide reductase under the tested conditions (Figure 3-4b). There are also two copies of the nitrite reductase *nirS* in PS. Both *nirS1* and *nirS2* were specifically induced albeit the normalized reads of *nirS2* were slightly higher than *nirS1*, indicated both paralogs could be functional during nitrate reduction (Figure 3-4a,b).

Interestingly, the NADH-depend nitrite reductase *nirBD* from the assimilatory nitrate reduction pathway were neither specifically induced nor expressed under the conditions tested, suggested the pathway was not functional in our cultures. Strain PS also harbors genes involved in the assimilatory nitrate reduction pathway (*nasA* locus tag: dsui_1817), and the nitrogen fixation pathway (*nifDKH* locus tag: dsui_0955-0957), though none of these genes was expressed (Figure 3-4c). This observation was not surprising as our growth medium contained ~5mM of ammonia, which was the end product of the assimilatory pathways. The presence of ammonia likely led to a product inhibition effect [155].

Molecular oxygen reduction under aerobic and (per)chlorate reducing conditions is mediated by a constitutively expressed cytochrome *cbb₃* oxidase

Strain PS contains two aerobic respiration pathways (Figure 3-1). In one pathway the cytochrome *cbb₃* oxidase (cyt *cbb₃*, locus tag: dsui_1627-1630) acts as a cytochrome *bc₁* (cyt *bc₁*, locus tag: dsui_1813, dsui_1814)-dependent oxidase, in which the cyt *bc₁* transfers electrons from quinol to the cyt *cbb₃* oxidase to reduce molecular oxygen to water [156-158]. In the other pathway the cytochrome *bd* (cyt *bd*, locus tag: dsui_1915, dsui_1916) respiratory oxygen reductase that also acts as a quinol oxidase uses ubiquinol or menaquinol as substrates to directly reduce oxygen [159]. Both cyt *cbb3* and cyt *bd* are known for their high affinity toward oxygen and their induction under low oxygen tension conditions [157, 159, 160]. Interestingly, our result revealed that cyt *cbb3* oxidase, and its electron donor cyt *bc₁* complex genes were constitutively expressed despite the varying aerobic/anaerobic growth conditions (Figure 3-5). This distinctive expression scheme was conceivably due to the carbon and electron donor rich but acceptor-limited environment where PS was isolated. The constitutive expression of high affinity oxidase may provide a selective advantage during competition for scarce oxygen. In contrast, the transcription of cyt *bd* oxygen reductase was induced under anaerobic nitrate reducing conditions, is consistence with previous studies [159]. The cyt *bd* oxygen reductase was also induced in one sample harvested on chlorate, but not perchlorate, implying a faster O_2 flux under chlorate reducing conditions (Figure 3-5).

Expression of TCA cycle and Electron transport chain complex I, II, and ATP synthase

Microorganisms shift to different metabolic modes depending on available electron donors or acceptors [34, 161]. In *Escherichia coli* aerobic metabolism the glycolytic conversion of glucose and the oxidative decarboxylation of pyruvate by the pyruvate dehydrogenase complex lead to the formation of acetyl-CoA. The produced acetyl-CoA feeds the TCA cycle to generate reducing equivalents [161]. Under anaerobic respiration conditions, however, the role of the pyruvate dehydrogenase complex is assumed by pyruvate formate-lyase and the metabolic flow in the C4 section of the TCA cycle is reversed [161]. Similarly, when grown with lactate, the chlorate reducing bacteria *Shewanella algae* ACDC flexibly shifts between incomplete oxidation of lactate to formate/acetate, and complete oxidation of lactate through the TCA cycle with NADH serving as the predominant electron carrier [34].

We checked the expression of genes involved in the incomplete lactate oxidation to formate and acetate and those involved in the complete oxidation via the TCA cycle. Surprisingly, the transcription of TCA cycle genes was relatively constant across

different growth conditions, similar to the cyt *bc₁* and cyt *cbb3* cytochromes (Figure 3-6). Expression of the genes involved in the incomplete oxidation of lactate showed relatively higher variations, but the absolute normalized reads were much lower (< 100), which led to these data to being sensitive to fold-changes measurement (Figure 3-6).

We also examined the expression of other components of the respiratory electron transport chain such as the complex I NAPH reductase (*nuo*, locus tag: dsui_3037-3050), complex II succinate dehydrogenase (*sdh*, locus tag: dsui_2211-2214), and ATP synthase (*atp*, locus tag: dsui_0851-0858) to determine whether there is any differential expression in response to changing the acceptors. The *nuo, sdh* and *atp* genes were all transcribed at a similarly high level accross all conditions tested (Figure 3-7), suggesting that the tested cultures were metabolically active.

Discussions

As expected, the transcription of the perchlorate reduction catalytic (PcrABCDOQ) and stress response proteins (YedYZ, SigF, NrsF, MtrX) were specifically induced under chlorate and perchlorate reducing conditions. The transcription of (per)chlorate reduction genes was detected at a baseline level, and was comparable to the response regulators RpoN, even under known inhibitory conditions. Whether this high level of normalized reads (induced and baseline) was a result of sequencing bias or represented genuine robust transcription is still unknown. However, an earlier study has confirmed the baseline expression of PS Cld, as the *cld* deletion led to chlorite stress hypersensitivity even under aerobic conditions [152]. The reasons of the baseline expression are still not clear. It could simply be a result of suboptimal regulation of a recently acquired metabolism, or alternatively, plays an important regulatory role, such as the production of the reactive intermediate chlorite as an induction signal for the metabolism. Constitutive expression of Cld could also be a way to preemptively defend against the toxic intermediate chlorite. In contrast, the transcription of perchlorate reduction sensory system was expressed at a baseline level but only moderately induced. This moderate induction was expected, as the overexpression of the sensory system would lead to inadvertent cross talk among non-cognate two-component systems [153], which usually results in disruption of signal transduction networks.

Our results suggested that under the tested conditions, denitrification was the dominant pathway for nitrate respiration. This was expected as the PS growth medium contains ~5 mM of ammonium chloride, which likely caused product inhibition of the ammonification and nitrogen fixation pathways [155]. In addition, the NirBD nitrite reductase is a NADH-dependent cytoplasmic enzyme that consumes reducing power to reduce nitrite without generating any proton motive force [154]. Therefore, the NirBD complex likely plays a nitrogen assimilation or nitrite detoxification role and is not involved in the nitrate respiration.

The transcription scheme of aerobic respiration pathways in PS was indeed unexpected. In PS the cyt *cbb₃* oxidase (*ccoNOQP*) was constitutively expressed. This observation is in contrast to other facultative anaerobic Proteobacteria such as *Rhodobacter sphaeroides*, *Paracoccus denitrificans*, *Pseudomonas aeruginosa* and *Rhizobium leguminosarum*, in which the redox-sensitive regulator Fnr induces cyt *cbb₃* oxidase expression under microaerobic or anaerobic conditions [156, 157, 162, 163]. Interestingly, the same constitutive expression of cyt *cbb₃* was also observed in a chlorate reducer, *Shewanella algae* ACDC [34], and another perchlorate reducer *Dechloromonas aromatica* RCB. These results implied the constitutive expression of cyt *cbb₃* oxidase could be a common theme among (per)chlorate and chlorate reducers, the constitutive expression could be an essential phenotype that is required for successful PRI and CRI (chlorate reduction

genomic island) adaptation. The experimentally determined K_m for purified *Bradyrhizobium japonicum cbb3* complex is in the order of 7 nM [164], significantly lower than other related oxygen reduction enzymes such as the cytochrome *bo3* oxidase (K_m = 150–350 µM) and cytochrome *aa3* oxidase (K_m = 100 - 1000 nM) [157, 159, 160]. The fact that the high oxygen affinity cytochrome *cbb3* oxidase was constitutively expressed implied that the native environment of PS was oxygen-limited, likely due to insufficient diffusion and poor solubility. Abolishment of the regulation of cyt *cbb3* complex potentially helped PS to better compete for the scarce oxygen, which offers a competitive advantage over other bacteria that require an additional induction phase.

The other oxygen reduction enzyme, cytochrome *bd* (*cydAB*), was only expressed under oxygen limited conditions in PS. In *E.coli,* the expression of the *cydAB* operon is controlled by global redox transcriptional regulators Arc and Fnr [160, 165], and only expressed when the oxygen tension is low [165]. Instead of being the dominant pathway for aerobic respiration, the cytochrome *bd* oxygen reductase likely serves as an oxygen scavenger to prevent the degradation of oxygen-sensitive enzymes such as nitrogenase or PcrAB [160, 166]. However, it is not clear why PS needs two oxygen reduction pathways that are both specialized for low-oxygen conditions if one pathway is already constitutively expressed.

Our results also showed PS lacked differential expression of TCA cycle genes. The absence of regulatory response across different growth conditions implied PS resided in a chemically stable environment. Presumably, the lack of physiology responses to different terminal acceptors made PS an ideal platform for the acquisition of perchlorate respiration. Further studies are needed to determine whether there is a correlation between the presence of perchlorate reduction and constitutive expression of oxygen reduction cytochromes and TCA cycle genes.

Conclusions

Recent studies have identified the common biochemical pathway and genetic systems involved in microbial perchlorate reduction. While PS serves as the model organism for studying microbial perchlorate reduction, no data was available on the expression profiles of PS under different growth conditions. Here we report the PS transcriptome under oxygen, nitrate, chlorate and perchlorate growth conditions. Our results provide new insight into this metabolically versatile model organism. Furthermore, the results of this study also serve as a hypotheses-generating foundation for future investigations.

Figures
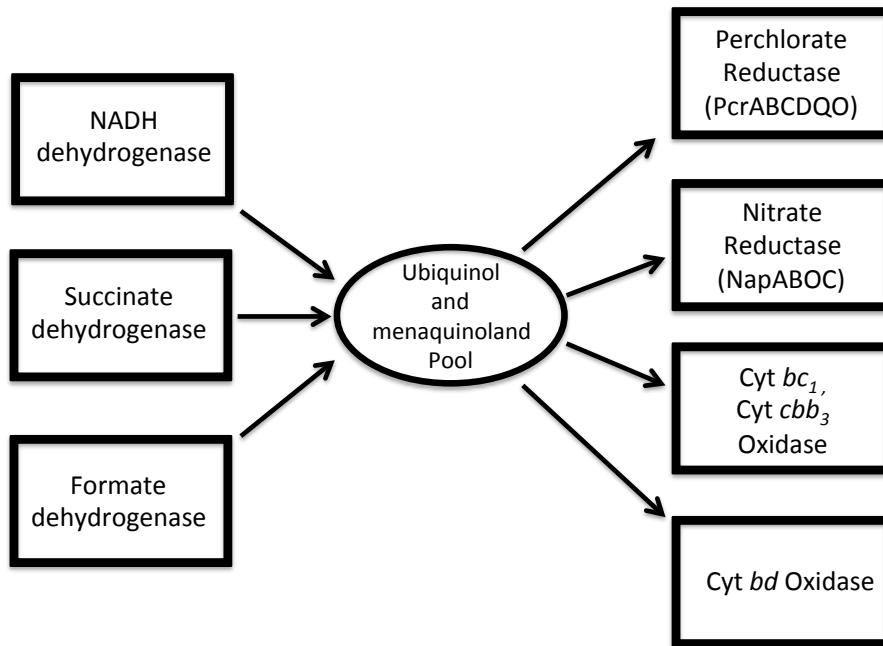
Figures 3-1 Respiratory flexibility of *Azospira suillum* PS

a PRI expression normalized reads

b PRI genes expression compared to aerobic condition
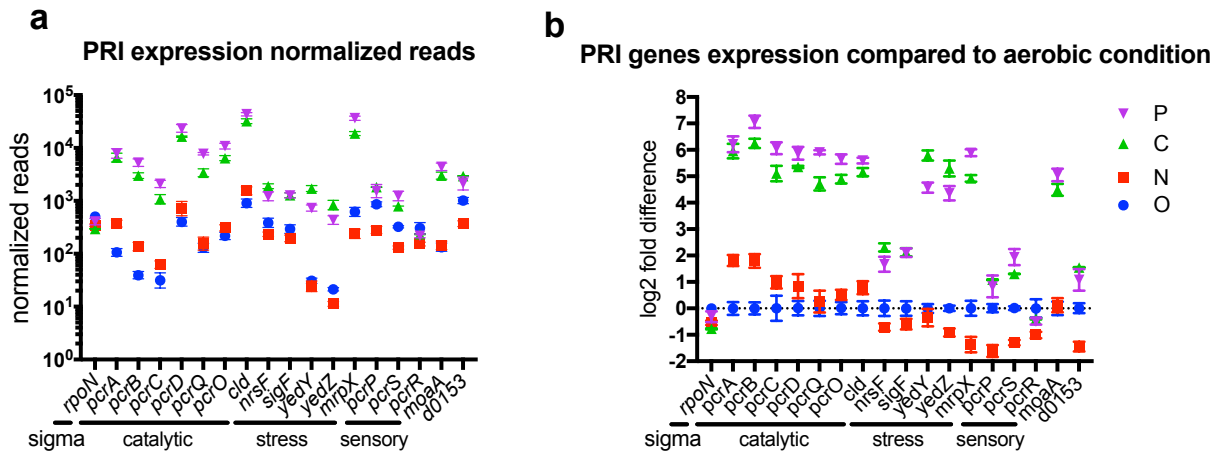
Figures 3-2 Transcription of (per)chlroate reduction genes in PS with perchlorate (P), chlorate (C), nitrate (N) and oxygen (O) as the terminal electron acceptors. (a) Total Rockhopper-normalized RNA-seq reads of each gene. (b) log2-fold change of normalized reads of each gene when compared to the aerobic condition.
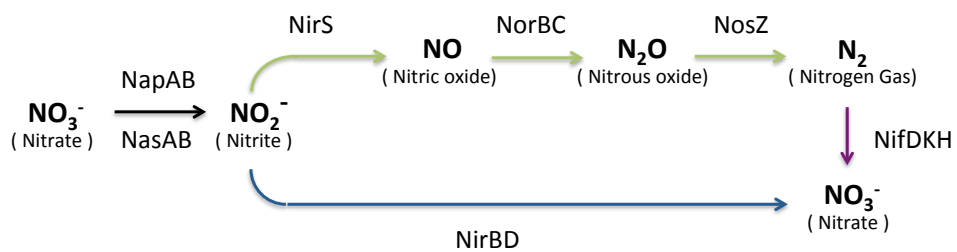
Figures 3-3 Nitrate reduction pathways and genes in *Azospira suillum* PS (green = denitrification, blue = ammonification, purple = nitrogen fixation).

a Nitrate Reduction Genes Expression Compared to Aerobic Condition

b Nitrate Reduction Genes Normalized Reads

c Expression of Other Nitrate Reduction Genes

Figures 3-4 Transcription of nitrate reduction genes in PS with oxygen (O), nitrate (N), chlorate (C), and perchlorate (P) as the terminal electron acceptors. (a) log2-fold change of normalized reads of each gene when compared to the aerobic condition. (b and c) Total Rockhopper-normalized RNA-seq reads of each gene.
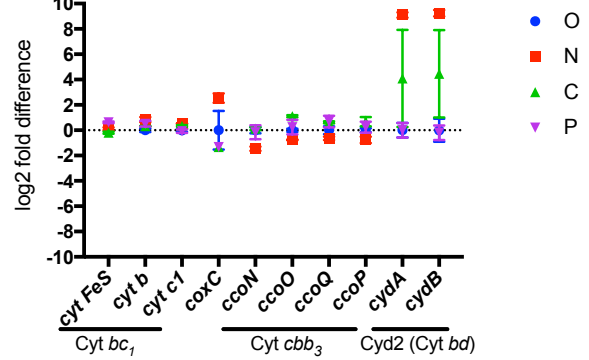
Figures 3-5 Transcription of oxygen reduction genes in PS with oxygen (O), nitrate (N), chlorate (C), and perchlorate (P) as the terminal electron acceptors. (a) Total Rockhopper-normalized RNA-seq reads of each gene. (b) log2-fold change of normalized reads of each gene when compared to the aerobic condition.
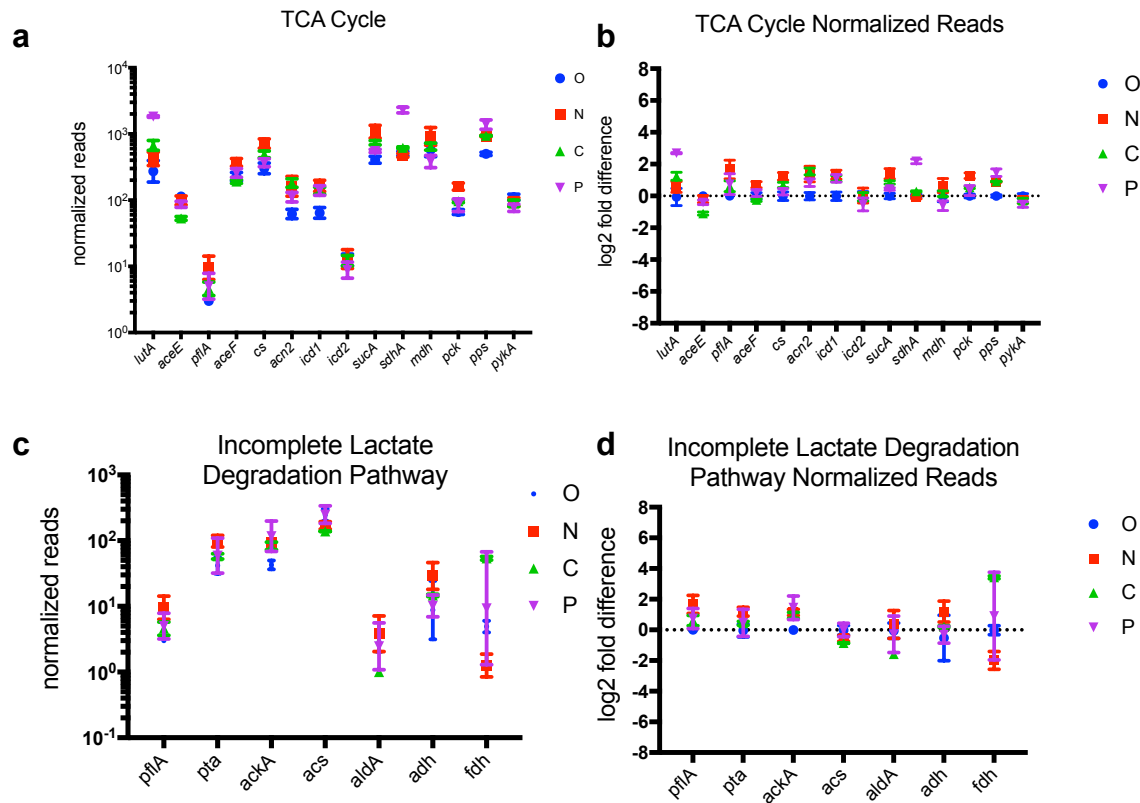
Figures 3-6 Transcription of enzymes involved in TCA cycle and incomplete lacate oxidation in PS with oxygen (O), nitrate (N), chlorate (C), and perchlorate (P) as the terminal electron acceptors. (a,c) Total Rockhopper-normalized RNA-seq reads of each gene. (b,d) log2-fold change of normalized reads of each gene when compared to the aerobic condition. *lutA*: lactate utilization protein A, *aceE*: Isocitrate lyase, *pflA*: pyruvate formate-lyase, *aceF*: pyruvate dehydrogenase, *cs*: citrate synthase, *acn*: aconitate hydratase, icd: isocitrate dehydrogenase, *sucA*: oxoglutarate dehydrogenase, *sdhA*: succinate dehydrogenase, *mdh*: malate dehydrogenase, *pck*: phosphoenolpyruvate carboxykinase, *pps*: phosphoenolpyruvate synthase, *pykA*: pyruvate kinase II, *pta*: phosphate acetyltransferase, *ackA*: acetate kinase, *aldA*: aldehyde dehydrogenase, *adh*: alcohol dehydrogenases, fdh, formate dehydrogenase.

Figure 3-7 Transcription of enzymes involved in respiratory complex I, II and ATP synthase in PS with oxygen (O), nitrate (N), chlorate (C), and perchlorate (P) as the terminal electron acceptors. (a) Total Rockhopper-normalized RNA-seq reads of each gene. (b) log2-fold change of normalized reads of each gene when compared to the aerobic condition.
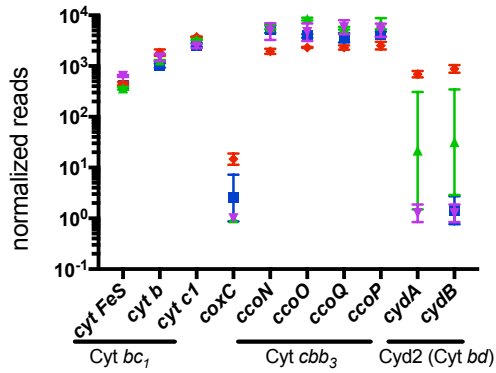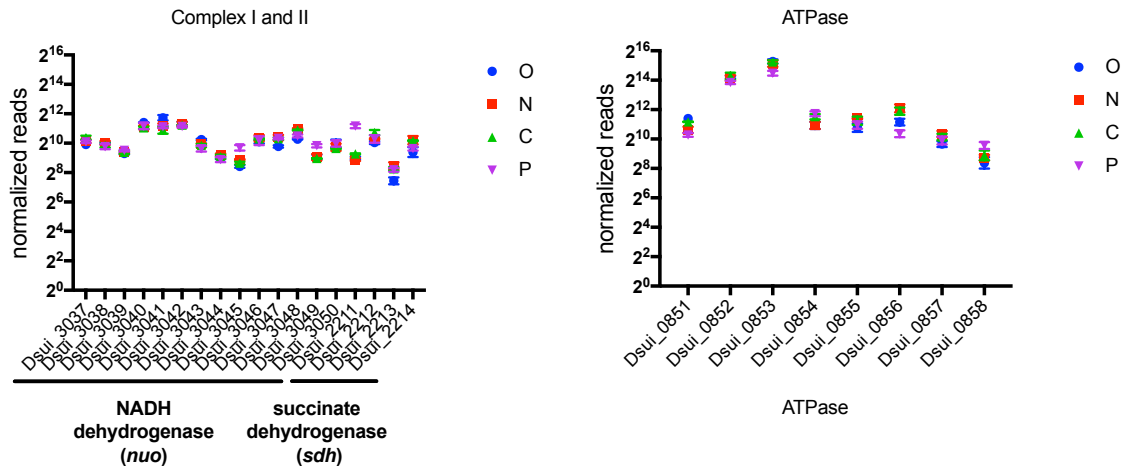
Chapter 4
Chlorite Dismutase and Chlorite Mediated Continuous Biomanufacturing Hygiene Control

Abstract

Batch and fed-batch bioreactors are commonly used in the biotech industry for the bioprocessing of value-added products from raw materials. While continuous bioprocessing with continuous-flow bioreactors has the potential to greatly improve process economics and production yield, these bioreactors are particularly sensitive to microbial contamination due to their long operation times. This contamination issue may be overcome by utilizing chlorite (ClO_2^-) as a biocide in systems containing chlorite-resistant bioprocessing strains. Chlorite has a broad biocidal activity, can be easily produced in industrial quantities, and is more cost-effective than common antibiotics (cost $1 per kg when purchased directly from the manufacturers). Chlorite dismutase (Cld) is a bacterial periplasmic enzyme that detoxifies chlorite into innocuous chloride and oxygen. Here, we report the construction of a chlorite resistant *Escherichia coli* strain by heterologous expression of Cld, followed by directed evolution. Initially, chlorite half maximal inhibitory concentration (IC_{50}) was approximately three times higher in Cld-expressing *E.coli* than the RFP-expressing and wild type *E.coli* negative controls. Through directed evolution, we identified an A21D mutation at the Cld translocation signal peptide that enhanced chlorite resistance and subsequently discovered that cytoplasmic expression of Cld (cCld) could lead to chlorite hyper-resistance, with a chlorite IC_{50} approximately 16 times higher than the negative controls. We then demonstrated that chlorite causes complete growth arrest and elicited strong stress-response in RFP-expressing *E.coli*, but not in cCld-expressing *E.coli*. Finally, we confirmed that the cCld expressing *E.coli* is compatible with continuous-flow bioreactors that contain chlorite as a biocide for contamination prevention and treatment.

Introduction

The biotech industry often relies on bioreactors to develop and bio-transform value-added products from raw materials. In 2015, the biotech industry in the United States generated 107.7 billion U.S. dollars of revenue and had an estimated total market value of some 890 billion U.S. dollars (www.statista.com/topics/1634/biotechnology-industry). Most industrial scale bioprocessing bioreactors are operated as batch, fed-batch, and continuous-flow bioreactors [167]. Batch reactors are simple, reliable and commonly used in the brewing and pharmaceutical industries [168-175], whereas fed-batch bioreactors are frequently implemented in processes that are subject to substrate inhibition [176, 177]. In theory, replacing the batch or fed-batch bioreactor system with a continuous-flow bioreactor would minimize equipment downtime, increase volumetric productivity, and reduce operational cost once the bioreactor reaches steady-state [178-180]. However, due to the prolonged continuous operation, accidental bioreactor contamination with environmental microbes or bacterial phages is a major risk and subsequent failure investigation could cause factory shutdowns that disrupt production schedule [100, 102, 103, 180-183]. Failure data collected from an industrial fermentation plant during a 15-year period suggest 1 in 10 bioreactors are subjected to microbial contamination [181]. Long-term continuous-flow bioreactor operation sometimes relies on antibiotic addition, which is ineffective against phage, environmentally unfriendly, and economically infeasible for low profit margin bio-commodity production [180, 184, 185].

We propose using chlorite as a biocide to solve the bioprocessing contamination problem. Chlorite (ClO_2^-) is a broad-spectrum alternative biocide that is known to be active against gram-negative and gram-positive bacteria [23-27, 29], bacteriophages [28], fungi [24], algae [26], and copepod parasites [30]. The chlorite toxicity is mediated by oxidation of cysteine and the thiol-containing antioxidant glutathione, resulting in detrimental cellular oxidative stress [23, 186]. The actual disinfection efficacy varies among these studies, presumably due to differences in microorganisms, chlorite concentrations, and media/buffer compositions.

The sodium chlorite salt is cheap, readily available, and relatively safe. Aside from being a disinfectant, recently published patents and scientific works established the use of acidified chlorite solution for meat and vegetable preservation [27, 29, 187-192]. Commercially available immunomodulatory medicine, such as Oxoferin and WF10, contain chlorite as an active ingredient [193-195]. Chlorite is exceptionally more cost-effective than traditional antibiotics, with one kilogram only costing about $1 when purchased directly from the manufacturer. Chlorite as a biocide should be compatible with current bioreactors as it has the lowest corrosion rate among chlorine-based

disinfectants used in water distribution systems and residual chlorite can be readily removed via precipitation with reduced iron [196].

We hypothesize that the enzyme chlorite dismutase (Cld) could be used to confer chlorite tolerance or resistance in the bioprocessing host. Cld is a bacterial heme-containing, periplasmic enzyme that catalyzes the decomposition of chlorite to chloride (Cl$^-$) and molecular oxygen (O$_2$) [197-202]. It is highly conserved and essential in perchlorate and chlorate (collectively (per)chlorate) respiring bacteria that utilize (per)chlorate as their terminal electron acceptor [18, 19, 33, 124, 148, 149, 203]. Heterologous expression of Cld in *Escherichia coli* has been reported numerous times [201, 204-211], but mostly with focus on purification and biochemical properties of the recombinant Cld. Here we report the construction of a chlorite hyper-resistant strain by functional expression of Cld (from *Shewanella algae* strain ACDC) in *E. coli,* followed by directed evolution. This strain exhibits a low Cld activity and is compatible with a continuous-flow bioreactor that contains chlorite as a biocide. We further show that chlorite can be applied in continuous-flow bioreactors to prevent contamination and rescue contaminated reactors back to a productive monoculture state.

Materials and Methods
Bacterial strains, cultivation, and plasmid construction

A list of bacterial strains and plasmids can be found in Table 4-1. *Escherichia coli* LMG194 (wt *E. coli*) was used for optimal protein induction and for its compatibility with the pBAD arabinose promoter [212]. All *E. coli* strains were grown in a modified version of RM medium (MRM medium), described in the pBAD TOPO® TA Expression Kit user manual, with a reduced amount of casamino acids (5g/L) and appropriate antibiotics (kanamycin 50µg/ml or spectinomycin 100µg/ml). All *Caulobacter crescentus* strains are derivatives of the lab-adapted NA1000 strain and were grown in peptone yeast extract (PYE) medium at 30C. Cultures were maintained in 15% glycerol stocks frozen at -80 °C.

A derivative of vector pSB4K5 (pSC101 origin of replication, ~5 copies per cell), which lacks *ccdB* and the pUC19 origin of replication but contains *araC* with the arabinose-inducible promoter [34], was used as the backbone to express *Shewanella algae* strain ACDC Cld (wtCld) (pICC63) and RFP (pICC49). The pICC63 and pICC49 plasmids were constructed by Clarks et al. for a previous study [34]. The cytoplasmic Cld (cCld) expressing plasmid, pOW61, was constructed by removing the translocation signal peptide (2-31 amino acids) of wtCld in pICC63 via "round-the-horn" site-directed mutagenesis (developed by Sean Moore, openwetware.org). The signal peptide was predicted with SignalP 4.1 Server [213]. All other plasmids are constructed via Gibson cloning with In-Fusion® HD Cloning Kit (Clontech) following the manufacture's instruction. A list of PCR primers used in this study can be found in Table 4-2. The plasmid pTMH173 that expresses FMO (flavin-containing monooxygenase from *Methylophaga aminisulfidivorans* MP) was constructed using Golden Gate Assembly. The FMO gene is flanked by the BioBricks promoter BBa_J23100 [214] and the terminator tSPY [215] .Constructed plasmid sequences were verified at the UC Berkeley DNA sequencing facility by Sanger sequencing.

Phage isolation and plaque assay

Influent wastewater samples were collected from the East Bay Municipal Utility District's wastewater treatment plant in Oakland, CA, and filtered through 0.22µM filters to remove debris and microbes. To make a phage enrichment culture, 5mL of filtered wastewater was mixed with 5mL of 2X LB medium and inoculated with 100µL of stationary *E. coli* cells, incubated for 48 hours at 37°C, 50RPM. Next, a sterile cotton swab was dipped into an overnight *E. coli* culture, smeared on an LB agar plate, and 10µL of the phage enrichment culture was then spotted on the plate. The plate was incubated overnight at 37°C. Positive lytic phage activity resulted in a clear zone on the *E. coli* lawn. Phage particles from the clear zone were picked into the phage buffer (10mM Tris, 1mM CaCl2 10mM MgCl2, 68mM NaCl, pH 7.5, adapted from the Phage

Hunting Program, University of Pittsburgh), followed by dilution to extinction and plating to obtain single plaques with pure phage cultures. Phage cultures were maintained at 4°C in the phage buffer. The pure phage culture was incubated with 4mM chlorite or water at 37°C, followed by plating on LB plates at different time points to test phage inactivation by chlorite. To test phage deactivation by chlorite, *C.crescentus* phage CR-30 was incubated with chlorite or water at 30C. Samples were taken at designated time points and mixed with PYE (0.3%) agar and log phase (OD660 0.1-04) *C. crescentus* culture before plating on PYE plates. Plaque forming unites were counted after 24 hours.

Protein expression in *E. coli*

Heterologous expression of Cld in the *E. coli* periplasm is difficult and usually requires a low induction temperature (20 °C) and/or addition of a heme-precursor [205, 207]. Our first attempt to express Cld with the inducible pET promoter was unsuccessful and produced mostly insoluble Cld that failed to provide chlorite resistance. Addition of the heme precursor hemin (10mM) did not affect Cld expression in any strain (data not shown). To overcome these expression problems, a low-copy number vector was used, which allows for the slow but steady expression of Cld (see plasmid construction section for details). To induce protein expression prior to experiments, *E. coli* strains were revived from freezer stocks by streaking out to single colonies on LB agar plates with the appropriate antibiotics. Single colonies from plates were picked into MRM medium and cultivated overnight at 37°C, 250 rpm. The next day, 100μL of the overnight cultures were inoculated into 10mL MRM medium and incubated at 37°C, 250 rpm. The incubation temperature was adjusted to 26°C and 0.02% w/v arabinose was added to induce the protein expression when the optical density at 600nm (OD600) reached approximately 0.4. Protein expression was induced for 18 hours before use in downstream experiments. All *E. coli* strains were treated with an identical procedure for protein induction, with the exception FMO expressing strains, which were under a constitutively active promoter.

Half maximal inhibitory concentration (IC$_{50}$) determination

For IC$_{50}$ determination, flat-bottom 96-well plates (Corning Costar, Tewksbury, MA) were inoculated with *E. coli* strains at a starting OD600 of 0.02 in 100μL of 2X MRM medium, with 0.02% w/v arabinose and appropriate antibiotics. 2X sodium chlorite stock solutions with various concentrations were prepared on the day of experiment, and 100μL was added to the plate to achieve the desired chlorite concentrations. 100μL of water was added to the negative control wells. The plate was then placed in a shaker and cultivated overnight at 37°C, 250 rpm. IC$_{50}$ were determined 24 hours after inoculation by measuring OD600. The OD600 difference between final and initial reads

was normalized to the no chlorite addition negative control to determine the final normalized growth.

Chlorite dismutase activity assay

Whole cells and cell lysates were used to determine the Cld activity. After induction of Cld or RFP expression, 10mL of RFP-expressing OW94, wtCld-expressing OW95, and cCld-expressing OW116 cells were normalized to an OD600nm of 2.0. Cells were then washed three times and resuspended in 1mL of 100mM potassium phosphate buffer (KPi buffer, 3.619g/L KH$_2$PO$_4$ and 4.63g/L K$_2$HPO$_4$). Cells in KPi buffer were then subjected to sonication (QSonica) at 4°C to generate cell lysate. A Qsonica sonicator was used with an amplitude of 50 and a total process time of 2 minutes. The protein concentration in the cell lysate was quantified with a BCA Protein Assay Kit (Thermo Fisher Scientific) following manufacture's protocol. To determine the Cld activity in different strains, 20µL of resuspended whole cells (normalized to an OD600nm of 2) or cell lysate (normalized to 0.5mg/mL) was transferred into a quartz cuvette (Fisher Scientific) containing 1mL of KPi buffer, and a final concentration of 500µM of chlorite was added followed by rapid mixing via pipetting. Chlorite concentration was monitored immediately after chlorite addition based on absorption at 260nm. Sodium chlorite from Sigma-Aldrich (CAS Number 7758-19-2) was used to generate a standard curve.

Directed evolution

OW95 cells were revived from freezer stocks, transferred into liquid MRM medium, and induced for Cld expression as described above. Initially, eight isogenic independent cultures were cultivated with a starting OD600nm of 0.01 in MRM medium with 1mM chlorite, 0.02% w/v arabinose, and 50µg/mL of kanamycin, at 37°C, 250 rpm. The resulting cultures were repeatedly transferred everyday with increasing chlorite concentrations (increments of 1mM) in the medium. Cultures were subjected to three transfers with the previous concentration of chlorite if they failed to tolerate the increased chlorite concentration. The directed evolution was concluded when we obtained a strain (OW105) that was able to grow in the presence of 8mM chlorite and reached a similar final OD600 as without chlorite control.

Western blots

For western blots, *E. coli* strains were harvested and normalized to an OD of 2.0, and cell lysate was generated as described in the above. Cell lysates were centrifuged, and the resulting supernatant was collected as the cell soluble fraction, whereas the membrane debris-containing pellet was resuspended in 8M urea and referred as the insoluble fraction. The insoluble fraction could also contain small amount of whole cells due to lysing inefficiency. The primary rabbit antibodies against Cld and horseradish

peroxidase conjugated anti-rabbit secondary antibodies were used at a 1:5000 dilution [216]. Immobilon western chemiluminescent hrp substrate (Millipore) was used following the manufacturer's protocol to reveal the blot. Purified *Azospira suillum* PS Cld (accession number: G8QM51, 96% identical to *S. algae* ACDC Cld) was used as a positive control.

Proteomic Analysis

For proteomic analysis, *E. coli* strains with or without chlorite (0.4mM for OW94, 4mM for OW116) were cultured and harvested at late log phase, centrifuged, resuspended, and lysed by sonication (QSonica) at 4°C. Less chlorite and a larger culture volume was used for OW94 due to poor cell yield in the presence of chlorite. Protein concentration was determined with a BCA Protein Assay Kit (Thermo Fisher Scientific) following manufacturer's protocol. A tryptic digestion procedure was used to prepare our samples for mass spectrometry [35]. Liquid chromatography coupled to tandem mass spectrometry of trypsin-digested samples was performed at the QB3 mass spectrometry facility at UC Berkeley and the resulting data were analyzed with the Progenesis software. A protein with a confidence score > 100, p-value < 0.05, and maximal normalized peptide abundance fold change > 2 is considered differentially expressed.

Chemostat setup and operation parameters

A 2L round-bottom autoclavable laboratory fermenter (BiOENGiNEERiNG), was operated as an iso-volumetric chemostat with 1L of MRM medium in the bioreactor vessel. Temperature, dissolved oxygen (dO), and pH were monitored during the course of the experiments. Temperature was set and maintained at 37°C. pH was set to 7.2 and adjusted automatically based on the real time pH value with 1M NaOH or 1M HCl. dO was set to 20% of the maximal dO value at 37°C with constant air flow of 2L/min. Constant dO was maintained by automatic agitation speed adjustment based on the real-time dO value. Agitation speed varied between 200-700 RPM, depending on oxygen demand. Two separate pumps were used to control medium inflow and waste outflow rates.

To determine the specific growth rate before and after spiking chlorite into the chemostat, after induction of Cld or RFP expression, 10mL of OW94, or OW116 cells were inoculated into the bioreactor containing 1L MRM medium with 0.02% w/v arabinose and 50μg/mL of kanamycin. The chemostat at first operated as a batch culture (dilution rate equal to 0), until the culture reached mid-log phase (OD600 of ~0.7-1.0), then dilution rate was set to be approximately equal to the cell growth rate. This allowed the bioreactor to achieve a zero net growth while maintaining a near-maximum specific growth rate. 4mM of chlorite was spiked into the chemostat 1 hour later, and the dilution rate was adjusted in an attempt to reestablish the equilibrium state. The

specific growth rate before chlorite spike was determined based on the batch mode growth, whereas specific growth rate after the chlorite spike was calculated as the dilution rate plus actual growth or wash out rate [217]. All growth data were plotted and calculated using the Prism 7 software. The batch growth kinetics of stationary cells were tested in 96-well plate under different chlorite concentrations in MRM medium at 37 °C, with shaking, on a Tecan Sunrise microplate readers.

To test the effectiveness of chlorite as a biocide in the chemostat, after induction of Cld and RFP expression, 10 mL of RFP and cCld expressing *E.coli* strain OW115 cells were inoculated into the bioreactor containing 1L MRM medium with 0.02% w/v arabinose. We deliberately contaminated our reactor with 10 mL of creek water from Strawberry Creek (Berkeley, CA), which is heavily contaminated by coliforms such as *E. coli* [218]. The dilution rate was increased from 0 to 0.3/hr after the inoculated culture reached mid-log phase. After the reactor was deemed contaminated (when the culture changed color from pink to milky white), 8mM chlorite was spiked into both the reactor and medium reservoir. The negative control run did not receive the chlorite spike treatment. Culture samples were taken from the reactor twice a day, diluted 100 times in sterile MRM medium, and counted in a Guava® easyCyte flow cytometer. Total and RFP-positive cells from 15μL of each sample were counted based on red fluorescent signal. Flow-cytometry data were visualized and analyzed via the cloud-based Cytobank tool [219].

To test how chlorite affects bio-indigo production, 10mL of Fmo and cCld expressing *E.coli* strain OW117 overnight culture was inoculated into the chemostat containing 1L of MRM medium and 4mM chlorite, with 1g/L of tryptophan added to the medium to enhance bio-indigo yield. The negative control did not receive chlorite. The dilution rate was adjusted from 0 to 0.08/hr after the inoculated culture reached late-log phase. After indigo production yield stabilized (after 30 hours), 10mL of the Strawberry Creek water enrichment culture at OD ~2.0 was added into the bioreactor. To make the Strawberry Creek water enrichment culture, 1mL of Strawberry Creek water was mixed with 9mL of MRM medium, at 37°C, 250 rpm, overnight. Chlorite concentration was monitored and re-adjusted to 4mM. Samples were taken from the reactor twice a day to determine the bio-indigo yield.

Bio-Indigo extraction and measurement

Indigo is poorly soluble in water thus was extracted from bioreactor samples using dimethyl sulfoxide (DMSO). 180μL of DMSO was added to 20μL of culture, mixed by vortexing, and centrifuged at 13,000 rcf for 10 minutes to remove cells debris. The supernatant containing soluble indigo was transferred to a 96-well plate, and the concentration of indigo was determined based on absorption at 650 nm. Indigo

purchased from Sigma-Aldrich (CAS Number 482-89-3) was used to generate a standard curve.

Results

Cld expressing *E. coli* results in chlorite resistance

During our study of perchlorate reducing bacteria, we have observed that the naturally perchlorate-reducing bacterium *Azospira suillum* PS grew aerobically in the presence of 40 μM chlorite, while the *cld* deletion (*Δcld*) mutant failed to grow (unpublished observations). Additionally, heterologous Cld expression protected against chlorite toxicity in aerobic *Shewanella oneidensis* MR-1 (unpublished observations) and *Caulobacter crescentus* culture (Figure 4-1a, data produced by Kathleen Ryan lab). These data suggested that Cld plays an important role in chlorite resistance under aerobic conditions. We also tested and observed chlorite-induced phage inactivation in *C.crescentus* and *E.coli* lytic phages similar to a previous study (Figure 4-1 b,c, data for figure b was produced by Kathleen Ryan lab) [28]. These results imply that chlorite-induced phage inactivation could be a general phenomenon. These preliminary results also indicate that chlorite could be a superior treatment than traditional antibiotics in terms of activity spectrum, potency, and process economics. This inspired us to pursue a biocide/biocide resistance system based on chlorite and Cld.

In order to obtain a chlorite resistant microbial host with industrial applications, the wtCld from a chlorate reducer, *Shewanella algae* ACDC, was heterologously expressed in *E. coli* strain LMG194. The resulting strain, wtCld-expressing OW95 showed a three-fold increase in chlorite resistance (IC_{50} = 1.74mM, 95% confidence interval [CI] 1.56 to 1.94mM) compared to our negative controls RFP-expressing *E. coli*, OW94 (IC_{50} = 0.56mM, 95%CI = 0.55-0.58mM), and the parental LMG194 (IC_{50} = 0.30mM 95% CI = 0.28-0.31mM) (Figure 4-2). The RFP negative control was used to account for non-specific protein reactivity toward chlorite. Interestingly, enhanced chlorite resistance was observed in OW95 if Cld expression was induced at 26 °C, but not at 37 °C. However, after induction at 26 °C, OW95 cultures displayed enhanced chlorite resistance when tested at 37 °C, indicating the wtCld was functional at 37 °C but failed to express or fold properly.

To further enhance chlorite resistance, we conducted a directed evolution experiment with OW95 by repeatedly subculturing (with overnight cultures) the strain into increasing concentrations of chlorite at 37 °C. At the end of the directed evolution experiment, we obtained a chlorite hyper-resistant strain OW105 (IC_{50} = 4.60 mM, 95%CI =4.26 to 4.98mM) (Figure 4-2), and identified the causative mutation as an alanine to aspartate (A21D) mutation in the translocation signal peptide of Cld (see method for more detail). Such mutation likely inhibited signal peptide processing and/or translocation through the inner membrane. To test this hypothesis, western blot analysis was conducted with OW95, OW105, and a cCld (translocation signal peptide removed) expressing strain OW116 to determine the consequences of A21D mutation

(Figure 4-3, 4-4). As a periplasmic enzyme, unprocessed (with its signal peptide) Cld is predicted to translocate through the inner membrane via the Sec pathway [220], followed by peptidase cleavage of the signal peptide to produce the mature Cld with a slight decrease in molecular weight. In the western blot, bands indicating processed mature Cld at ~35 kDa could be seen in the purified Cld positive control, both soluble and insoluble fractions of OW95, and the soluble fraction of OW116, but was absent in OW105, and samples without arabinose induction. The mature Cld band in OW116 was significantly fainter than ones in OW95, which implies potential Cld copy number control in the cytoplasm. As expect, when induced with arabinose, a band corresponding to the unprocessed Cld was present in the OW95 insoluble fraction, but not in OW116, as cytoplasmic Cld does not go through peptidase processing. Interestingly, mature Cld was absent but one band that likely corresponds to unprocessed Cld was present in the insoluble fraction of OW105. Taken together, these results suggest that the A21D mutation in OW105-Cld resulted in loss of localization and/or signal peptide processing capability. Based on this observation, we predicted the cCld could potentially enhance chlorite tolerance. Strikingly, OW116 showed the highest chlorite resistance (IC_{50} = 8.94 mM, 95%CI = 8.07 to 9.93mM) (Figure 4-2) among different Cld-expressing strains, demonstrating that expression of cCld is more advantageous than the A21D mutant Cld or wtCld.

One explanation of the enhanced chlorite resistance in cCld expressing OW116 is through heightened chlorite decomposition activity, which is undesirable, as it would cause rapid chlorite degradation and loss of medium selectivity. Therefore, to compare Cld activity among different strains, we measured the chlorite dismutase activity of whole cells and cell lysates of OW94, OW95 and OW116 (Figure 4-5). As expected, OW94 did not react with chlorite, whereas OW95 demonstrated rapid Cld activity in both whole cells and cell lysate. Unexpectedly we did not detect significant Cld activity in OW116 whole cells and only observed low, though significant, Cld activity in OW116 cell lysate, indicating membrane impermeability limiting the influx of chlorite into the cytoplasm. The Cld activity in OW95 and OW116 cell lysates were much lower than published Cld activity in (per)chlorate reducer cell lysates [221-223], which ranged from 130 to 1928 umol of chlorite mg^{-1} minute^{-1}. These results suggested that the increased chlorite resistance in OW116 was not due to heightened Cld activity, but other unknown mechanisms involving the enzyme's cellular localization.

Exposure to chlorite causes growth arrest and oxidative stress, but these effects are greatly diminished in the cCld-expressing OW116

While our previous chlorite IC_{50} experiment determines the chlorite resistance based on cell yield, it does not account for changes of the specific growth rate. During continuous

bioprocessing, the bioreactor dilution (production) rate could be restricted by the specific growth rate of the processing organism; a slow-growing strain is unwanted and could potentially hamper overall volumetric yield. To understand the impact of chlorite on the specific growth rate of batch cultures, we assayed the growth kinetics of OW94 and OW116 under different chlorite concentrations (Figure 4-6). As chlorite concentration increased, the specific growth rate of OW94 drastically decreased (Figure 4-6a, c), but only reduced slightly in OW116 (Figure 4-6b, d). To investigate if a similar result can be seen in actively growing cultures, we spiked 4mM chlorite into bioreactors with growing OW94 or OW116 during the equilibrium growth state (Figure 4-6c, d, Figure 4-7). During equilibrium growth, the dilution rate is roughly equal to the maximum specific growth rate, resulting in a zero net growth while the cells are growing at near maximum growth rate. Before the chlorite spike, OW94 and OW116 were growing with a specific growth rate of 0.88 ± 0.39 and 0.87 ± 0.13 hr $^{-1}$, respectively. After the chlorite spike, OW94 never reached a new equilibrium growth state and washed out overtime despite our attempts to reestablish its equilibrium growth state by changing the dilution rate. Its specific growth rate also dropped to near or below zero $(0.01 \pm 0.07$ hr $^{-1})$ after the spike, indicating complete growth arrest and/or cell lyses. As expected, OW116 was still able to grow after the chlorite spike due to the protective effect of cCld; however, the specific growth rate of OW116 was reduced by ~20% to 0.64 ± 0.10 hr $^{-1}$.

To further investigate why the growth rate of OW116 was reduced and to gain insight for possible future strain improvement, we conducted proteomic experiments to compare the stress-induced protein expression profiles of OW94 and OW116, with and without chlorite. A total 52 proteins from the chlorite sensitive strain OW94 and 11 proteins from the chlorite resistant strain OW116 displayed peptide abundance changes greater than 2-fold in response to chlorite addition (Table 4-3). Eight stress response proteins were induced in OW94 (Figure 4-8): stress-induced chaperone Spy (Accession: P77754) and ClpB (Accession: P63284); periplasmic and membrane proteases DegP (Accession: P0C0V0) and HtpX (Accession: P23894); oxidative stress and redox homeostasis proteins Tpx (Accession: P0A862), Bcp (Accession: P0AE52), and TrxA (Accession: P0AA25); and acid stress protein GadB (Accession: P69910). These findings indicted that OW94 was experiencing chlorite-induced oxidative stress, which led to protein denaturation, misfolding and degradation, as well as a disturbed redox environment. In OW116 only the proteases DegP and HtpX were similarly induced, whereas other stress proteins up-regulated in OW94 remained mostly unchanged (Figure 4-8), implying a much milder effect of chlorite-induced oxidative stress.

Chlorite/Cld can be used as a biocide/biocide-resistance system for treatment or prevention of contamination in a continuous flow bioreactor

The final goal of this study was to demonstrate that chlorite in combination with Cld can be applied as a biocide/biocide resistant system to treat and prevent bioreactor contamination. To examine if addition of chlorite could rescue a contaminated bioreactor, we deliberately contaminated our reactor with 1% (v/v) raw environmental water sample from a site that is known to be heavily contaminated by coliforms [218], and subsequently treated it with 10mM chlorite. An *E.coli* strain expressing both cCld and RFP (OW115) that mimics an industrial protein production strain was used to inoculate bioreactors. Flow cytometry was performed to track RFP positive (RFP+) cells vs. total cells in the bioreactors. In the absence of chlorite, the RFP+ OW115 cells were slowly outcompeted by contaminants, as evidenced by the change in color of the cultures from red/pink to milky white (Figure 4-9a). Strikingly, after 10mM chlorite was spiked into the reactor, the culture returned to its original pink color as the contaminants were inhibited and washed out from the reactors. Flow cytometry showed a steady decline of the RFP+ population before the chlorite spike (Figure 4-9 a-d), followed by RFP+ cells recovery and reestablishment as the dominant population after the spike, consistent with our visual observation (Figure 4-9 a-d). In control cultures without chlorite addition, RFP-expressing cells continuously declined without recovery (Figure 6e). Our data thus indicate that chlorite can be used as a biocide to effectively eliminate contaminants in a continuous-flow bioreactor.

To demonstrate that chlorite can also protect a commodity bioprocessing strain from contamination, we constructed an *E.coli* strain (OW117) that constitutively expressed cCld and the indigo-producing, flavin-containing monooxygenase (FMO) from *Methylophaga aminisulfidivorans* MP [224, 225]; and a control *E.coli* strain (OW118) that constitutively expresses only FMO. An enriched microbial community (SCW enrichment) from Strawberry Creek was used to mimic environmental contaminants. We switched from the pBAD promoter to a constitutively active promoter due to an unknown compatibility problem of FMO with Cld and pBAD promoter (data not shown). In batch growth without chlorite, SCW enrichment culture showed faster growth kinetics than both OW117 and OW118 (Figure 4-10a); however, only OW118 could endure medium with chlorite due to the presence of cCld (Figure 4-10b, c). Unlike the robust chlorite resistance seen in OW116, chlorite addition resulted in a more severe defective growth phenotype in OW118, indicating that expression of flavin-containing protein likely exacerbated the chlorite-induced stress. To test whether the chlorite/Cld system also protects OW117 against SCW enrichment in a continuous flow system, we inoculated bioreactors with OW117 with and without the addition of 4 mM chlorite (Figure 4-10d). After two days of bio-indigo production, 10mL of the SCW enrichment

culture with an OD of ~2.0 was added to the bioreactors. As expected, indigo yields plummeted after the addition of contaminants in the absence of chlorite, presumably because OW117 failed to compete with the environmental microbes. However, in the presence of chlorite, indigo was steadily produced until the end of the experiment, indicating that chlorite addition can successfully prevent contamination of a continuous flow bioreactor.

Discussion

Contamination remains a major challenge in continuous bioprocessing as the processing strain can be easily outcompeted by microbial contaminants. Antibiotic use in continuous-flow bioreactor is undesirable due to its high cost. In contrast, the chlorite/Cld system offers a cheap, effective, and environmentally friendly alternative for bioreactor hygiene control and maintenance.

Heterologous expression of Cld in *E. coli* has been previously shown in many studies on the biochemical properties and enzymatic mechanisms of Cld, which have used purified Cld from *E. coli* [201, 204-211]. Nevertheless, this study is the first to demonstrate that Cld-expressing *E. coli* can tolerate high concentrations of chlorite. Expression of wtCld has been problematic; likely due to protein misfolding and/or co-factor limitation combined with sudden bursts of protein expression upon induction with a strong promoter such as the T7 promoter used in pET expression vectors. By using a lower copy vector and inducing at a relatively low temperature, we were able to functionally express wtCld that was correctly processed and translocated to the periplasm (as evidenced by shifted protein size).

Although we eventually discovered that cCld provides better protection against chlorite, the reasons for the remarkable difference of chlorite resistance and enzyme activity in OW95 and OW116 still remain obscure. One possibility is that cytoplasmic Cld expression is not as vigorous as periplasmic expression; western blot with normalized cell input showed a noticeably fainter cCld band compared to wtCld (Figure 4-3, 4-4). In addition, negatively charged chlorite molecules must pass through the inner membrane via transporters, therefore limiting the influx of chlorite into the cytoplasm. The enhanced chlorite resistance by cytoplasmic expression of the natural periplasmic Cld was unexpected, but rather unsurprising, as most of the aerobic electron transporting chain redox active sites that would be vulnerable to chlorite attack are cytoplasmic-facing enzymes. Although wtCld could rapidly detoxify the chlorite in the periplasm, there is no resistant mechanism to deal with chlorite once it passes through the inner membrane. In support of this, unlike wtCld, cCld no longer provide chlorite resistance under anaerobic growth condition with nitrate (which has the redox sites in the periplasm that are vulnerable to chlorite attack) (Figure 4-11).

Despite the expression of cCld in OW116, chlorite addition also reduced the specific growth rate by ~20-30% (Figure 4d), which was likely caused by the absence of Cld in the periplasm. Consistent with this idea, our proteomics data suggested that this is likely caused by chlorite-induced protein mis-folding and degradation, as periplasmic serine endoprotease DegP [226-228] and membrane-bound zinc metalloprotease HtpX [229, 230], both involved in heat shock stress, were also induced in response to chlorite

addition. This reduced growth rate probably can be alleviated by the co-expression of wtCld and cCld (to provide resistance in both the periplasm and cytoplasm), but expression of wtCld will inevitably increase chlorite degradation, which is undesirable for maintaining a stable chlorite concentration with biocide resistant activity. Further organism-specific genetic engineering are needed to completely erase any side effect of the chlorite addition.

It is important to note that this is only a proof-of-concept study, limitations exist and additional strain specific engineering are needed to optimize the biotransformation and bioprocessing yield with the chlorite/Cld system. For example, while we demonstrated that chlorite as a biocide is capable to treat and prevent microbial contamination in continuous-flow bioreactors, addition of chlorite during bio-indigo production resulted in yield decrease (data not shown), suggesting that chlorite could antagonistically react and damage the redox-active production enzymes (in our case the flavin enzyme Fmo). The current chlorite/Cld system is not applicable in anaerobic processes, as cCld does not provide protect cells against chlorite under anaerobic nitrate reducing condition. In addition, the processing host must contain a functional heme biosynthesis and/or uptake pathways for the expression Cld. Another potential issue with the chlorite/Cld system is contamination by environmental bacteria that naturally expresses Cld, such as (per)chlorate-reducing bacteria. However, to our knowledge, all known (per)chlorate reducers only harbor the periplasmic Cld, which provides minimal chlorite resistance compared to the cytoplasmic Cld thus cannot survive in our system.

Conclusion

In this study, we have demonstrated that cytoplasmic expression of *S. algae* strain ACDC Cld in *E. coli* can prevent and treat microbial contamination during continuous bioprocessing. The high chlorite resistance and low chlorite dismutase activity observed in cCld-expressing cells is ideal for maintaining a stable population of the desired strain in chlorite-containing bioreactors. We recommend a concentration of 4mM chlorite for *E.coli* continuous-flow bioreactors for maximal contaminant inhibition without adverse effects. This work establishes the use of chlorite and Cld as an alternative method for robust continuous bioprocessing and bioreactor hygiene control, which we wish to assist the transition from batch and fed-batch reactors to continuous-flow bioreactor in the biotech industry, and could significantly enhance the bioprocessing economics.

a

b

c
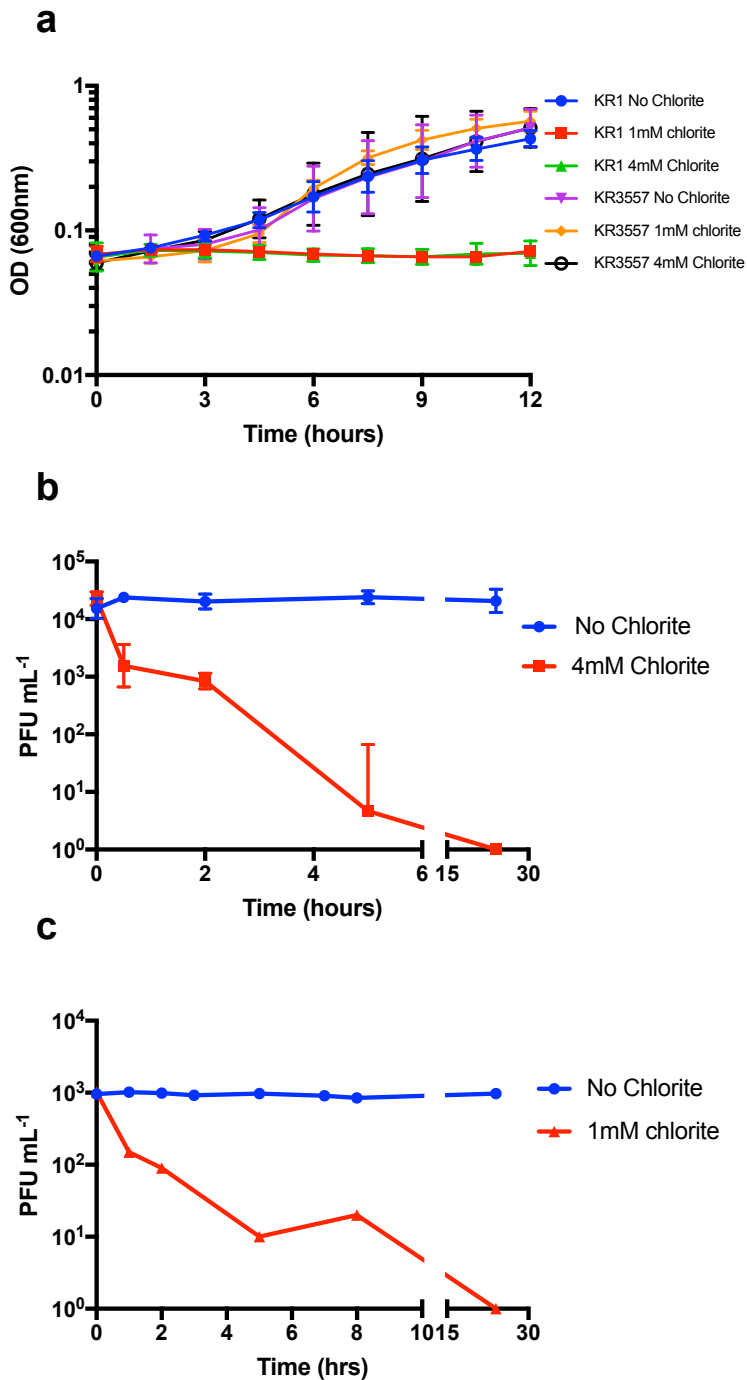
Figure 4-1. (a) Cld-expressing C. *crescentus* (KR3557) and C. *crescentus* with empty vector (KR1) growth with different chlorite concentrations. (b) *E.coli* and (c) C. *crescentus* phages deactivation by chlorite. For a and b, error bars represent the standard deviation of three biological replicates (n=3).
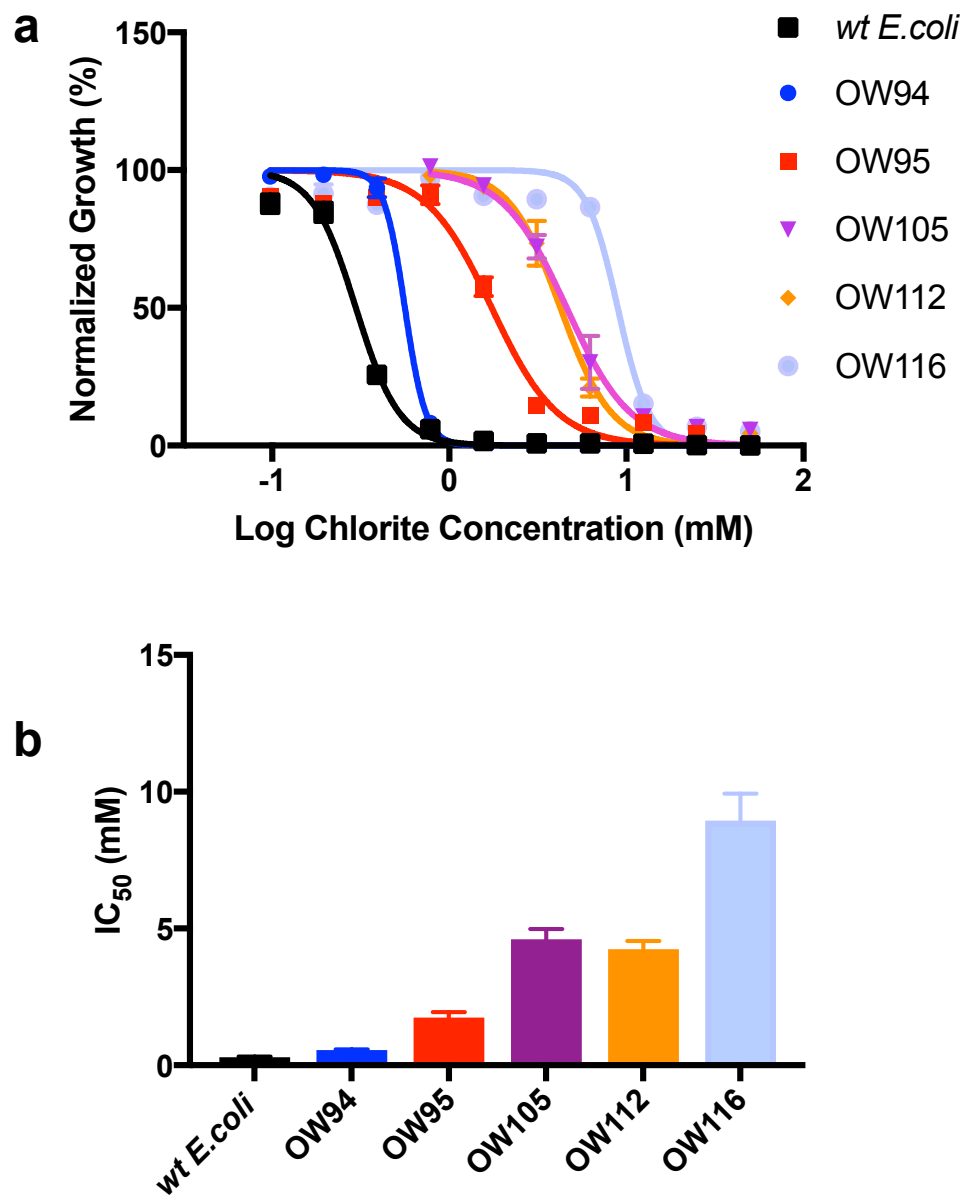
Figure 4-2. (a) Chlorite dose-response curves and (b) chlorite IC_{50} of different *E.coli* strains used in this study. Error bars represent the standard deviation of three biological replicates (n=3).

	Purified PS-Cld	OW95				OW116				OW105			
Fraction		S	S	I	I	S	S	I	I	S	S	I	I
Arabinose		-	+	-	+	-	+	-	+	-	+	-	+
35kda ->													
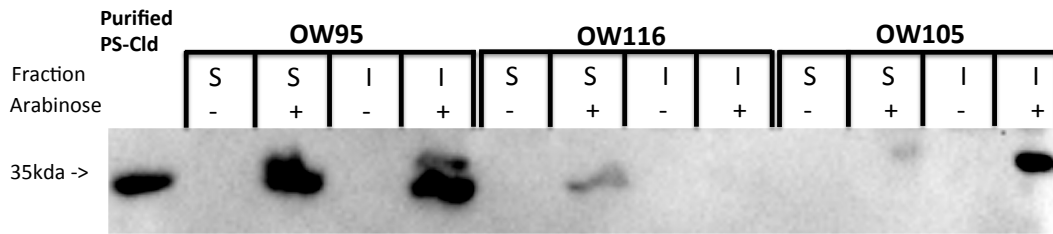
Figure 4-3. Cld Western blot of wtCld expressing *E.coli* OW95, and cCld expressing *E.coli* OW116, and A21D mutant Cld expressing *E.coli* OW105. Letter S and I indicate soluble and insoluble cellular fractions of the input. + and − signs indicate whether arabinose was added for protein induction. Purified Cld was loaded as a positive control. The uncropped full western blot image can be find at Figure 4-4.
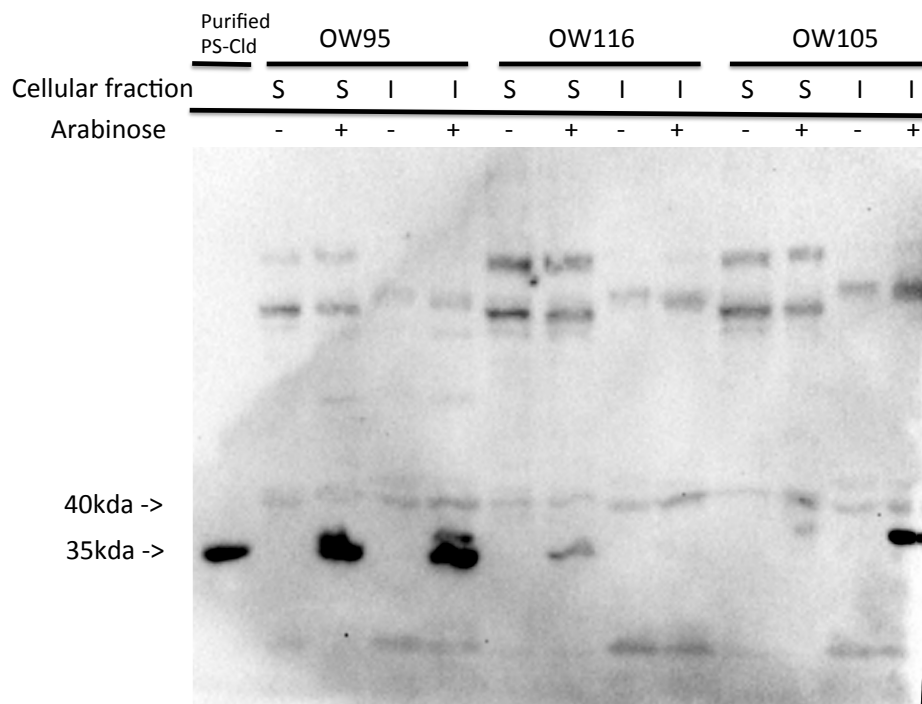
Figure 4-4. The uncropped full western blot image.
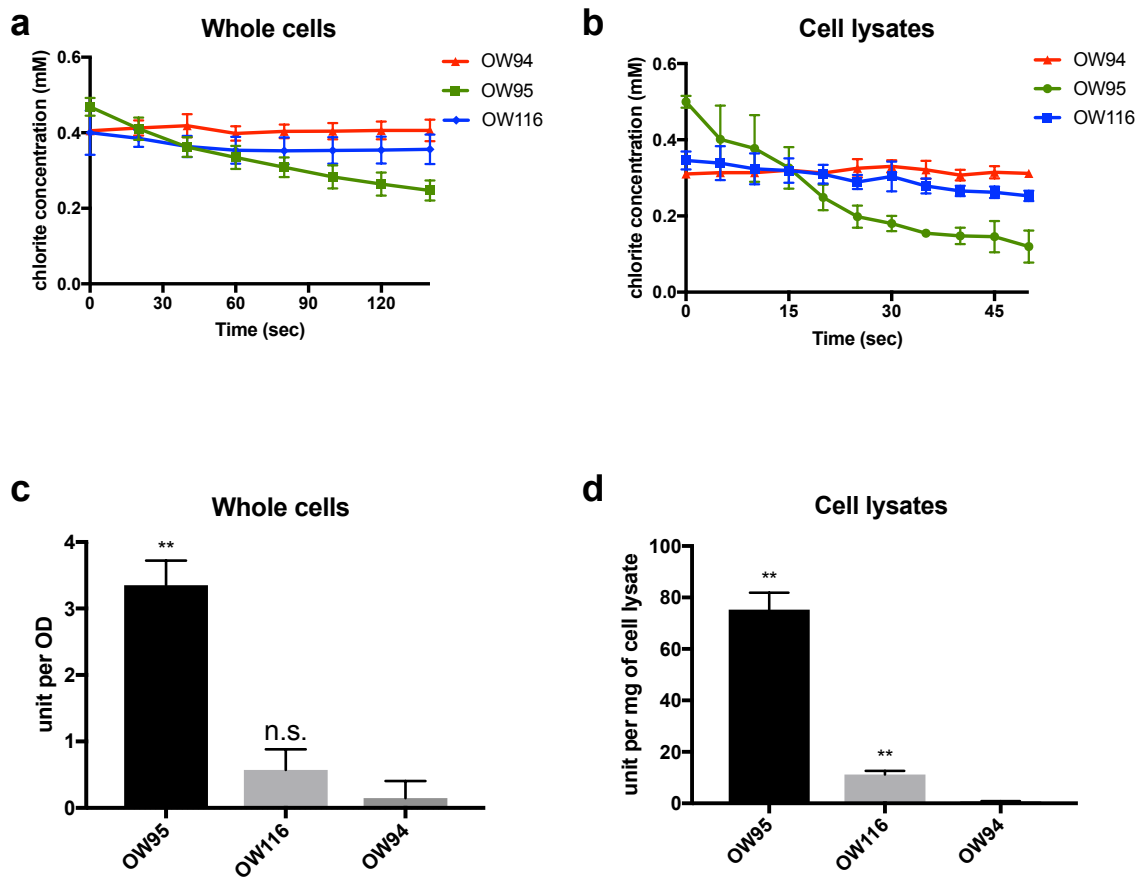
Figure 4-5 (a, b) Chlorite decomposition of whole cells and cell lysates of different strains overtime, respectively. (c, d) Cld activity of whole cells and cell lysates of different strains based on Figure 3a and 3b. One unit is defined as 1 μmol of chlorite decomposed by 1 OD/mL of cells or 1 mg of crude protein per minutes. ** indicates a *p*-value ≤ 0.01, n.s. indicates a P value > 0.05. *p*-values are calculated based on T test vs. negative control OW94.
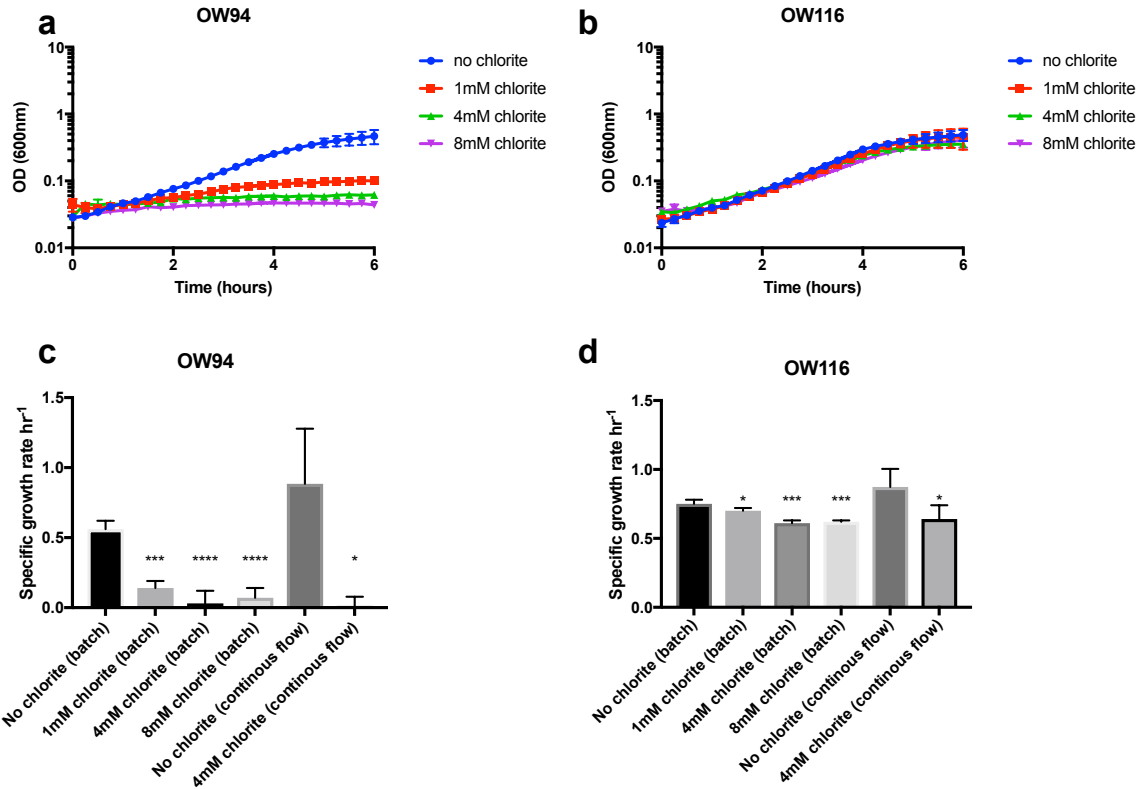
Figure 4-6 (a, b) Batch growth curves from RFP-expressing *E.coli* (OW94) and cCld-expressing *E.coli* (OW116) stationary cultures with different chlorite concentrations. (c, d) OW94 and OW116 specific growth rates of from batch culture stationary cells (batch) and continuous-flow bioreactor mid-log cells (continuous-flow). ****, ***, and * indicate a P value that ≤ 0.0001, ≤ 0.001, and ≤ 0.05, respectively. For batch cultures, *p*-values are calculated based on one-way ANOVA test vs. batch no chlorite controls. For continuous-flow cultures, *p*-values are calculated based on T test vs. continuous-flow no chlorite controls.
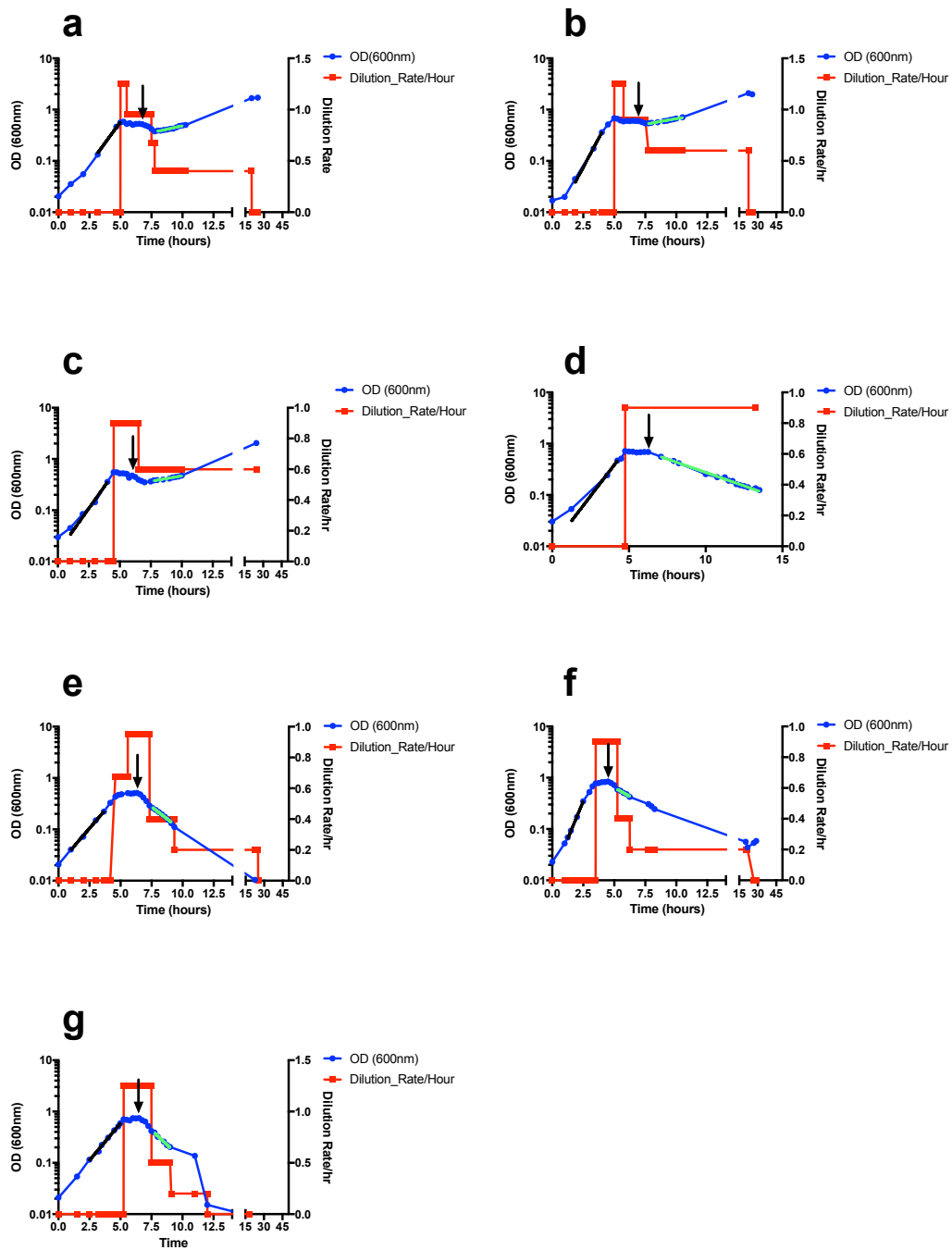
Figure 4-7. cCld expressing *E.coli* OW116 (a-d) and RFP expressing *E.coli* OW94 (e-g) bioreactors, showing changes in OD600nm before and after chlorite spike. Dilution rate was adjusted to maintain a growth equilibrium state before and after chlorite addition. Black and green bars indicate ranges used for specific growth rate calculation. Black arrows indicate chlorite spiking.
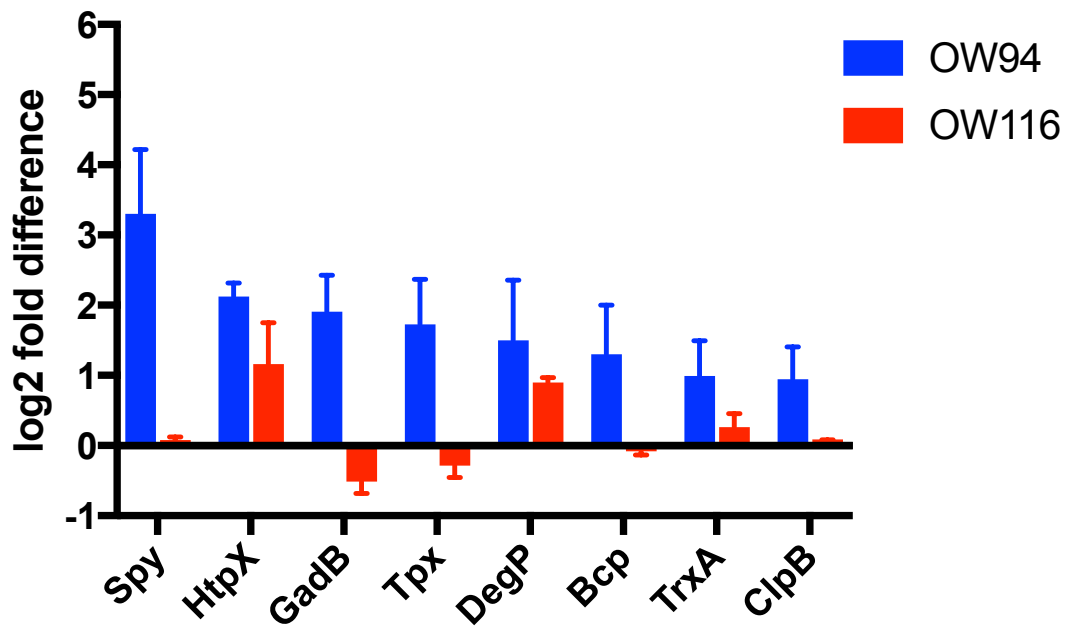
Figure 4-8. Differentially expressed stress-induced proteins in response to chlorite addition in OW94 and OW116. Fold change is calculated based on normalized peptides abundance. A protein with a confidence score > 100, p-value < 0.05, and maximal normalized peptide abundance fold change > 2, is considered differentially expressed.
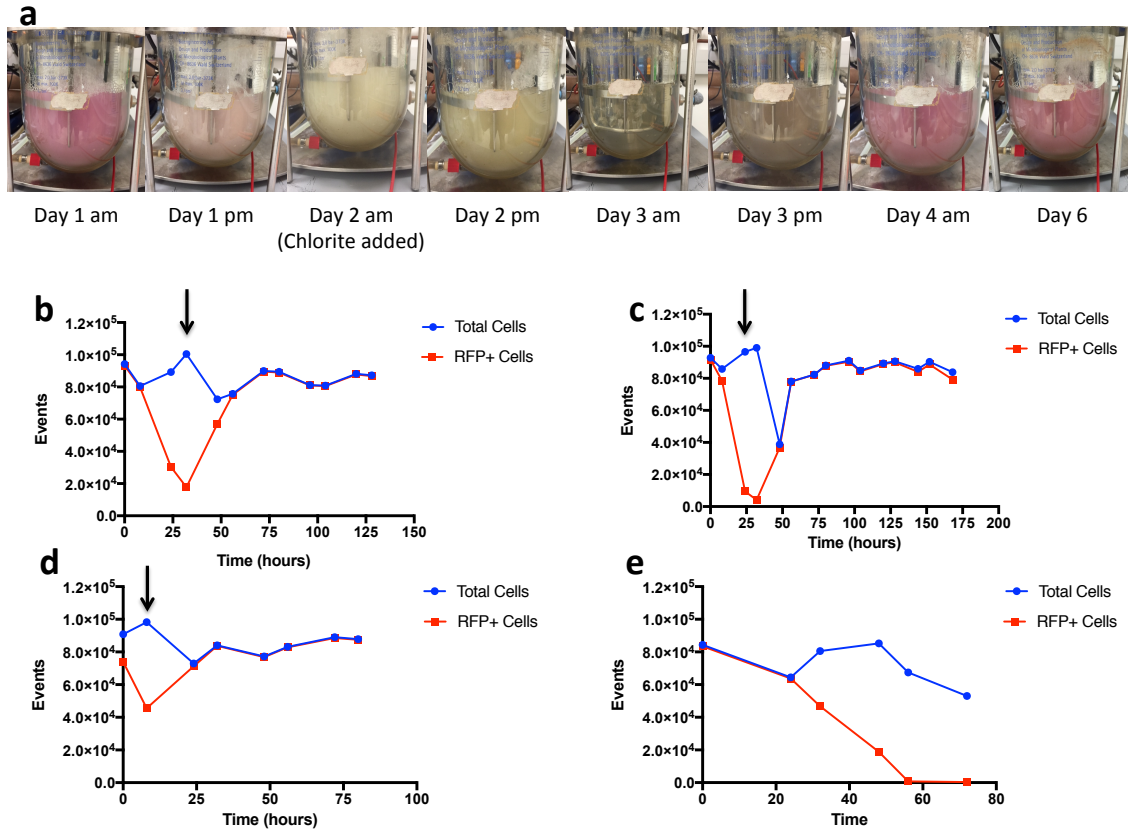
Figure 4-9. (a) Visual changes of RFP and cCld expressing OW115 bioreactor overtime, Strawberry Creek water was added along with OW115 inoculum at day 0 (not shown here), and chlorite was added at day 2 morning. (b-d) Flow cytometry quantification of total cells and RFP+ cells in three separated bioreactor runs. Black arrow indicates chlorite spiking. (e) Control reactor without chlorite that was contaminated.
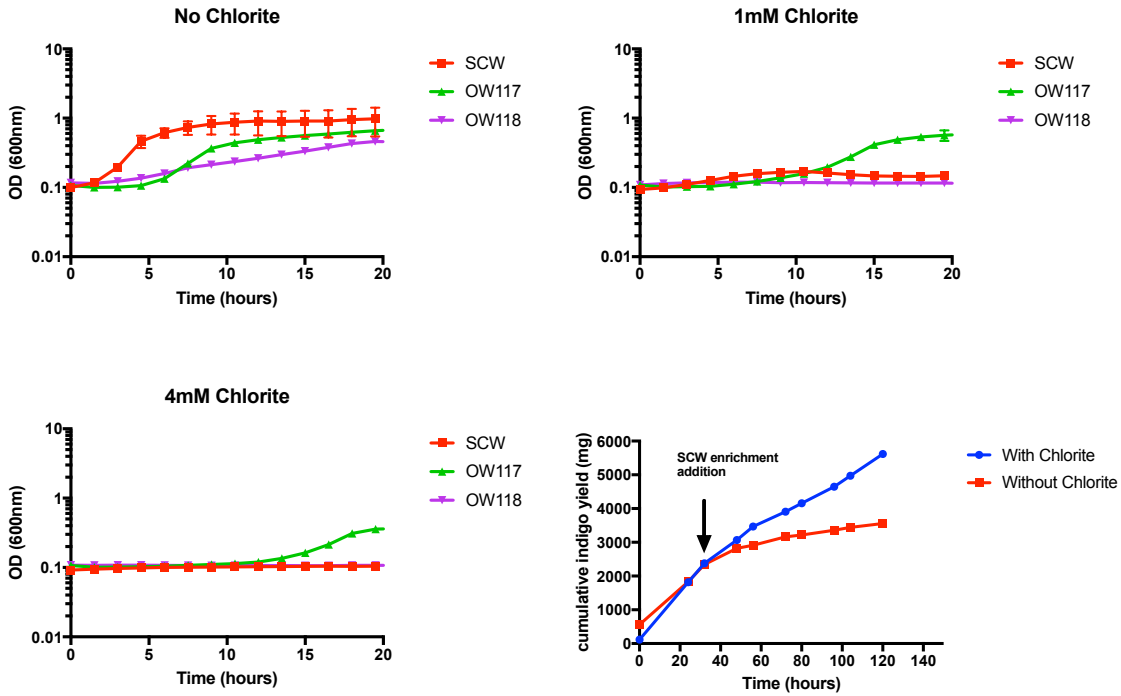
Figure 4-10. (a-c) Batch growth curves of Strawberry Creek enrichment (SCW), cCld and Fmo expressing *E.coli* (OW117), and Fmo expressing *E.coli* (OW118) with different chlorite concentrations. (d) Cumulative indigo yield in OW117 bioreactor, with or without chlorite. Contaminant was added after 30 hours.
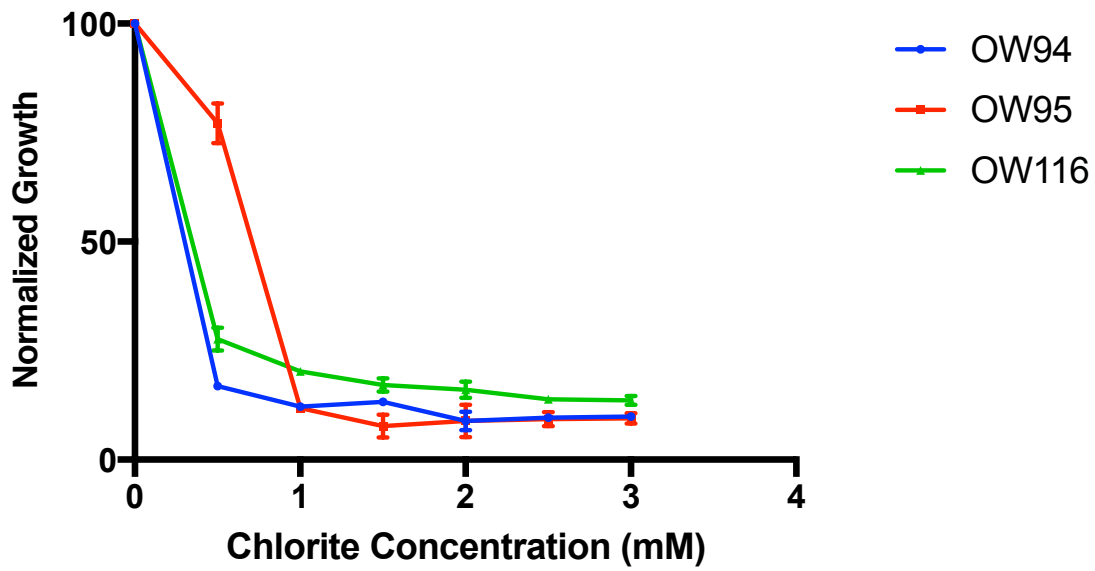
Figure 4-11. Chlorite dose-response curves under anaerobic nitrate reducing conditions of different strains. OW94, RFP expressing *E.coli*, OW95 wtCld expressing *E.coli*, OW116 cCld expressing *E.coli*.

Table 4-1. List of Strains and plasmids used in this study

Strain Name	Plasmid	Genotype / Description	Reference
E. coli LMG194	none	F- ΔlacX74 galE thi rpsL ΔphoA (Pvu II) Δara714 leu::Tn10, used as the pareantal strain for this study	Thermo Fisher Scientific
E. coli OW94	pICC49	Used for the expression of RFP by pICC49	This study
E. coli OW95	pICC63	Used for the expression of wtCld by pICC63	This study
E. coli OW105	pOW64	Resulting strain from the directed evolution of OW95, highly resistant to chlorite	This study
E. coli OW112	pOW64	LMG194 with the evovled plasmid, pOW64, from OW105	This study
E. coli OW115	pOW68	Used for the expression of RFP and cytoplasmic Cld	This study
E. coli OW116	pOW61	Used for the expression of cytoplasmic Cld	This study
E. coli OW117	pOW73	Used for the expression of Fmo and cytoplasmic Cld	This study
E. coli OW118	pTMH173	Used for the expression of Fmo	This study
C. crescentus KR1	pJS14	Empty vector control	Gift from Jeffrey Skerker
C. crescentus KR3557	pCAM1	Used for expression of wtCld	This study

Plasmid	Marker	Description	Reference
pICC49	Kanamycin	pICC44 containing rfp driven by the pBad promoter	Constructed by Iain Clark
pICC63	Kanamycin	pICC44 containing Shewanella algae strain acdc cld driven by the pBad promoter	Constructed by Iain Clark
pOW61	Kanamycin	pICC44 containing cytoplasmic Shewanella algae strain acdc cld driven by the pBad promoter	This study
pOW64	Kanamycin	plasmids extracted from OW105, same as pICC63 except a A21D mutation in Cld	This study
pOW68	Kanamycin	pICC44 containing rfp and cld driven by the pBad promoter	This study
pTMH173	Spectinomycin	containing fmo driven by the BBa_J23110 promoter	This study
pOW73	Spectinomycin	containing fmo and cytoplasmic cld driven by the BBa_J23110 promoter	This study
pJS14	Chloramphenicol	pJS14 empty vector	Gift from Jeffrey Skerker
pCAM1	Chloramphenicol	pJS14 containing Pseudomonas chloritidismutans cld driven by pXyl promoter	This study

Table 4-2 List of primers used in this study

Primer Name	Sequence	Description
pOW61L	CATGGATATCCCCTTGTGTGAAATAATC	round the horn PCR for making pOW61 from pICC63
pOW61R	CAGGCAATGCAACCCATGC	round the horn PCR for making pOW61 from pICC63
pICC49L	TTATTAAGCACCGGTGGAGTGAC	linearization of pICC49 for gibson assembly of pOW68
pICC49R	CGCTGATAGTGCTAGTGTAGATCG	linearization of pICC49 for gibson assembly of pOW68
pOW61cldF	ACTCCACCGGTGCTTAATAAATTTCACACAAGGGGATATCCATGC	making insert fragment from pOW61 for gibson assembly of pOW68
pOW61cldR	CTACACTAGCACTATCAGCGGAGGAACAGCCTTGCCGT	making insert fragment from pOW61 for gibson assembly of pOW68
pTMH173L	TTAGGATCCAGCCTCCTTGG	linearization of pTMH173 for gibson assembly of pOW73
pTMH173R	CTCGAGTTCAGCCAAAAAACTTAAGA	linearization of pTMH173 for gibson assembly of pOW73
pOW61cldF2	CCAAGGAGGCTGGATCCTAAAAGGTCGTCACTCCACCG	making insert fragment from pOW61 for gibson assembly of pOW73
pOW61cldR2	GTTTTTTGGCTGAACTCGAGTTACTCGGCAAGCGCCT	making insert fragment from pOW61 for gibson assembly of pOW73

Table 4-3 All differentially expressed proteins, and proteomic raw data of OW94 and OW116

	Confidence score	Anova (p)	Max fold change	Description
Peptides that significantly induced in OW116				
Accession	Confidence score	Anova (p)	Max fold change	Description
P0ABJ9	140.22	0.001	2.651	Cytochrome bd-I ubiquinol oxidase subunit 1 OS=Escherichia coli (strain K12) GN=cydA PE=1 SV=1
P12996	151.66	0.001	2.530	Biotin synthase OS=Escherichia coli (strain K12) GN=bioB PE=1 SV=2
P23894	133.09	0.042	2.370	Protease HtpX OS=Escherichia coli (strain K12) GN=htpX PE=1 SV=1
P00904	247.05	0.002	2.285	Bifunctional protein TrpGD OS=Escherichia coli (strain K12) GN=trpGD PE=1 SV=3
P0A763	100.34	0.001	2.269	Nucleoside diphosphate kinase OS=Escherichia coli (strain K12) GN=ndk PE=1 SV=2
P07014	167.40	0.001	2.139	Succinate dehydrogenase iron-sulfur subunit OS=Escherichia coli (strain K12) GN=sdhB PE=1 SV=1
P0AFG6	191.01	0.001	2.089	Component of 2-oxoglutarate dehydrogenase complex
P0ABI8	114.26	0.028	2.054	Cytochrome bo(3) ubiquinol oxidase subunit 1
P00909	253.07	0.002	2.040	Tryptophan biosynthesis protein TrpCF OS=Escherichia coli (strain K12) GN=trpC PE=1 SV=4
P0AFG3	494.22	0.000	1.949	2-oxoglutarate dehydrogenase E1 component OS=Escherichia coli (strain K12) GN=sucA PE=1 SV=1
P0A877	252.51	0.001	1.943	Tryptophan synthase alpha chain OS=Escherichia coli (strain K12) GN=trpA PE=1 SV=1
Peptides that significantly induced in OW94				
Accession	Confidence score	Anova (p)	Max fold change	Description
P00904	247.0545	0.003	11.248	Bifunctional protein TrpGD OS=Escherichia coli (strain K12) GN=trpGD PE=1 SV=3
P77754	236.7783	0.004	11.239	Periplasmic chaperone Spy OS=Escherichia coli (strain K12) GN=spy PE=1 SV=1
P00895	459.6082	0.005	7.309	Anthranilate synthase component 1 OS=Escherichia coli (strain K12) GN=trpE PE=1 SV=2
P0A903	187.6007	0.016	6.334	Outer membrane protein assembly factor BamC
P0C8J8	166.8629	0.002	4.764	D-tagatose-1,6-bisphosphate aldolase subunit GatZ
P23894	133.0922	0.000	4.380	Protease HtpX OS=Escherichia coli (strain K12) GN=htpX PE=1 SV=1
P0A877	252.5115	0.001	4.160	Tryptophan synthase alpha chain OS=Escherichia coli (strain K12) GN=trpA PE=1 SV=1
P69910;P69908	316.1407	0.004	3.921	Glutamate decarboxylase beta OS=Escherichia coli (strain K12) GN=gadB PE=1 SV=1
P0A879	241.5478	0.012	3.655	Tryptophan synthase beta chain OS=Escherichia coli (strain K12) GN=trpB PE=1 SV=2
P0A862	114.7718	0.010	3.542	Thiol peroxidase OS=Escherichia coli (strain K12) GN=tpx PE=1 SV=2
P0A8W8	139.1088	0.024	3.489	UPF0304 protein YfbU OS=Escherichia coli (strain K12) GN=yfbU PE=1 SV=1
P00561	359.1206	0.001	3.468	Bifunctional aspartokinase/homoserine dehydrogenase 1
P0ABK5	309.4595	0.035	3.424	Cysteine synthase A OS=Escherichia coli (strain K12) GN=cysK PE=1 SV=2
P37051	113.5089	0.009	3.420	Formyltetrahydrofolate deformylase
P06999	104.0634	0.014	3.239	ATP-dependent 6-phosphofructokinase isozyme 2
P0C0V0	221.6097	0.040	3.203	Periplasmic serine endoprotease DegP OS=Escherichia coli (strain K12) GN=degP PE=1 SV=1

P04846	101.6631	0.055	3.187	Lipoprotein 28 OS=Escherichia coli (strain K12) GN=nlpA PE=1 SV=1
P0AFG6	191.0053	0.034	3.047	Component of 2-oxoglutarate dehydrogenase complex
P0A6K6	155.2563	0.047	2.856	Phosphopentomutase OS=Escherichia coli (strain K12) GN=deoB PE=1 SV=1
P07650	192.7061	0.037	2.741	Thymidine phosphorylase OS=Escherichia coli (strain K12) GN=deoA PE=1 SV=3
P0AE52	117.0318	0.039	2.662	Putative peroxiredoxin bcp OS=Escherichia coli (strain K12) GN=bcp PE=1 SV=1
P17315	178.1409	0.018	2.661	Colicin I receptor OS=Escherichia coli (strain K12) GN=cirA PE=1 SV=2
P27306	209.3588	0.012	2.623	Soluble pyridine nucleotide transhydrogenase OS=Escherichia coli (strain K12) GN=sthA PE=1 SV=5
P0ADG7	309.5558	0.055	2.579	Inosine-5'-monophosphate dehydrogenase OS=Escherichia coli (strain K12) GN=guaB PE=1 SV=1
P07004	164.0568	0.005	2.574	Gamma-glutamyl phosphate reductase OS=Escherichia coli (strain K12) GN=proA PE=1 SV=2
P22188	177.0993	0.005	2.485	UDP-N-acetylmuramoyl-L-alanyl-D-glutamate--2,6-diaminopimelate ligase
P08506	240.3077	0.020	2.442	D-alanyl-D-alanine carboxypeptidase DacC OS=Escherichia coli (strain K12) GN=dacC PE=1 SV=2
P0AAI5	142.3683	0.006	2.436	3-oxoacyl-[acyl-carrier-protein] synthase 2 OS=Escherichia coli (strain K12) GN=fabF PE=1 SV=2
P0AD61	405.905	0.047	2.421	Pyruvate kinase I OS=Escherichia coli (strain K12) GN=pykF PE=1 SV=1
P0AET8	104.1525	0.004	2.400	7-alpha-hydroxysteroid dehydrogenase OS=Escherichia coli (strain K12) GN=hdhA PE=1 SV=1
P37330	146.4155	0.002	2.330	Malate synthase G OS=Escherichia coli (strain K12) GN=glcB PE=1 SV=3
P37759	146.9646	0.030	2.316	dTDP-glucose 4,6-dehydratase 1 OS=Escherichia coli (strain K12) GN=rfbB PE=3 SV=2
P33602	373.2806	0.006	2.307	NADH-quinone oxidoreductase subunit G OS=Escherichia coli (strain K12) GN=nuoG PE=1 SV=4
P76536	163.3851	0.030	2.276	Probable deferrochelatase/peroxidase YfeX OS=Escherichia coli (strain K12) GN=yfeX PE=1 SV=2
P07014	167.4006	0.013	2.260	Succinate dehydrogenase iron-sulfur subunit OS=Escherichia coli (strain K12) GN=sdhB PE=1 SV=1
P33195	409.453	0.006	2.254	Glycine dehydrogenase (decarboxylating) OS=Escherichia coli (strain K12) GN=gcvP PE=1 SV=3
P26646	148.8732	0.003	2.204	Probable acrylyl-CoA reductase AcuI OS=Escherichia coli (strain K12) GN=acuI PE=1 SV=1
P0A6X7	109.1504	0.026	2.180	Integration host factor subunit alpha OS=Escherichia coli (strain K12) GN=ihfA PE=1 SV=1
P0AEM9	232.9604	0.024	2.149	L-cystine-binding protein FliY OS=Escherichia coli (strain K12) GN=fliY PE=1 SV=1
P10378	123.7031	0.013	2.120	Enterobactin synthase component E OS=Escherichia coli (strain K12) GN=entE PE=1 SV=3
P0A6W5	150.4752	0.031	2.106	Transcription elongation factor GreA OS=Escherichia coli (strain K12) GN=greA PE=1 SV=1
P62620	198.3892	0.001	2.089	4-hydroxy-3-methylbut-2-en-1-yl diphosphate synthase (flavodoxin)
P08839	417.0484	0.041	2.088	Phosphoenolpyruvate-protein phosphotransferase
P0AA25	105.5885	0.034	2.075	Thioredoxin-1 OS=Escherichia coli (strain K12) GN=trxA PE=1 SV=2
P06959	455.0288	0.035	2.024	Dihydrolipoyllysine-residue acetyltransferase component of pyruvate dehydrogenase complex
P45577	135.6506	0.016	2.023	RNA chaperone ProQ OS=Escherichia coli (strain K12) GN=proQ PE=1 SV=2
P63284	732.9446	0.034	1.988	Chaperone protein ClpB OS=Escherichia coli (strain K12) GN=clpB PE=1 SV=1
P76116	174.8977	0.016	1.968	Uncharacterized protein YncE OS=Escherichia coli (strain K12)

				GN=yncE PE=1 SV=1
P37902	114.2336	0.044	1.966	Glutamate/aspartate import solute-binding protein
P15254	535.6712	0.024	1.949	Phosphoribosylformylglycinamidine synthase
P00954	190.3508	0.006	1.943	Tryptophan--tRNA ligase OS=Escherichia coli (strain K12) GN=trpS PE=1 SV=3

Chapter 5 Future Directions

Regulation of perchlorate and nitrate reductions

In the presence of both nitrate and perchlorate, (per)chlorate reducers almost always preferentially use nitrate over perchlorate. In chapter 2 of this dissertation we demonstrate that both pathways can actually co-occur and are not mutually exclusive. The exact inhibition mechanism of nitrate on the perchlorate pathway, if any, remains a mystery. Independent regulation of nitrate and perchlorate respiratory pathways likely plays an important role in controlling environmental electron acceptor preferential usage. As such, dissecting regulatory mechanisms remains an important goal for future studies. In nitrate reducing Alpha- and Gammaproteobacteria, nitrate respiration is regulated by the Crp/Fnr family of global transcriptional regulators, in addition to nitrate specific NarXL and NarQP two component systems that sense environmental activators, such as nitrate and nitrite [142, 146]. However, there is little known about the nitrate regulatory circuit in PS. The nitrate/nitrite sensors NarXL and NarQP are absent, and multiple Crp/Fnr transcriptional regulators are present, but there is difficulty in predicting which transcriptional regulator is involved in nitrate metabolism regulation.

The perchlorate metabolism regulatory circuit is also not characterized in PS. The PAS domain containing the protein PcrP, histidine kinase sensor PcrS, and response regulator PcrR comprise the putative transcriptional regulatory system that senses internal and/or external signals [98]. Based on homology to other systems, PcrS is likely regulated by PcrP to influence the phosphorylation state of PcrR which in turn interacts with RpoN to induce transcription of the *pcr* operon [98], However, the regulatory signal(s) that influence *pcr* operon induction via PcrPSR transcriptional regulatory system are still unknown. Future molecular and biochemical studies on PcrPSR are needed to gain better understanding of the perchlorate metabolism regulatory circuit.

Heterologous expression of perchlorate reduction pathway

The unique physical chemistry of perchlorate is proposed to play an important role in maintaining water in the liquid state on the Martian surface [231]. Future manned Mars colonization likely involves in situ resources utilization activities such as terraforming or extraterrestrial farming, which both require prior bioremediation of perchlorate. Currently there is no perchlorate reducer that are able to grow and perform perchlorate

reduction under the extreme Martian environments. A potential solution is to bioengineer an extremophile that can tolerate the harsh Martian environment to become a (per)chlorate reducer for bioremediation purposes.

The perchlorate reduction genes are encoded on a horizontally transferable perchlorate reduction genomic island (PRI). PRI harbors a total of 17 genes involved in the catalytic, sensory, and stress-responses aspects of perchlorate reduction. Among these genes only the catalytic and sensory genes are essential for perchlorate reduction in PS [149]. In theory, expression of the core perchlorate reduction genes, *pcrABCDQO* and *cld*, under a new, host-compatible promoter would provide the recipient host the necessary information to carry out perchlorate respiration, as long as the recipient is able to produce the enzyme cofactors (molybdopterin and heme) required. In fact, work conducted by my undergraduate research assistant Nazar Akhverdyan demonstrates that heterologous expression of *cld* in *E.coli* enabled cellular growth by indirect chlorite respiration, in both batch and continuous cultures (Akhverdyan, dissertation in press, 2018). Under anaerobic conditions, Cld in these *E.coli* strains dismutate chlorite to molecular oxygen, which is subsequently reduced to water by the quinol oxidase cytochrome *bd* to generate proton motive force. Future studies could utilize high-throughput golden gate cloning [232] coupled to PCR mutagenesis and/or directed evolution to bioengineer model microorganisms such as *E.coli* or an actual extremophile to become a (per)chlorate reducer for bioremediation purposes.

Cld expression and optimization in diverse hosts

While in chapter 4 we have successfully demonstrated the application of the biocide/biocide-resistant system to treat general contamination, further tests are needed to expand our technology to a broad diversity of known biomanufacturing systems and disparate processing organisms. The potential future objectives include: (1) Optimize Cld expression and chlorite resistance in eukaryotic (*Saccharomyces cerevisiae*, *Pichia pastoris*) and mammalian (Chinese Hamster Ovarian) cell lines. (2) Create a universal biocide-resistant cassette by utilizing phage or CRISPR/Cas9 mediated site-specific genome integration. These cassettes could then be readily transformed/transfected into existing industrial processing strains to avoid development of new cell lines. (3) As laboratory studies progress, future studies should seek out industrial trial opportunities and validate the system in pilot-scale bioreactors with actual industrial processing organisms.

Chapter 6 Conclusions

In closing, my Ph.D. dissertation sought to elucidate the molecular mechanisms and physiology of perchlorate respiration in the model (per)chlorate reducing bacteria, *A. suillum* PS; and my efforts were successful in transforming our fundamental knowledge of perchlorate reduction into applied biotechnologies to solve practical industry problems.

In this work, I demonstrate two genes (*pcrQ* and *pcrO*) that encode electron transfer cytochromes are essential for perchlorate respiration; but completely redundant and fully replaceable with their homologs *napC* and *napO* in the denitrification pathway. Nitrate often co-occurs in perchlorate-contaminated environments. As such, nitrate inhibition of perchlorate metabolism presents an obstacle in the bioattenuation of perchlorate in these environments, as electron donor amendment will stimulate unproductive nitrate reduction rather than perchlorate reduction. By rewiring the terminal electron transport pathways in PS we were able to engineer strains that preferentially reduce perchlorate or concurrently reduce both nitrate and perchlorate. This study improves our understanding of nitrate and perchlorate respiratory pathways in dissimilatory perchlorate reducing bacteria and identifies key functionally redundant electron carrier proteins in these pathways. These redundancies are important to consider for the past and future co-evolution of perchlorate and nitrate respiratory pathways as well as other oxyanion respiratory pathways by related enzymes.

I also conducted transcriptomic analysis of PS under different growth conditions to establish the expression profiles of enzymes involved in nitrate, chlorate, perchlorate, and aerobic respirations. The results of the transcriptomic study not only provide new insights into the model (per)chlorate reducing bacteria PS, but also serve as a hypotheses-generating foundation for future investigations.

Although the obvious application of perchlorate metabolisms lies in the bioremediation of (per)chlorate in contaminated environments, a diversity of innovative biotechnological applications has been proposed based on the unique metabolic abilities of perchlorate reducers. In this dissertation I briefly summarized the potential biotechnological applications of microbial (per)chlorate reduction, and constructed a biocide/biocide-resistant molecular marker for microbial contamination treatment and prevention during biomanufacturing. This system is based on the biocide chlorite, a toxic intermediate generated during perchlorate reduction, and the corresponding detoxifying enzyme, chlorite dismutase. This work establishes an alternative method for

robust continuous bioprocessing and bioreactor hygiene control, which we expect to assist the transition from batch and fed-batch reactors to continuous-flow bioreactor in the industry, and potentially reduce the upstream biomanufacturing cost by 20-50%.

Reference

1. Urbansky ET: **Perchlorate as an environmental contaminant**. *Environ Sci & Potlut Res* 2002, **9**(3):187-192.
2. Rajagopalan S, Anderson T, Cox S, Harvey G, Cheng Q, Jackson WA: **Perchlorate in Wet Deposition Across North America**. *Environmental Science & Technology* 2009, **43**(3):616-622.
3. Nilsson T, Rova M, Smedja Bäcklund A: **Microbial metabolism of oxochlorates: A bioenergetic perspective**. *Biochimica et Biophysica Acta (BBA) - Bioenergetics* 2013, **1827**(2):189-197.
4. Motzer WE: **Perchlorate: Problems, Detection, and Solutions**. *Environmental Forensics* 2001, **2**(4):301-311.
5. Dasgupta PK, Martinelango PK, Jackson WA, Anderson TA, Tian K, Tock RW, Rajagopalan S: **The Origin of Naturally Occurring Perchlorate: The Role of Atmospheric Processes**. *Environmental Science & Technology* 2005, **39**(6):1569-1575.
6. Catling D, Claire M, Zahnle K, Quinn R, Clark B, Hecht M, Kounaves S: **Atmospheric origins of perchlorate on Mars and in the Atacama**. *Journal of Geophysical Research: Planets (1991–2012)* 2010, **115**(E1).
7. Mastrocicco M, Di Giuseppe D, Vincenzi F, Colombani N, Castaldelli G: **Chlorate origin and fate in shallow groundwater below agricultural landscapes**. *Environmental Pollution* 2017, **231**(Part 2):1453-1462.
8. Kounaves SP, Stroble ST, Anderson RM, Moore Q, Catling DC, Douglas S, McKay CP, Ming DW, Smith PH, Tamppari LK *et al*: **Discovery of Natural Perchlorate in the Antarctic Dry Valleys and Its Global Implications**. *Environmental Science & Technology* 2010, **44**(7):2360-2364.
9. Urbanski T: **Chemistry and Technology of Explosives, vol. 4, pp. 602-620, Pergamon Press, New York**. 1988.
10. Urbansky ET: **Perchlorate Chemistry: Implications for Analysis and Remediation**. *Bioremediation Journal* 1998, **2**(2):81-95.
11. Roote D: **Technology Status Report–Perchlorate Treatment Technologies**. *Ground-Water Remediation Technologies Analysis Center* 2001.
12. Wolff J: **Perchlorate and the Thyroid Gland**. *Pharmacological Reviews* 1998, **50**(1):89-106.
13. Stanbury JB, Wyngaarden JB: **Effect of perchlorate on the human thyroid gland**. *Metabolism: clinical and experimental* 1952, **1**(6):533-539.
14. Clark JJJ: **Toxicology of Perchlorate**. In: *Perchlorate in the Environment*. Edited by Urbansky ET. Boston, MA: Springer US; 2000: 15-29.

15.   Abt E, Spungen J, Pouillot R, Gamalo-Siebers M, Wirtz M: **Update on dietary intake of perchlorate and iodine from U.S. food and drug administration/'s total diet study: 2008-2012**. *Journal of Exposure Science & Environmental Epidemiology* 2016.

16.   Engelbrektson A, Hubbard CG, Tom LM, Boussina A, Jin YT, Wong H, Piceno YM, Carlson HK, Conrad ME, Anderson G: **Inhibition of microbial sulfate reduction in a flow-through column system by (per) chlorate treatment**. *Frontiers in microbiology* 2014, **5**:315.

17.   Deshwal B, Lee H-K: **Kinetics and mechanism of chloride based chlorine dioxide generation process from acidic sodium chlorate**. *Journal of hazardous materials* 2004, **108**(3):173-182.

18.   Youngblut MD, Wang O, Barnum TP, Coates JD: **(Per) chlorate in Biology on Earth and Beyond**. *Annual Review of Microbiology* 2016, **70**:435-457.

19.   Coates JD, Achenbach LA: **Microbial perchlorate reduction: rocket-fuelled metabolism**. *Nature Reviews Microbiology* 2004, **2**(7):569-580.

20.   Condie LW: **Toxicological problems associated with chlorine dioxide**. *Journal (American Water Works Association)* 1986:73-78.

21.   Daniel FB, Condie LW, Robinson M, Stober JA, York RG, Olson GR, Wang S-R: **Comparative Subchronic Toxicity Studies of Three Disinfectants (PDF)**. *Journal (American Water Works Association)* 1990, **82**(10):61-69.

22.   Vanwijk DJ, Hutchinson TH: **The Ecotoxicity of Chlorate to Aquatic Organisms: A Critical Review**. *Ecotoxicology and Environmental Safety* 1995, **32**(3):244-253.

23.   Ingram PR, Homer NZ, Smith RA, Pitt AR, Wilson CG, Olejnik O, Spickett CM: **The interaction of sodium chlorite with phospholipids and glutathione: a comparison of effects in vitro, in mammalian and in microbial cells**. *Archives of Biochemistry and Biophysics* 2003, **410**(1):121-133.

24.   Ingram PR, Pitt AR, Wilson CG, Olejnik O, Spickett CM: **A comparison of the effects of ocular preservatives on mammalian and microbial ATP and glutathione levels**. *Free radical research* 2004, **38**(7):739-750.

25.   Gagnon G, Rand J, O'leary K, Rygel A, Chauret C, Andrews R: **Disinfectant efficacy of chlorite and chlorine dioxide in drinking water biofilms**. *Water Research* 2005, **39**(9):1809-1817.

26.   van Wijk DJ, Kroon SG, Garttener-Arends IC: **Toxicity of chlorate and chlorite to selected species of algae, bacteria, and fungi**. *Ecotoxicology and environmental safety* 1998, **40**(3):206-211.

27.   Allende A, McEvoy J, Tao Y, Luo Y: **Antimicrobial effect of acidified sodium chlorite, sodium chlorite, sodium hypochlorite, and citric acid on Escherichia coli O157: H7 and natural microflora of fresh-cut cilantro**. *Food Control* 2009, **20**(3):230-234.

28.   Bichai F, Barbeau B: **Assessing the disinfecting power of chlorite in drinking water**. *Water quality research journal of Canada* 2006, **41**(4):375-382.

29.   Luo Y, Lu S, Zhou B, Feng H: **Dual effectiveness of sodium chlorite for enzymatic browning inhibition and microbial inactivation on fresh-cut apples**. *LWT - Food Science and Technology* 2011, **44**(7):1621-1625.

30.   Dempster RP, Morales P, Glennon FX: **Use of Sodium Chlorite to Combat Anchorworm Infestations of Fish**. *The Progressive Fish-Culturist* 1988, **50**(1):51-55.

31.   Åslander A: **Experiments on the Eradication of Canada Thistle: Cirsium Arvense, with Chlorates and Other Herbicides**: US Government Printing Office; 1928.

32.   Youngblut MD, Tsai C-L, Clark IC, Carlson HK, Maglaqui AP, Gau-pan PS, Redford SA, Wong A, Tainer JA, Coates JD: **Perchlorate Reductase is Distinguished by Active Site Aromatic Gate Residues**. *Journal of Biological Chemistry* 2016.

33.   Clark IC, Melnyk RA, Engelbrektson A, Coates JD: **Structure and evolution of chlorate reduction composite transposons**. *Mbio* 2013, **4**(4):e00379-00313.

34.   Clark IC, Melnyk RA, Iavarone AT, Novichkov PS, Coates JD: **Chlorate reduction in Shewanella algae ACDC is a recently acquired metabolism characterized by gene loss, suboptimal regulation and oxidative stress**. *Molecular microbiology* 2014, **94**(1):107-125.

35.   Clark IC, Melnyk RA, Youngblut MD, Carlson HK, Iavarone AT, Coates JD: **Synthetic and evolutionary construction of a chlorate-reducing Shewanella oneidensis MR-1**. *MBio* 2015, **6**(3):e00282-00215.

36.   Clark IC, Youngblut M, Jacobsen G, Wetmore KM, Deutschbauer A, Lucas L, Coates JD: **Genetic dissection of chlorate respiration in Pseudomonas stutzeri PDA reveals syntrophic (per) chlorate reduction**. *Environmental Microbiology* 2016, **18**(10):3342-3354.

37.   Thorell HD, Stenklo K, Karlsson J, Nilsson T: **A gene cluster for chlorate metabolism in Ideonella dechloratans**. *Applied and environmental microbiology* 2003, **69**(9):5585-5592.

38.   Coates J, Jackson A: **Principles of perchlorate treatment. In situ bioremediation of perchlorate in groundwater**. In.: Springer Verlag, Norwell, MA; 2008.

39.   Srinivasan A, Viraraghavan T: **Perchlorate: health effects and technologies for its removal from water resources**. *International Journal of Environmental Research and Public Health* 2009, **6**(4):1418-1442.

40.   Stepanov VG, Xiao Y, Tran Q, Rojas M, Willson RC, Fofanov Y, Fox GE, Roberts DJ: **The presence of nitrate dramatically changed the predominant microbial community in perchlorate degrading cultures under saline conditions**. *BMC Microbiology* 2014, **14**(1):225.

41. Carlström CI, Loutey DE, Wang O, Engelbrektson A, Clark I, Lucas LN, Somasekhar PY, Coates JD: **Phenotypic and genotypic description of Sedimenticola selenatireducens strain CUZ, a marine (per) chlorate-respiring gammaproteobacterium, and its close relative the chlorate-respiring Sedimenticola strain NSS**. *Applied and environmental microbiology* 2015, **81**(8):2717-2726.

42. Carlström CI, Wang O, Melnyk RA, Bauer S, Lee J, Engelbrektson A, Coates JD: **Physiological and Genetic Description of Dissimilatory Perchlorate Reduction by the Novel Marine Bacterium Arcobacter sp. Strain CAB**. *mBio* 2013, **4**(3).

43. Okeke BC, Giblin T, Frankenberger Jr WT: **Reduction of perchlorate and nitrate by salt tolerant bacteria**. *Environmental Pollution* 2002, **118**(3):357-363.

44. Xiao Y, Roberts DJ: **Kinetics Analysis of a Salt-Tolerant Perchlorate-Reducing Bacterium: Effects of Sodium, Magnesium, and Nitrate**. *Environmental Science & Technology* 2013, **47**(15):8666-8673.

45. Ahn CH, Oh H, Ki D, Van Ginkel SW, Rittmann BE, Park J: **Bacterial biofilm-community selection during autohydrogenotrophic reduction of nitrate and perchlorate in ion-exchange brine**. *Appl Microbiol Biotechnol* 2009, **81**(6):1169-1177.

46. Chung J, Shin S, Oh J: **Characterization of a microbial community capable of reducing perchlorate and nitrate in high salinity**. *Biotechnology letters* 2009, **31**(7):959-966.

47. Zuo G, Roberts D, Lehman S, Jackson G, Fox G, Willson R: **Molecular assessment of salt-tolerant, perchlorate-and nitrate-reducing microbial cultures**. *Water Science and Technology* 2009, **60**(7):1745-1756.

48. Giblin TL, Herman DC, Frankenberger W: **Removal of perchlorate from ground water by hydrogen-utilizing bacteria**. *Journal of Environmental Quality* 2000, **29**(4):1057-1062.

49. Logan BE, LaPoint D: **Treatment of perchlorate-and nitrate-contaminated groundwater in an autotrophic, gas phase, packed-bed bioreactor**. *Water Research* 2002, **36**(14):3647-3653.

50. Miller JP, Logan BE: **Sustained perchlorate degradation in an autotrophic, gas-phase, packed-bed bioreactor**. *Environmental science & technology* 2000, **34**(14):3018-3022.

51. Nerenberg R, Rittmann B: **Hydrogen-based, hollow-fiber membrane biofilm reactor for reduction of perchlorate and other oxidized contaminants**. *Water Science and Technology* 2004, **49**(11-12):223-230.

52. Son A, Lee J, Chiu PC, Kim BJ, Cha DK: **Microbial reduction of perchlorate with zero-valent iron**. *Water research* 2006, **40**(10):2027-2032.

53.   Sahu AK, Conneely T, Nüsslein KR, Ergas SJ: **Biological perchlorate reduction in packed bed reactors using elemental sulfur**. *Environmental science & technology* 2009, **43**(12):4466-4471.

54.   Xu J, Song Y, Min B, Steinberg L, Logan BE: **Microbial degradation of perchlorate: principles and applications**. *Environmental Engineering Science* 2003, **20**(5):405-422.

55.   Hatzinger PB: **Perchlorate Biodegradation for Water Treatment**. *Environmental Science & Technology* 2005, **39**(11):239A-247A.

56.   Brown JC, Anderson RD, Min JH, Boulos L, Prasifka D, Juby GJ: **Fixed-bed biological treatment of perchlorate-contaminated drinking water**. *Journal (American Water Works Association)* 2005, **97**(9):70-81.

57.   Thrash JC, Coates JD: **Review: direct and indirect electrical stimulation of microbial metabolism**. *Environmental science & technology* 2008, **42**(11):3921-3931.

58.   Thrash JC, Van Trump JI, Weber KA, Miller E, Achenbach LA, Coates JD: **Electrochemical stimulation of microbial perchlorate reduction**. *Environmental science & technology* 2007, **41**(5):1740-1746.

59.   Rook JJ: **Haloforms in drinking water**. *Journal (American Water Works Association)* 1976, **68**:168-172.

60.   Coates JD, Thrash CJ: **Bioelectrical treatment of xenobiotics**. In.: US Patent Office; 2007.

61.   Shea C, Clauwaert P, Verstraete W, Nerenberg R: **Adapting a denitrifying biocathode for perchlorate reduction**. *Water Science & Technology* 2008, **58**(10):1941.

62.   Clark IC, Carlson HK, Iavarone AT, Coates JD: **Bioelectrical redox cycling of anthraquinone-2, 6-disulfonate coupled to perchlorate reduction**. *Energy & Environmental Science* 2012, **5**(7):7970-7978.

63.   Dang Y, Holmes DE, Zhao Z, Woodard TL, Zhang Y, Sun D, Wang L, Nevin KP, Lovley DR: **Enhancing anaerobic digestion of complex organic waste with carbon-based conductive materials**. *Bioresource Technology* 2016, **220**:516-522.

64.   Lovley DR: **Electromicrobiology**. *Annual Reviews in Microbiology* 2012, **66**(1):391-409.

65.   El Aribi H, Le Blanc YJ, Antonsen S, Sakuma T: **Analysis of perchlorate in foods and beverages by ion chromatography coupled with tandem mass spectrometry (IC-ESI-MS/MS)**. *Analytica Chimica Acta* 2006, **567**(1):39-47.

66.   Jackson P, Gokhale S, Streib T, Rohrer J, Pohl C: **Improved method for the determination of trace perchlorate in ground and drinking waters by ion chromatography**. *Journal of Chromatography A* 2000, **888**(1):151-158.

67.   Valentín-Blasini L, Blount BC, Delinsky A: **Quantification of iodide and sodium-iodide symporter inhibitors in human urine using ion**

chromatography tandem mass spectrometry. *Journal of Chromatography A* 2007, **1155**(1):40-46.

68. Coates JD, Heinnickel M, Achenbach LA: **An enzymatic bioassay for perchlorate**. In.: DTIC Document; 2010.

69. Heinnickel M, Smith SC, Koo J, O'Connor SM, Coates JD: **A bioassay for the detection of perchlorate in the ppb range**. *Environmental science & technology* 2011, **45**(7):2958-2964.

70. Glavin DP, Freissinet C, Miller KE, Eigenbrode JL, Brunner AE, Buch A, Sutter B, Archer PD, Atreya SK, Brinckerhoff WB *et al*: **Evidence for perchlorates and the origin of chlorinated hydrocarbons detected by SAM at the Rocknest aeolian deposit in Gale Crater**. *Journal of Geophysical Research: Planets* 2013, **118**(10):1955-1973.

71. Navarro‐González R, Vargas E, Rosa Jdl, Raga AC, McKay CP: **Reanalysis of the Viking results suggests perchlorate and organics at midlatitudes on Mars**. *Journal of Geophysical Research: Planets* 2010, **115**(E12).

72. Jackson WA, Davila AF, Sears DWG, Coates JD, McKay CP, Brundrett M, Estrada N, Böhlke JK: **Widespread occurrence of (per)chlorate in the Solar System**. *Earth and Planetary Science Letters* 2015, **430**:470-476.

73. Davila AF, Willson D, Coates JD, McKay CP: **Perchlorate on Mars: a chemical hazard and a resource for humans**. *International Journal of Astrobiology* 2013, **12**(4):321-325.

74. Urbansky ET, Brown SK: **Perchlorate retention and mobility in soils**. *Journal of environmental monitoring : JEM* 2003, **5**(3):455-462.

75. Gieg LM, Jack TR, Foght JM: **Biological souring and mitigation in oil reservoirs**. *Applied Microbiology and Biotechnology* 2011, **92**(2):263.

76. Gregoire P, Engelbrektson A, Hubbard CG, Metlagel Z, Csencsits R, Auer M, Conrad ME, Thieme J, Northrup P, Coates JD: **Control of sulfidogenesis through bio‐oxidation of H2S coupled to (per) chlorate reduction**. *Environmental microbiology reports* 2014, **6**(6):558-564.

77. Youssef N, Elshahed MS, McInerney MJ: **Microbial processes in oil fields: culprits, problems, and opportunities**. *Advances in applied microbiology* 2009, **66**:141-251.

78. Carlson HK, Kuehl JV, Hazra AB, Justice NB, Stoeva MK, Sczesnak A, Mullan MR, Iavarone AT, Engelbrektson A, Price MN: **Mechanisms of direct inhibition of the respiratory sulfate-reduction pathway by (per) chlorate and nitrate**. *The ISME journal* 2015, **9**(6):1295-1305.

79. Voordouw G, Grigoryan AA, Lambo A, Lin S, Park HS, Jack TR, Coombe D, Clay B, Zhang F, Ertmoed R: **Sulfide remediation by pulsed injection of nitrate into a low temperature Canadian heavy oil reservoir**. *Environmental science & technology* 2009, **43**(24):9512-9518.

80. Hubert C: **Microbial ecology of oil reservoir souring and its control by nitrate injection**. In: *Handbook of Hydrocarbon and Lipid Microbiology.* Springer; 2010: 2753-2766.

81. Lovley DR, Goodwin S: **Hydrogen concentrations as an indicator of the predominant terminal electron accepting reactions in aquatic sediments.** *Geochim Cosmochim Acta* 1988, **52**:2993-3003.

82. Callbeck CM, Agrawal A, Voordouw G: **Acetate production from oil under sulfate-reducing conditions in bioreactors injected with sulfate and nitrate**. *Applied and environmental microbiology* 2013, **79**(16):5059-5068.

83. Moura I, Bursakov S, Costa C, Moura JJ: **Nitrate and nitrite utilization in sulfate-reducing bacteria**. *Anaerobe* 1997, **3**(5):279-290.

84. Mehta-Kolte MG, Loutey D, Wang O, Youngblut MD, Hubbard CG, Wetmore KM, Conrad ME, Coates JD: **Mechanism of H2S Oxidation by the Dissimilatory Perchlorate-Reducing Microorganism Azospira suillum PS**. *mBio* 2017, **8**(1):e02023-02016.

85. Carmona M, Zamarro MT, Blázquez B, Durante-Rodríguez G, Juárez JF, Valderrama JA, Barragán MJ, García JL, Díaz E: **Anaerobic catabolism of aromatic compounds: a genetic and genomic view**. *Microbiology and Molecular Biology Reviews* 2009, **73**(1):71-133.

86. Díaz E, Jiménez JI, Nogales J: **Aerobic degradation of aromatic compounds**. *Current opinion in biotechnology* 2013, **24**(3):431-442.

87. Samanta SK, Singh OV, Jain RK: **Polycyclic aromatic hydrocarbons: environmental pollution and bioremediation**. *TRENDS in Biotechnology* 2002, **20**(6):243-248.

88. Basu A, Apte SK, Phale PS: **Preferential utilization of aromatic compounds over glucose by Pseudomonas putida CSV86**. *Applied and environmental microbiology* 2006, **72**(3):2226-2230.

89. Jiménez JI, Miñambres B, García JL, Díaz E: **Genomic analysis of the aromatic catabolic pathways from Pseudomonas putida KT2440**. *Environmental microbiology* 2002, **4**(12):824-841.

90. Lovley D: **Potential for anaerobic bioremediation of BTEX in petroleum-contaminated aquifers**. *Journal of Industrial Microbiology & Biotechnology* 1997, **18**(2):75-81.

91. Fuchs G, Boll M, Heider J: **Microbial degradation of aromatic compounds—from one strategy to four**. *Nature Reviews Microbiology* 2011, **9**(11):803-816.

92. Ismail W, Gescher J: **Epoxy Coenzyme A Thioester pathways for degradation of aromatic compounds**. *Applied and environmental microbiology* 2012, **78**(15):5043-5051.

93. Coates JD, Chakraborty R, Lack JG, O'connor SM, Cole KA, Bender KS, Achenbach LA: **Anaerobic benzene oxidation coupled to nitrate reduction in**

pure culture by two strains of Dechloromonas. *Nature* 2001, **411**(6841):1039-1043.

94. Brundrett M, Horita J, Anderson T, Pardue J, Reible D, Jackson WA: **The use of chlorate, nitrate, and perchlorate to promote crude oil mineralization in salt marsh sediments**. *Environ Sci & Potlut Res* 2015, **22**(20):15377-15385.

95. Coates JD, Bruce RA, Haddock JD: **Anoxic bioremediation of hydrocarbons**. *Nature* 1998, **396**:730.

96. Coates JD, Bruce RA, Patrick JA, Achenbach LA: **Hydrocarbon bioremediative potential of (per)chlorate-reducing bacteria**. *Bioremediation Journal* 1999, **3**:323-334.

97. Miller LG, Baesman SM, Carlstrom CI, Coates JD, Oremland RS: **Methane oxidation linked to chlorite dismutation.** *Frontiers in Microbiology* 2014, **5**.

98. Melnyk RA, Clark IC, Liao A, Coates JD: **Transposon and Deletion Mutagenesis of Genes Involved in Perchlorate Reduction in Azospira suillum PS**. *mBio* 2014, **5**(1).

99. Melnyk RA, Youngblut MD, Clark IC, Carlson HK, Wetmore KM, Price MN, Iavarone AT, Deutschbauer AM, Arkin AP, Coates JD: **Novel Mechanism for Scavenging of Hypochlorite Involving a Periplasmic Methionine-Rich Peptide and Methionine Sulfoxide Reductase**. *mBio* 2015, **6**(3):e00233-00215.

100. Callanan MJ, Klaenhammer TR: **Bacteriophages in industry**. *eLS* 2008.

101. Jones DT, Shirley M, Wu X, Keis S: **Bacteriophage infections in the industrial acetone butanol (AB) fermentation process**. *Journal of molecular microbiology and biotechnology* 2000, **2**(1):21-26.

102. Marcó MB, Moineau S, Quiberoni A: **Bacteriophages and dairy fermentations**. *Bacteriophage* 2012, **2**(3):149-158.

103. Verreault D, Gendron L, Rousseau GM, Veillette M, Massé D, Lindsley WG, Moineau S, Duchaine C: **Detection of Airborne Lactococcal Bacteriophages in Cheese Manufacturing Plants**. *Applied and Environmental Microbiology* 2011, **77**(2):491-497.

104. Dassama LM, Yosca TH, Conner DA, Lee MH, Blanc Ba, Streit BR, Green MT, DuBois JL, Krebs C, Bollinger Jr JM: **O2-evolving chlorite dismutase as a tool for studying O2-utilizing enzymes**. *Biochemistry* 2012, **51**(8):1607-1616.

105. Garcia-Ochoa F, Gomez E: **Bioreactor scale-up and oxygen transfer rate in microbial processes: an overview**. *Biotechnology Advances* 2009, **27**(2):153-176.

106. Karimi A, Golbabaei F, Mehrnia MR, Neghab M, Mohammad K, Nikpey A, Pourmand MR: **Oxygen mass transfer in a stirred tank bioreactor using different impeller configurations for environmental purposes**. *Iranian journal of environmental health science & engineering* 2013, **10**(1):6.

107. Krebs C, Dassama LM, Matthews ML, Jiang W, Price JC, Korboukh V, Li N, Bollinger JM: **Novel approaches for the accumulation of oxygenated**

intermediates to multi-millimolar concentrations. *Coordination chemistry reviews* 2013, **257**(1):234-243.

108.   Martín M, Montes FJ, Galán MA: **Bubbling process in stirred tank reactors II: Agitator effect on the mass transfer rates**. *Chemical Engineering Science* 2008, **63**(12):3223-3234.

109.   Mölder E, Mashirin A, Tenno T: **Measurement of the Oxygen Mass Transfer Through the Air-Water Interface (5 pp)**. *Environ Sci & Potlut Res* 2005, **12**(2):66-70.

110.   Rui Z, Li X, Zhu X, Liu J, Domigan B, Barr I, Cate JH, Zhang W: **Microbial biosynthesis of medium-chain 1-alkenes by a nonheme iron oxidase**. *Proceedings of the National Academy of Sciences* 2014, **111**(51):18237-18242.

111.   Wang C, Chang W-c, Guo Y, Huang H, Peck SC, Pandelia ME, Lin G-m, Liu H-w, Krebs C, Bollinger JM: **Evidence that the fosfomycin-producing epoxidase, HppE, is a non–heme-iron peroxidase**. *Science* 2013, **342**(6161):991-995.

112.   Coates JD, Michaelidou U, Bruce RA, O'Connor SM, Crespi JN, Achenbach LA: **Ubiquity and Diversity of Dissimilatory (Per)chlorate-Reducing Bacteria**. *Applied and Environmental Microbiology* 1999, **65**(12):5234-5241.

113.   Taylor PN, Okosieme OE, Murphy R, Hales C, Chiusano E, Maina A, Joomun M, Bestwick JP, Smyth P, Paradice R *et al*: **Maternal perchlorate levels in women with borderline thyroid function during pregnancy and the cognitive development of their offspring: data from the Controlled Antenatal Thyroid Study**. *The Journal of clinical endocrinology and metabolism* 2014, **99**(11):4291-4298.

114.   Greer MA, Goodman G, Pleus RC, Greer SE: **Health effects assessment for environmental perchlorate contamination: the dose response for inhibition of thyroidal radioiodine uptake in humans**. *Environmental Health Perspectives* 2002, **110**(9):927-937.

115.   Coates JD, Achenbach LA: **Microbial perchlorate reduction: rocket-fuelled metabolism**. *Nat Rev Micro* 2004, **2**(7):569-580.

116.   Youngblut MD, Wang O, Barnum TP, Coates JD: **(Per)chlorate in Biology on Earth and Beyond**. *Annual Review of Microbiology* 2016, **70**(1):435-457.

117.   Wang O, Coates J: **Biotechnological Applications of Microbial (Per)chlorate Reduction**. *Microorganisms* 2017, **5**(4):76.

118.   Carlstrom CI, Loutey DE, Wang O, Engelbrektson A, Clark I, Lucas LN, Somasekhar PY, Coates JD: **Phenotypic and genotypic description of Sedimenticola selenatireducens strain CUZ, a marine (per)chlorate-respiring gammaproteobacterium, and its close relative the chlorate-respiring sedimenticola strain NSS**. *Appl Environ Microbiol* 2015, **81**(8):2717-2726.

119.   Achenbach LA, Michaelidou U, Bruce RA, Fryman J, Coates JD: **Dechloromonas agitata gen. nov., sp. nov. and Dechlorosoma suillum gen. nov., sp. nov., two novel environmentally dominant (per) chlorate-reducing bacteria and their**

phylogenetic position. *International Journal of Systematic and Evolutionary Microbiology* 2001, **51**(2):527-533.

120. Herman DC, Frankenberger WT: **Bacterial Reduction of Perchlorate and Nitrate in Water**. *Journal of Environmental Quality* 1999, **28**(3):1018-1024.

121. Chaudhuri SK, O'Connor SM, Gustavson RL, Achenbach LA, Coates JD: **Environmental Factors That Control Microbial Perchlorate Reduction**. *Applied and Environmental Microbiology* 2002, **68**(9):4425-4430.

122. Choi H, Silverstein J: **Inhibition of perchlorate reduction by nitrate in a fixed biofilm reactor**. *Journal of Hazardous Materials* 2008, **159**(2–3):440-445.

123. Nozawa-Inoue M, Scow KM, Rolston DE: **Reduction of Perchlorate and Nitrate by Microbial Communities in Vadose Soil**. *Applied and Environmental Microbiology* 2005, **71**(7):3928-3934.

124. Melnyk RA, Engelbrektson A, Clark IC, Carlson HK, Byrne-Bailey K, Coates JD: **Identification of a Perchlorate Reduction Genomic Island with Novel Regulatory and Metabolic Genes**. *Applied and Environmental Microbiology* 2011, **77**(20):7401-7404.

125. Michaelidou U, Achenbach LA, Coates JD: **Isolation and Characterization of Two Novel (Per)Chlorate-Reducing Bacteria from Swine Waste Lagoons**. In: *Perchlorate in the Environment.* Edited by Urbansky ET. Boston, MA: Springer US; 2000: 271-283.

126. Bruce RA, Achenbach LA, Coates JD: **Reduction of (per)chlorate by a novel organism isolated from paper mill waste**. *Environmental Microbiology* 1999, **1**(4):319-329.

127. Lam C, O'Mullan P, Eveleigh D: **Transformation of Zymononas mobilis by electroporation**. *Appl Microbiol Biotechnol* 1993, **39**(3):305-308.

128. Kovach ME, Elzer PH, Hill DS, Robertson GT, Farris MA, Roop RM, 2nd, Peterson KM: **Four new derivatives of the broad-host-range cloning vector pBBR1MCS, carrying different antibiotic-resistance cassettes**. *Gene* 1995, **166**(1):175-176.

129. Melnyk R, Coates J: **The Perchlorate Reduction Genomic Island: Mechanisms and Pathways of Evolution by Horizontal Gene Transfer**. *BMC Genomics* 2015, **16**(1):862.

130. Potter LC, Cole JA: **Essential roles for the products of the napABCD genes, but not napFGH, in periplasmic nitrate reduction by Escherichia coli K-12**. *The Biochemical journal* 1999, **344 Pt 1**:69-76.

131. Roldan MD, Sears HJ, Cheesman MR, Ferguson SJ, Thomson AJ, Berks BC, Richardson DJ: **Spectroscopic characterization of a novel multiheme c-type cytochrome widely implicated in bacterial electron transport**. *Journal of Biological Chemistry* 1998, **273**(44):28785-28790.

132. Brondijk TH, Fiegen D, Richardson DJ, Cole JA: **Roles of NapF, NapG and NapH, subunits of the Escherichia coli periplasmic nitrate reductase, in ubiquinol oxidation**. *Mol Microbiol* 2002, **44**(1):245-255.

133. Kloer DP, Hagel C, Heider J, Schulz GE: **Crystal structure of ethylbenzene dehydrogenase from Aromatoleum aromaticum**. *Structure* 2006, **14**(9):1377-1388.

134. Kern M, Mager AM, Simon J: **Role of individual nap gene cluster products in NapC-independent nitrate respiration of Wolinella succinogenes**. *Microbiology* 2007, **153**(Pt 11):3739-3747.

135. Stewart V, Lu Y, Darwin AJ: **Periplasmic nitrate reductase (NapABC enzyme) supports anaerobic respiration by Escherichia coli K-12**. *J Bacteriol* 2002, **184**(5):1314-1323.

136. Sparacino-Watkins C, Stolz JF, Basu P: **Nitrate and periplasmic nitrate reductases**. *Chemical Society reviews* 2014, **43**(2):676-706.

137. Simpson PJ, Richardson DJ, Codd R: **The periplasmic nitrate reductase in Shewanella: the resolution, distribution and functional implications of two NAP isoforms, NapEDABC and NapDAGHB**. *Microbiology* 2010, **156**(Pt 2):302-312.

138. Kraft B, Strous M, Tegetmeyer HE: **Microbial nitrate respiration – Genes, enzymes and environmental distribution**. *Journal of Biotechnology* 2011, **155**(1):104-117.

139. Kengen SWM, Rikken GB, Hagen WR, van Ginkel CG, Stams AJM: **Purification and Characterization of (Per)Chlorate Reductase from the Chlorate-Respiring Strain GR-1**. *Journal of Bacteriology* 1999, **181**(21):6706-6711.

140. Coursolle D, Gralnick JA: **Modularity of the Mtr respiratory pathway of Shewanella oneidensis strain MR-1**. *Mol Microbiol* 2010, **77**(4):995-1008.

141. Sturm G, Richter K, Doetsch A, Heide H, Louro RO, Gescher J: **A dynamic periplasmic electron transfer network enables respiratory flexibility beyond a thermodynamic regulatory regime**. *The ISME journal* 2015, **9**(8):1802-1811.

142. González PJ, Correia C, Moura I, Brondino CD, Moura JJG: **Bacterial nitrate reductases: Molecular and biological aspects of nitrate reduction**. *Journal of Inorganic Biochemistry* 2006, **100**(5–6):1015-1023.

143. Mesa S, Bedmar EJ, Chanfon A, Hennecke H, Fischer H-M: **Bradyrhizobium japonicum NnrR, a Denitrification Regulator, Expands the FixLJ-FixK(2) Regulatory Cascade**. *Journal of Bacteriology* 2003, **185**(13):3978-3982.

144. Arai H, Kodama T, Igarashi Y: **Cascade regulation of the two CRP/FNR‐related transcriptional regulators (ANR and DNR) and the denitrification enzymes in Pseudomonas aeruginosa**. *Molecular microbiology* 1997, **25**(6):1141-1148.

145.   Lambden PR, Guest JR: **Mutants of Escherichia coli K12 unable to use fumarate as an anaerobic electron acceptor**. *Journal of general microbiology* 1976, **97**(2):145-160.

146.   Rabin RS, Stewart V: **Dual response regulators (NarL and NarP) interact with dual sensors (NarX and NarQ) to control nitrate- and nitrite-regulated gene expression in Escherichia coli K-12**. *Journal of Bacteriology* 1993, **175**(11):3259-3268.

147.   Tan Z, Reinhold-Hurek B: **Dechlorosoma suillum Achenbach et al. 2001 is a later subjective synonym of Azospira oryzae Reinhold-Hurek and Hurek 2000**. *International Journal of Systematic and Evolutionary Microbiology* 2003, **53**(4):1139-1142.

148.   Melnyk RA, Coates JD: **The Perchlorate Reduction Genomic Island: Mechanisms and Pathways of Evolution by Horizontal Gene Transfer**. *BMC genomics* 2015, **16**(1):862.

149.   Melnyk RA, Clark IC, Liao A, Coates JD: **Transposon and Deletion Mutagenesis of Genes Involved in Perchlorate Reduction in Azospira suillum PS**. *mBio* 2014, **5**(1):e00769-00713.

150.   Wang O, Melnyk RA, Mehta-Kolte MG, Youngblut MD, Carlson HK, Coates JD: **Functional Redundancy in Perchlorate and Nitrate Electron Transport Chains and Rewiring Respiratory Pathways to Alter Terminal Electron Acceptor Preference**. *Frontiers in Microbiology* 2018, **9**(376).

151.   McClure R, Balasubramanian D, Sun Y, Bobrovskyy M, Sumby P, Genco CA, Vanderpool CK, Tjaden B: **Computational analysis of bacterial RNA-Seq data**. *Nucleic acids research* 2013, **41**(14):e140.

152.   Melnyk RA, Youngblut MD, Clark IC, Carlson HK, Wetmore KM, Price MN, Iavarone AT, Deutschbauer AM, Arkin AP, Coates JD: **Novel Mechanism for Scavenging of Hypochlorite Involving a Periplasmic Methionine-Rich Peptide and Methionine Sulfoxide Reductase**. *mBio* 2015, **6**(3).

153.   Rowland MA, Deeds EJ: **Crosstalk and the evolution of specificity in two-component signaling**. *Proceedings of the National Academy of Sciences* 2014, **111**(15):5550.

154.   Malm S, Tiffert Y, Micklinghoff J, Schultze S, Joost I, Weber I, Horst S, Ackermann B, Schmidt M, Wohlleben W *et al*: **The roles of the nitrate reductase NarGHJI, the nitrite reductase NirBD and the response regulator GlnR in nitrate assimilation of Mycobacterium tuberculosis**. *Microbiology* 2009, **155**(4):1332-1339.

155.   McCarty GW, Bremner JM: **Inhibition of assimilatory nitrate reductase activity in soil by glutamine and ammonium analogs**. *Proceedings of the National Academy of Sciences* 1992, **89**(13):5834.

156. Buschmann S, Warkentin E, Xie H, Langer JD, Ermler U, Michel H: **The Structure of *cbb*₃ Cytochrome Oxidase Provides Insights into Proton Pumping**. *Science* 2010, **329**(5989):327.

157. Pitcher RS, Watmough NJ: **The bacterial cytochrome cbb3 oxidases**. *Biochimica et biophysica acta* 2004, **1655**(1-3):388-399.

158. Trumpower BL: **Cytochrome bc1 complexes of microorganisms**. *Microbiological reviews* 1990, **54**(2):101-129.

159. Borisov VB, Gennis RB, Hemp J, Verkhovsky MI: **The cytochrome bd respiratory oxygen reductases**. *Biochimica et biophysica acta* 2011, **1807**(11):1398-1413.

160. Junemann S: **Cytochrome bd terminal oxidase**. *Biochimica et biophysica acta* 1997, **1321**(2):107-127.

161. Partridge JD, Scott C, Tang Y, Poole RK, Green J: **Escherichia coli transcriptome dynamics during the transition from anaerobic to aerobic conditions**. *The Journal of biological chemistry* 2006, **281**(38):27806-27815.

162. C. CJ, J. DT: **Differences in two Pseudomonas aeruginosa cbb3 cytochrome oxidases**. *Molecular Microbiology* 2004, **51**(4):1193-1203.

163. Cosseau C, Batut J: **Genomics of the ccoNOQP-encoded cbb3 oxidase complex in bacteria**. *Archives of microbiology* 2004, **181**(2):89-96.

164. Preisig O, Zufferey R, Thöny-Meyer L, Appleby CA, Hennecke H: **A high-affinity cbb3-type cytochrome oxidase terminates the symbiosis-specific respiratory chain of Bradyrhizobium japonicum**. *Journal of Bacteriology* 1996, **178**(6):1532-1538.

165. Fernando G, A. AJ, P. GR: **Oxygen regulation of the Escherichia coli cytochrome d oxidase (cydAB) operon: roles of multiple promoters and the Fnr‐1 and Fnr‐2 binding sites**. *Molecular Microbiology* 2000, **37**(6):1456-1469.

166. Poole RK, Hill S: **Respiratory protection of nitrogenase activity in Azotobacter vinelandii--roles of the terminal oxidases**. *Bioscience reports* 1997, **17**(3):303-317.

167. Modak JM, Lim HC: **Optimal mode of operation of bioreactor for fermentation processes**. *Chemical engineering science* 1992, **47**(15-16):3869-3884.

168. Birch JR, Racher AJ: **Antibody production**. *Advanced drug delivery reviews* 2006, **58**(5-6):671-685.

169. Yang JD, Lu C, Stasny B, Henley J, Guinto W, Gonzalez C, Gleason J, Fung M, Collopy B, Benjamino M: **Fed‐batch bioreactor process scale‐up from 3‐L to 2,500‐L scale for monoclonal antibody production from cell culture**. *Biotechnology and bioengineering* 2007, **98**(1):141-154.

170. Robinson M-P, Ke N, Lobstein J, Peterson C, Szkodny A, Mansell TJ, Tuckey C, Riggs PD, Colussi PA, Noren CJ: **Efficient expression of full-length antibodies in the cytoplasm of engineered bacteria**. *Nature communications* 2015, **6**.

171. Carter P, Kelley RF, Rodrigues ML, Snedecor B, Covarrubias M, Velligan MD, Wong WLT, Rowland AM, Kotts CE, Carver ME *et al*: **High Level Escherichia**

coli Expression and Production of a Bivalent Humanized Antibody Fragment. *Nat Biotech* 1992, **10**(2):163-167.

172. Cabilly S, Riggs AD, Pande H, Shively JE, Holmes WE, Rey M, Perry LJ, Wetzel R, Heyneker HL: **Generation of antibody activity from immunoglobulin polypeptide chains produced in Escherichia coli**. *Proceedings of the National Academy of Sciences* 1984, **81**(11):3273-3277.

173. Huston JS, Levinson D, Mudgett-Hunter M, Tai MS, Novotný J, Margolies MN, Ridge RJ, Bruccoleri RE, Haber E, Crea R: **Protein engineering of antibody binding sites: recovery of specific activity in an anti-digoxin single-chain Fv analogue produced in Escherichia coli**. *Proceedings of the National Academy of Sciences* 1988, **85**(16):5879-5883.

174. Ghose TK, Tyagi R: **Rapid ethanol fermentation of cellulose hydrolysate. I. Batch versus continuous systems**. *Biotechnology and Bioengineering* 1979, **21**(8):1387-1400.

175. Cardona CA, Sánchez ÓJ: **Fuel ethanol production: process design trends and integration opportunities**. *Bioresource technology* 2007, **98**(12):2415-2457.

176. Modak J, Lim H, Tayeb Y: **General characteristics of optimal feed rate profiles for various fed‐batch fermentation processes**. *Biotechnology and bioengineering* 1986, **28**(9):1396-1407.

177. Luli GW, Strohl WR: **Comparison of growth, acetate production, and acetate inhibition of Escherichia coli strains in batch and fed-batch fermentations**. *Applied and environmental microbiology* 1990, **56**(4):1004-1011.

178. Li S-Y, Srivastava R, Suib SL, Li Y, Parnas RS: **Performance of batch, fed-batch, and continuous A–B–E fermentation with pH-control**. *Bioresource technology* 2011, **102**(5):4241-4250.

179. Cysewski GR, Wilke CR: **Process design and economic studies of alternative fermentation methods for the production of ethanol**. *Biotechnology and Bioengineering* 1978, **20**(9):1421-1444.

180. Bayrock D, Thomas K, Ingledew W: **Control of Lactobacillus contaminants in continuous fuel ethanol fermentations by constant or pulsed addition of penicillin G**. *Appl Microbiol Biotechnol* 2003, **62**(5-6):498-502.

181. Junker B, Lester M, Leporati J, Schmitt J, Kovatch M, Borysewicz S, Maciejak W, Seeley A, Hesse M, Connors N: **Sustainable reduction of bioreactor contamination in an industrial fermentation pilot plant**. *Journal of bioscience and bioengineering* 2006, **102**(4):251-268.

182. Jones DT, Shirley M, Wu X, Keis S: **Bacteriophage infections in the industrial acetone butanol (AB) fermentation process**. *Journal of molecular microbiology and biotechnology* 2000, **2**(1):21-26.

183. Madigan MT, Martinko JM, Parker J: **Brock biology of microorganisms**, vol. 11: prentice hall Upper Saddle River, NJ; 1997.

184. Costanzo SD, Murby J, Bates J: **Ecosystem response to antibiotics entering the aquatic environment**. *Marine Pollution Bulletin* 2005, **51**(1):218-223.

185. Okeke IN, Lamikanra A, Edelman R: **Socioeconomic and behavioral factors leading to acquired bacterial resistance to antibiotics in developing countries**. *Emerging Infectious Diseases* 1999, **5**(1):18-27.

186. Ison A, Odeh IN, Margerum DW: **Kinetics and mechanisms of chlorine dioxide and chlorite oxidations of cysteine and glutathione**. *Inorganic chemistry* 2006, **45**(21):8768-8775.

187. Kross RD, Kemp GK: **Method for optimizing the efficacy of chlorous acid disinfecting sprays for poultry and other meats**. In.: Google Patents; 2000.

188. Kemp GK, Aldrich M, Waldroup A: **Acidified sodium chlorite antimicrobial treatment of broiler carcasses**. *Journal of food Protection* 2000, **63**(8):1087-1092.

189. Stopforth JD, Mai T, Kottapalli B, Samadpour M: **Effect of Acidified Sodium Chlorite, Chlorine, and Acidic Electrolyzed Water on Escherichia coli O157:H7, Salmonella, and Listeria monocytogenes Inoculated onto Leafy Greens**. *Journal of Food Protection* 2008, **71**(3):625-628.

190. Lim K, Mustapha A: **Effects of Cetylpyridinium Chloride, Acidified Sodium Chlorite, and Potassium Sorbate on Populations of Escherichia coli O157:H7, Listeria monocytogenes, and Staphylococcus aureus on Fresh Beef**. *Journal of Food Protection* 2004, **67**(2):310-315.

191. Harris K, Miller MF, Loneragan GH, Brashears MM: **Validation of the Use of Organic Acids and Acidified Sodium Chlorite To Reduce Escherichia coli O157 and Salmonella Typhimurium in Beef Trim and Ground Beef in a Simulated Processing Environment**. *Journal of Food Protection* 2006, **69**(8):1802-1807.

192. Oyarzabal OA, Hawk C, Bilgili SF, Warf CC, Kemp GK: **Effects of Postchill Application of Acidified Sodium Chlorite To Control Campylobacter spp. and Escherichia coli on Commercial Broiler Carcasses**. *Journal of Food Protection* 2004, **67**(10):2288-2291.

193. Jakopitsch C, Pirker KF, Flemmig J, Hofbauer S, Schlorke D, Furtmüller PG, Arnhold J, Obinger C: **Mechanism of reaction of chlorite with mammalian heme peroxidases**. *Journal of inorganic biochemistry* 2014, **135**:10-19.

194. McGrath M, Kahn J, Herndier B: **Development of WF10, a novel macrophage-regulating agent**. *Current opinion in investigational drugs (London, England: 2000)* 2002, **3**(3):365-373.

195. Maraprygsavan P, Mongkolsuk J, Arnhold J, Kuehne F-W: **The chlorite-based drug WF10 constantly reduces hemoglobin A1c values and improves glucose control in diabetes patients with severe foot syndrome**. *Journal of Clinical & Translational Endocrinology* 2016, **4**:53-58.

196. Iatrou A, Knocke WR: **Removing chlorite by the addition of ferrous iron**. *Journal-American Water Works Association* 1992, **84**(11):63-68.

197. van Ginkel CG, Rikken GB, Kroon AG, Kengen SW: **Purification and characterization of chlorite dismutase: a novel oxygen-generating enzyme**. *Archives of microbiology* 1996, **166**(5):321-326.

198. Hofbauer S, Schaffner I, Furtmüller PG, Obinger C: **Chlorite dismutases–a heme enzyme family for use in bioremediation and generation of molecular oxygen**. *Biotechnology journal* 2014, **9**(4):461-473.

199. Schaffner I, Hofbauer S, Krutzler M, Pirker KF, Furtmüller PG, Obinger C: **Mechanism of chlorite degradation to chloride and dioxygen by the enzyme chlorite dismutase**. *Archives of biochemistry and biophysics* 2015, **574**:18-26.

200. Lee AQ, Streit BR, Zdilla MJ, Abu-Omar MM, DuBois JL: **Mechanism of and exquisite selectivity for O–O bond formation by the heme-dependent chlorite dismutase**. *Proceedings of the National Academy of Sciences* 2008, **105**(41):15654-15659.

201. Streit BR, Blanc B, Lukat-Rodgers GS, Rodgers KR, DuBois JL: **How active-site protonation state influences the reactivity and ligation of the heme in chlorite dismutase**. *Journal of the American Chemical Society* 2010, **132**(16):5711-5724.

202. DuBois JL, Ojha S: **Production of dioxygen in the dark: dismutases of oxyanions**. In: *Sustaining Life on Planet Earth: Metalloenzymes Mastering Dioxygen and Other Chewy Gases.* Springer; 2015: 45-87.

203. Clark IC, Youngblut M, Jacobsen G, Wetmore KM, Deutschbauer A, Lucas L, Coates JD: **Genetic dissection of chlorate respiration in Pseudomonas stutzeri PDA reveals syntrophic (per) chlorate reduction**. *Environmental microbiology* 2016.

204. de Geus DC, Thomassen EA, Hagedoorn P-L, Pannu NS, van Duijn E, Abrahams JP: **Crystal structure of chlorite dismutase, a detoxifying enzyme producing molecular oxygen**. *Journal of molecular biology* 2009, **387**(1):192-206.

205. Thorell HD, Karlsson J, Portelius E, Nilsson T: **Cloning, characterisation, and expression of a novel gene encoding chlorite dismutase from Ideonella dechloratans**. *Biochimica et Biophysica Acta (BBA)-Gene Structure and Expression* 2002, **1577**(3):445-451.

206. Danielsson Thorell H, Beyer NH, Heegaard NH, Öhman M, Nilsson T: **Comparison of native and recombinant chlorite dismutase from Ideonella dechloratans**. *European journal of biochemistry* 2004, **271**(17):3539-3546.

207. Streit BR, DuBois JL: **Chemical and steady-state kinetic analyses of a heterologously expressed heme dependent chlorite dismutase**. *Biochemistry* 2008, **47**(19):5271-5280.

208. Maixner F, Wagner M, Lücker S, Pelletier E, Schmitz‐Esser S, Hace K, Spieck E, Konrat R, Le Paslier D, Daims H: **Environmental genomics reveals a functional**

chlorite dismutase in the nitrite‑oxidizing bacterium 'Candidatus Nitrospira defluvii'. *Environmental microbiology* 2008, **10**(11):3043-3056.

209. Kostan J, Sjöblom B, Maixner F, Mlynek G, Furtmüller PG, Obinger C, Wagner M, Daims H, Djinović-Carugo K: **Structural and functional characterisation of the chlorite dismutase from the nitrite-oxidizing bacterium "Candidatus Nitrospira defluvii": identification of a catalytically important amino acid residue**. *Journal of structural biology* 2010, **172**(3):331-342.

210. Hofbauer S, Bellei M, Sündermann A, Pirker KF, Hagmüller A, Mlynek G, Kostan J, Daims H, Furtmüller PG, Djinović-Carugo K: **Redox thermodynamics of high-spin and low-spin forms of chlorite dismutases with diverse subunit and oligomeric structures**. *Biochemistry* 2012, **51**(47):9501-9512.

211. Mlynek G, Sjöblom B, Kostan J, Füreder S, Maixner F, Gysel K, Furtmüller PG, Obinger C, Wagner M, Daims H: **Unexpected diversity of chlorite dismutases: a catalytically efficient dimeric enzyme from Nitrobacter winogradskyi**. *Journal of bacteriology* 2011, **193**(10):2408-2417.

212. Guzman LM, Belin D, Carson MJ, Beckwith J: **Tight regulation, modulation, and high-level expression by vectors containing the arabinose PBAD promoter**. *J Bacteriol* 1995, **177**(14):4121-4130.

213. Petersen TN, Brunak S, von Heijne G, Nielsen H: **SignalP 4.0: discriminating signal peptides from transmembrane regions**. *Nature methods* 2011, **8**(10):785-786.

214. Anderson J, Dueber JE, Leguia M, Wu GC, Goler JA, Arkin AP, Keasling JD: **BglBricks: A flexible standard for biological part assembly**. *Journal of Biological Engineering* 2010, **4**(1):1.

215. Chen Y-J, Liu P, Nielsen AAK, Brophy JAN, Clancy K, Peterson T, Voigt CA: **Characterization of 582 natural and synthetic terminators and quantification of their design constraints**. *Nature Methods* 2013, **10**:659.

216. O'Connor SM, Coates JD: **Universal immunoprobe for (per) chlorate-reducing bacteria**. *Applied and environmental microbiology* 2002, **68**(6):3108-3113.

217. Jannasch HW: **Estimations of bacterial growth rates in natural waters**. *Journal of Bacteriology* 1969, **99**(1):156-160.

218. Hans K, Maranzana S: **Strawberry Creek Water Quality- 2006 Status Report**. *University of California, Berkeley Office of Environment, Health & Safety (EH&S)* 2006.

219. Kotecha N, Krutzik PO, Irish JM: **Web‑Based Analysis and Publication of Flow Cytometry Experiments**. *Current protocols in cytometry* 2010:10.17. 11-10.17. 24.

220. Bagos PG, Nikolaou EP, Liakopoulos TD, Tsirigos KD: **Combined prediction of Tat and Sec signal peptides with hidden Markov models**. *Bioinformatics* 2010, **26**(22):2811-2817.

221.   Lindqvist MH, Johansson N, Nilsson T, Rova M: **Expression of chlorite dismutase and chlorate reductase in the presence of oxygen and/or chlorate as the terminal electron acceptor in Ideonella dechloratans**. *Applied and environmental microbiology* 2012, **78**(12):4380-4385.

222.   Van Ginkel C, Rikken G, Kroon A, Kengen S: **Purification and characterization of chlorite dismutase: a novel oxygen-generating enzyme**. *Archives of microbiology* 1996, **166**(5):321-326.

223.   Coates JD, Michaelidou U, Bruce RA, O'Connor SM, Crespi JN, Achenbach LA: **Ubiquity and diversity of dissimilatory (per) chlorate-reducing bacteria**. *Applied and Environmental Microbiology* 1999, **65**(12):5234-5241.

224.   Chen Y, Patel NA, Crombie A, Scrivens JH, Murrell JC: **Bacterial flavin-containing monooxygenase is trimethylamine monooxygenase**. *Proceedings of the National Academy of Sciences* 2011, **108**(43):17791-17796.

225.   Choi HS, Kim JK, Cho EH, Kim YC, Kim JI, Kim SW: **A novel flavin-containing monooxygenase from Methylophaga sp. strain SK1 and its indigo synthesis in Escherichia coli**. *Biochemical and biophysical research communications* 2003, **306**(4):930-936.

226.   Strauch KL, Johnson K, Beckwith J: **Characterization of degP, a gene required for proteolysis in the cell envelope and essential for growth of Escherichia coli at high temperature**. *Journal of Bacteriology* 1989, **171**(5):2689-2696.

227.   Krojer T, Garrido-Franco M, Huber R, Ehrmann M, Clausen T: **Crystal structure of DegP (HtrA) reveals a new protease-chaperone machine**. *Nature* 2002, **416**(6879):455-459.

228.   Lipinska B, Zylicz M, Georgopoulos C: **The HtrA (DegP) protein, essential for Escherichia coli survival at high temperatures, is an endopeptidase**. *Journal of bacteriology* 1990, **172**(4):1791-1797.

229.   Sakoh M, Ito K, Akiyama Y: **Proteolytic activity of HtpX, a membrane-bound and stress-controlled protease from Escherichia coli**. *Journal of Biological Chemistry* 2005, **280**(39):33305-33310.

230.   Shimohata N, Chiba S, Saikawa N, Ito K, Akiyama Y: **The Cpx stress response system of Escherichia coli senses plasma membrane proteins and controls HtpX, a membrane protease with a cytosolic active site**. *Genes to Cells* 2002, **7**(7):653-662.

231.   Ojha L, Wilhelm MB, Murchie SL, McEwen AS, Wray JJ, Hanley J, Massé M, Chojnacki M: **Spectral evidence for hydrated salts in recurring slope lineae on Mars**. *Nature Geoscience* 2015, **8**:829.

232.   Lee ME, DeLoache WC, Cervantes B, Dueber JE: **A Highly Characterized Yeast Toolkit for Modular, Multipart Assembly**. *ACS Synthetic Biology* 2015, **4**(9):975-986.